Contents

Zusammenfassung

Das Ziel dieser Arbeit ist die Untersuchung der Abstrahlung korrelierter Photonen durch zeitweise beschleunigte Ladungsträger. Desweiteren untersuchen wir die Korrelationen dieser Photonen, d.h. wir betrachten die Verschränkung zwischen den abgestrahlten Photonen. Um dieses Ziel zu erreichen entwickeln wir ein Rahmenwerk der skalaren und spinoriellen Quantenelektrodynamik in einem linearen, homogenen und endlich ausgedehnten klassischen elektrischen Hintergrundfeld. Als erstes konstruieren wir die Lösungen der zugehörigen relativistischen Wellengleichungen und benutzen diese Lösungen um die Materiefelder zu quantisieren. Durch die Wirkung des elektrische Hintergundfeldes kann das Vakuum nicht eindeutig definert werden. Das kann als Instabilität des Vakuumss interpretiert werden, was bedeutet, dass Elektron-Positron-Paare entstehen und somit der Teilchen-Inhalte eines Zustands wächst. Die resultierende Rate der Elektron-Positron-Paarerzeugung wird in der Mitte dieser Arbeit betrachtet. Im Hauptteil dieser Arbeit leiten wir Ausdrücke für die Streumatrix-Elemente der Photonenabstrahlung durch geladene Teilchen in erster und zweiter Ordnung Störungstheorie her. Für die erste Ordnung benutzen wir eine ultrarelativistische Nährung um geschlossene analytische Ausdrücke für die Wirkungsquerschnitte herzuleiten. Wir zeigen, dass es, im Widerspruch zu den klassischen Ergebnissen, bei der Abstrahlung von Photonen durch Electronen, aufgrund des Spins, im Allgemeinen keinen blinden Fleck in der Beschleunigungsrichtung gibt. Zuletzt untersuchen wir noch die Korrelationseigenschaften der durch beschleunigte Electronen abgestrahlten Photonen in zweiter Ordnung Störungstheorie. Wir stellen fest, dass Photonenpaare in ihren Polarisationsfreiheitsgraden maximal verschränkt sind, wenn sie in Beschleunigungsrichtung

abgestrahlt werden und, dass sie sich nährungweise in einem Produktzustand befinden, wenn die beiden Photonen in ein und dieselbe Richtung senkrecht zur Beschleunigungsrichtung abgestrahlt werden.

Abstract

The aim of this thesis is to investigate the emission of correlated photons from transiently accelerated charges. Furthermore, we want to investigate the correlations of such photons, with other words entanglement. To reach this goal we develop a framework of scalar and spinor quantum electrodynamics in a classical, electric background field which is linear, homogenous and finite extended. First of all we construct the solutions of the corresponding relativistic wave equations and use these solutions to quantize the matter fields. Due to the presence of the electric field the vacuum state cannot be defined unambiguously. This can be interpred as an unstability of the vacuum which means that electron-positron pairs emerge and thus the particle content of a state increases. The resulting rate of electron-positron pair production is investigated in the middle of this thesis. In the main part of this thesis we derive expressions for the scattering matrix elements of photon emission from charged particles in first and second order perturbation theory. For the first order we use an ultrarelativistic approximation to derive closed analytic expressions for the cross section. We show that, due to the spin, there is not a blind spot for photon emission from electrons in the acceleration direction in general. Finally we investigate the correlation properties of emitted photon pairs in second order perturbation theory. This result contradicts the results of classical electrodynamics. Moreover, we find that emitted photon pairs are maximally entangled in their polarization degrees of freedom if they are emitted in the acceleration direction and that they are approximately in a product state if both photons are emitted in the same direction perpendicular to the acceleration direction.

Chapter 1

Introduction

Does a linearly accelerated charged particle radiate and, if it does, what are the properties of the arising radiation? Classical electrodynamics gives a clear answer to this question: Linearly accelerated particles radiate and the angular distribution of this radiation is given by the relativistic Larmor formula [1]

$$\frac{dP}{d\Omega} = \frac{e^2\dot{x}^2}{4\pi c^3}\frac{\sin\theta^2}{(1-\frac{\dot{x}}{c}\cos\theta)^5}. \tag{1.1}$$

However, the classical description of the interaction between the electromagentic field and matter is in many experimental and technical relevant situations not adequate, it must be replaced by a quantum mechanical description. The state of the art method for describing electrodynamical phenomena in the framework of quantum theory is Quantum Optics. How does Quantum Optics answer our question? At the first glance the answer is, again, the Larmor formular [2]. If one then goes one step further in the accuracy of the calculations and considers the back reaction of the emitted photon on the charged particle one gets the simultanious emission of two photons; a photon pair. Due to the quantum properties of the electromagnetic field the correlations between these photons can be much stronger than classical correlations, i.e. the photon pair is entangled to some degree [3]. Hence accelerated electrons could be a source of entangled photon pair radiation

with energy in the keV domain. This could be of enormous value for experiments in Quantum Optics and experimental Quantum Information [4]. In Quantum Optics all these results are derived while assuming the accelerated charged particle to be simply a classical point particle without any inner degree of freedom - like spin. In contrast to this model the charged particles that are used in most of the experimental cases have spin and thus the quantum optical description outlined above can only be adequate to some extent since effects caused by the spin are neglected. In Quantum Optics one deals with such inner degrees of freedom by modelling them as an n-level system, that is a harmonic oscillator with n levels with an appropriate coupling to the external electromagnetic field [2]. By investigating a quantum optical model for an uncharged particle with inner degrees of freedom we arrive at the following statement: If such a particle is in the ground state and is then accelerated, there is a finite probability that it will be found in an excited state after the acceleration; the energy spectrum of the excitation probability is thermal, that is the occupation probabilities of the energy eigenstates of the n-lever system undergoing an acceleration a are the same as if the system were coupled to a thermal bath with temperature $kT = \frac{\hbar a}{2\pi c}$. This theoretical prediction is called the Unruh effect [5] and has been thoroughly investigated in several publications by different authors although it has not yet been experimentally observed. It can be interpreted as the statement that for non inertial observers the quantum vacuum is ambigious, i.e. the particle content of the environment depends on the acceleration [6]. In this way the Unruh effect is closely related to the Hawking effect for black holes [7]. Obviously we must also consider the Unruh effect for a charged accelerated particle with inner degrees of freedom in the calculations[1].

We see that the quantum optical description of an accelerated charged particle explains most of the corresponding macroscopic phenomena but is insufficient if one wants to take a closer look. Quantum Electrodynamics is, in contrast, a theory that deals with electrons and their interaction with the electromagnetic field in a highly precise way. In this theory both the electromagnetic field and matter are treated in second quantization, thus all the quantum mechanical properties corresponding

[1]Unfortunately the acceleration in every existing linear accelerator is to small or the acceleration time is to short to enable the detection of a themalization of the particles at the Unruh temperature [8].

to space and momentum of photons and massive charged particles are accessible which allows the investigation of entanglement within these variables. A further great advantage of this theory is that the spin is completely inherent because we describe the electron as an excitation of a spinor field; no artificial inner degrees of freedom have to be established like in Quantum Optics. Furthermore, instead of giving the charged particle a fixed trajectory, as it is done in most of the quantum optical approaches in QED, the acceleration is achieved by an external electric field and all recoil effects due to photon emission processes are included. In this thesis we show that these advantages lead to significant differences in the predictions of the photon emission probability in contrast to predictions given by Quantum Optics. This is relevant especially in experiments geared towards the detection of photon pair radiaton, like those described in ref. [4]. Our results show that it is questionable that the quantum optical description used in ref. [3] and [4] to describe these experiments is sufficient.

Unfortunately in QED the effects of the interaction between the matter field and the electromagnetic field can, in most cases, only be calculated in a perturbative way, order by order. Because of this QED is mainly used for the calculation of cross sections of processes with only a few particles in Minkovski space. To succesfully model the acceleration of a particle in this perturbative framework and to investigate the emission of photons from an accelerated particle it is necessary to consider processes of very high order. This is hardly a solvable problem. However, we can model the acceleration of particles approximately if we use a classical, linear electric background field and negelect the backreaction of the charged particle on this background field. Radiation can be considered by splitting the electromagnetic field into the classical background field that accelerates the charged particles and a quantum mechanical radiation field. In ref. [9] the authors use this framework in first order perturbation theory to investigate the emission of photons from infinitely, uniformly accelerated electrons. In this thesis we use the framework of QED to investigate the emission of photons from charges that are transiently accelerated by a linear finite extended electric field like that which can easily be realized in a plate capicitor (see figure 1.1). Furthermore we investigate the correlations of the emitted photons in second order perturbation theory.

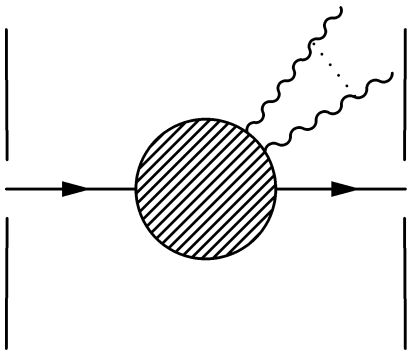

Figure 1.1: Charged particle accelerated by the electric field of a plate capacitor interacting with the electromagnetic field.

In chapter 2 we derive the solutions of the relativistic wave equations for scalar and spinor particles in a classical finite extended electric field and investigate the propagation of wave packets. In chaper 3 we outline the procedure of second quantization and construct the many particle quantum theory for scalar and spinor particles in an external field. In chapter 4 we discuss the instability of the vacuum and the pair creation rate. The central part of this thesis is chapter 5. We use the developed many particle quantum theory of scalar and spinor particles and their interaction with the electromagnetic field to derive the probability of photon emission by transiently accelerated charges in first and second order perturbation theory. In section 5.4 of this chapter we discuss the correlations between emitted photon pairs in second order perturbation thory. In chapter 6 we give conclusions and an outlook on potential further work.

Chapter 2

Relativistic quantum mechanics

In relativistic quantum mechanics a scalar or spinor particle can be modelled as a wave packet of the solutions of the Klein-Gordon or Dirac equation respectively. Acceleration can be brought into play by coupling the wave equations minimally to a linear electric field. In the next two subsections we calculate the solutions of the relativistic wave equations coupled to a finite extended linear electric field. For the scalar particle we additionally derive ultrarelativistic approximations of the solutions of the wave equation, compare them with the corresponding WKB solutions and investigate the propagation of wave packets in this electromagnetic background field.

2.1 Scalar particles

2.1.1 Solutions of the wave equation

The Klein-Gordon equation is

$$\left[D^\mu D_\mu + \frac{m^2c^2}{\hbar^2}\right]\Phi = 0 \tag{2.1}$$

where $D_\mu = \partial_\mu + i\frac{q}{\hbar}A_\mu$ and the inner product on Minkowki space is
$\eta_{\mu\nu} = diag(1,-1,-1,-1)$. A_μ is the electromagnetic four-vector potential and m is the mass of the scalar particle. We decide to describe electrons as particles and positrons as antiparticles, thus we

have $q = -e$. We consider the following four-vector potential illustrated in figure 2.1:

$$A_0 = \begin{cases} x_{3,0}E/c & : & & & x_3 & < & -x_{3,0} \\ -x_3E/c & : & -x_{3,0} & \leq & x_3 & \leq & x_{0,3} \\ -x_{3,0}E/c & : & x_{3,0} & < & x_3 & & \end{cases} \tag{2.2}$$

$$\text{and} \quad A_\mu = 0 \quad \text{for} \quad \mu \neq 0.$$

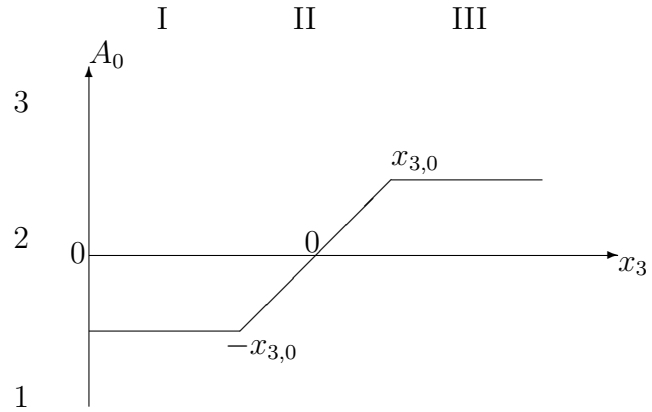

Figure 2.1: A diagram of the potential $-eA_0$. It can be separated into three spacial sections I, II and III with different solutions of the wave equation (2.1) and into three energy domains 1, 2 and 3 with different particle and antiparticle content. Section 1: $cp_0 < -eEx_{3,0}$, Section 2: $-eEx_{3,0} \leq cp_0 \leq eEx_{3,0}$, Section 3: $eEx_{3,0} < cp_0$.

Now we devide the domain of Φ, i.e. the x_3-axis into three sections corresponding to the three sections of the potential I, II and III and make the ansatz

$$\Phi(x,t) := \phi(x_3)e^{\frac{i}{\hbar}p_\perp x_\perp}e^{-i\frac{p_0}{\hbar}ct} \tag{2.3}$$

where $p_\perp$ is the part of the vector p lying perpendicular to the x_3 direction. By defining $m_\perp^2c^2 := m^2c^2 + p_\perp^2$ we get three ordinary linear second order differential equations in x_3. **Section I** ($x_3 < -x_{3,0}$)

$$\frac{d^2\phi_I}{dx_3^2} + \frac{(p_0 + eEx_{3,0})^2}{c^2\hbar^2}\phi_I - \frac{m_\perp^2c^2}{\hbar^2}\phi_I = 0 \tag{2.4}$$

Section II $(-x_{3,0} \leq x_3 \leq x_{3,0})$

$$\frac{d^2\phi_{II}}{dx_3^2} + \frac{(p_0 - eEx_3)^2}{c^2\hbar^2}\phi_{II} - \frac{m_\perp^2 c^2}{\hbar^2}\phi_{II} = 0 \tag{2.5}$$

Section III $(x_{3,0} < x_3)$

$$\frac{d^2\phi_{III}}{dx_3^2} + \frac{(p_0 - eEx_{3,0})^2}{c^2\hbar^2}\phi_{III} - \frac{m_\perp^2 c^2}{\hbar^2}\phi_{III} = 0. \tag{2.6}$$

For the sake of simplicity we define new dimensionless variables and parameters.

$$\begin{gathered} \tilde{p}_0 := \sqrt{\tfrac{c}{2eE\hbar}}p_0 \qquad \tilde{p}_\perp := \sqrt{\tfrac{c}{2eE\hbar}}p_\perp \qquad z := \sqrt{\tfrac{2eE}{\hbar c}}x_3 \\ \tilde{t} := \sqrt{\tfrac{2eE}{\hbar c}}ct \qquad \mu_\perp^2 := \tfrac{m_\perp^2 c^4}{2eE\hbar c} \end{gathered} \tag{2.7}$$

To get a feeling for these dimensionless variables we give some experimentally relevant values: for $E = 10^6 \frac{\hbar V}{\hbar m}$, $x_{3,0} = 10^{-5}\hbar m$ and $p_\perp = 0$ we find $z_0 = 3.65 \times 10^6$ and $\mu_\perp = 7.4 \times 10^5$.

With the definitions (2.7) the differential equations (2.4), (2.5) and (2.6) become **Section I** $(x_3 < -x_{3,0})$

$$\frac{d^2\phi_I}{dz^2} + (\tilde{p}_0 + z_0/2)^2\phi_I - \mu_\perp^2\phi_I = 0 \tag{2.8}$$

Section II $(-x_{3,0} \leq x_3 \leq x_{3,0})$

$$\frac{d^2\phi_{II}}{dz^2} + (\tilde{p}_0 - z/2)^2\phi_{II} - \mu_\perp^2\phi_{II} = 0 \tag{2.9}$$

Section III $(x_{3,0} < x_3)$

$$\frac{d^2\phi_{III}}{dz^2} + (\tilde{p}_0 - z_0/2)^2\phi_{III} - \mu_\perp^2\phi_{III} = 0 \tag{2.10}$$

For sections I and III the solutions are straight forward. For section II we make a additional

transformation to $\tilde{z} := e^{-i\frac{3}{4}\pi}(z - 2\tilde{p}_0) := \gamma(z - 2\tilde{p}_0)$ and get with the definition $n := i\mu^2 - \frac{1}{2}$

$$\frac{d^2\phi_{II}}{d\tilde{z}^2} + \left(n + \frac{1}{2} - \frac{\tilde{z}^2}{4}\right)\phi_{II} = 0. \tag{2.11}$$

This is the parabolic cylinder equation known from harmonic analysis. A special complete set of solutions consists of the so-called parabolic cylinder functions $D_n[\tilde{z}]$ and $D_n[-\tilde{z}]$ [10]. We use these solutions due to their asymptotic properties, which appear appropriate for the following interpretation as in- and out-propagating particle and antiparticle states like it is done in [11], [12] and [13]. Doing this we arrive at the following general solutions: **Section I** ($x_3 < -x_{3,0}$)

$$\phi_I(z) = a_1 e^{-i\tilde{p}(-)z} + b_1 e^{i\tilde{p}(-)z} \tag{2.12}$$

Section II ($-x_{3,0} \leq x_3 \leq x_{3,0}$)

$$\phi_{II}(z) = AD_n[\gamma(z - 2\tilde{p_0})] + BD_n[-\gamma(z - 2\tilde{p_0})] \tag{2.13}$$

Section III ($x_{3,0} < x_3$)

$$\phi_{III}(z) = a_2 e^{-i\tilde{p}(+)z} + b_2 e^{i\tilde{p}(+)z} \tag{2.14}$$

where $\tilde{p}(-) = ((\tilde{p}_0 + \frac{z_0}{2})^2 - \mu_\perp^2)^{\frac{1}{2}}$ and $\tilde{p}(+) = ((\tilde{p}_0 - \frac{z_0}{2})^2 - \mu_\perp^2)^{\frac{1}{2}}$ and the factors a_1, b_1, a_2, b_2, A and B must be specified by connection conditions between the three sections of the wave function's domain and by the interpretation as in- and out-propagating states.

In the next step we have to fix the free parameters in equations (2.12) to (2.14). Since the Klein-Gordon equation is a second order differential equation and the potential A_μ is continuous, the solutions ϕ for the whole domain have to be twice continuously differentiable, i.e. $\phi \in C_2^\infty(\mathbb{R})$. These connecting conditions give us four equations.

$$\phi_I(-z_0) = \phi_{II}(-z_0) \qquad \phi_{II}(z_0) = \phi_{III}(z_0)$$

$$\phi_I'(-z_0) = \phi_{II}'(-z_0) \qquad \phi_{II}'(z_0) = \phi_{III}'(z_0)$$

where the prime indicates the derivative with respect to z. We can now fix the two remaining free parameters by normalization of the wave functions and, at this point, everything is fixed by physical and mathematical constraints. The last parameter, however, can only be fixed by the identification of in- and out-propagating states and this is totally ambigious. In literature we find two different approaches to identify in- and out-propagating states; one is followed by ref.[14] and the other by ref.[15] and [16]. They are illustrated by the diagrams in figures 2.2 and 2.3. Both identification schemes are based on a wave packet picture, i.e. by investigation of the group velocity $v_g = c\frac{\tilde{p}}{\tilde{p}_0 + \frac{z_0}{2}}$ of a wave packet constructed from these wave functions. The identification scheme of ref. [14] can be summarized by the statement: an in-propagating state from the left is a state with no in-propagating wavepacket from the right and analogous for in-propagating states from the right and out-propagating states. Similary the identification scheme of ref. [15] can be summarized by the statement: an in-propagating state from the left is a state without out-propagating wave packet on the left and analogous for the other states. We find that the transformation that connects the two schemes is CPT, i.e. the subsequent application of time reversal, point reflection (parity) and charge conjugation. There is no argument for ruling out one of these identification schemes or any other identification scheme using linear combinations of the wave functions constructed with the identification scheme of ref. [14] and ref. [15]. Nevertheless, in the following we construct the left and right in-propagating states in the scheme of ref. [14] only since, in the context of the one particle theory, it seems more natural that the incident particle is reflected than that it is annihilated by a particle coming from the right. The corresponding out-propagating states can be obtained by complex conjugation of the spatial part of the wave function. This can easily be seen by looking at the exponential form of the wave functions in section I and III of the z-axis, which indicates that complex conjugation flips the sign of the group velocity.

To construct the wave functions we start with the investigation of the group velocity. For an

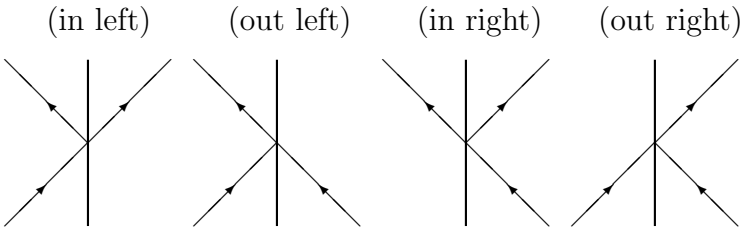

Figure 2.2: A diagram of the identification scheme of ref. [14]. The vertical line represents the source of reflection, i.e. the electromagnatic fild.

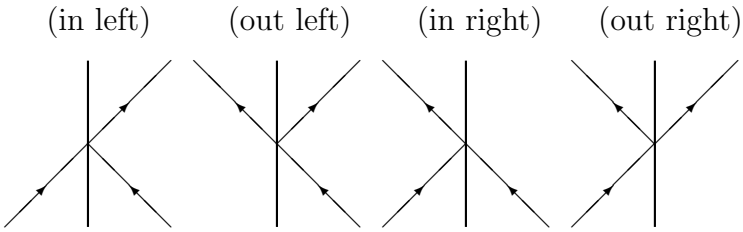

Figure 2.3: A diagram of the identification scheme of ref. [15].

in-propagating state from the left the group velocity has to be positive on the left. One can easily see that the sign of v_g depends on the energy range. Thus we have to split the energy range into three domains as it is shown in figure 2.1. We name the domains 1, 2 and 3 under barrier regime, pair creation regime and over barrier regime respectively. The reason for denoting domain 2 as pair creation regime will become clear in the following. Due to the ansatz (2.3) we define the wave functions

$$\Phi^{(p,a)}_{in,p(\pm)} := \phi^{(p,a)}_{in,p(\pm)} e^{ip_\perp x_\perp - ip_0^{(p,a)}(p(\pm),p_\perp)t}. \tag{2.15}$$

The explicit expressions for the functions $\phi^{(p,a)}_{in,p(\pm)}$ are given in the appendix 7.2. We term states as particle $^{(p)}$ and antiparticle $^{(a)}$ states due to their asymptotic charge density, here and in the following the indices $p(+)$ and $p(-)$ denote a left or right state respectively. The charge density for Klein Gordon fields is given by

$$\rho[\Phi](x) = -ie(\Phi^*(x)D_0\Phi(x) - (D_0\Phi(z))^*\Phi(z)). \tag{2.16}$$

Since the covariant derivative D_0 depends only on x_3 we can restrict our investigations to one dimension and get

$$\rho[\phi](z) = -e(p_0 - eA_0(z))\phi^*(z)\phi(z). \tag{2.17}$$

Thus the density is negative for $p_0 > A_0(z)$ and positive for $p_0 < A_0(z)$. Since we are only interested in a definition of states in the asymptotic regime where $z \to \pm\infty$ we term the left(right) states with negative charge density on the left(right) side of the potential barrier as particle states $\phi^{(p)}_{in,p(-)}$ and the left(right) states with positive charge density on the left(right) side as antiparticle states $\phi^{(a)}_{in,p(-)}$. Obviously this definition corresponds to the three energy domains. We obtain that particle and antiparticle states coexist only in the energy domain 2. Since this leads to an unstable vacuum state this domain is termed pair creation regime.

The next task is to investigate the normalization and orthogonality of the wave functions. For this purpose let us define the Klein-Gordon inner product which is, up to a factor e, equivalent to the charge, that is the intergral over the charge density (2.16).

$$(\Phi_1, \Phi_2)_{KG} = -i \int d^3x (\Phi_1^* D_0 \Phi_2 - (D_0\Phi_1)^* \Phi_2). \tag{2.18}$$

In ref. [14] the author sketches a proof for the orthogonality of the functions constructed with the above method with respect to the Klein Gordon inner product, i.e.

$$\begin{aligned} (\Phi^{(p,a)}_{in,out,p(\pm)}, \Phi^{(p,a)}_{in,out,p'(\pm)})_{KG} &= \epsilon_{p,a} 2\pi\hbar\delta(p(\pm) - p'(\pm))(2\pi\hbar)^2\delta^{(2)}(p_\perp - p'_\perp) \\ (\Phi^{(p,a)}_{in,out,p(-)}, \Phi^{(p,a)}_{in,out,p'(+)})_{KG} &= 0 \end{aligned} \tag{2.19}$$

where $\epsilon_p = -1$ and $\epsilon_a = 1$.

It will be outlined in chapter 3 that these are the required properties of the solutions of the wave function to get a well defined quantum field theory. However, to calculate these properties explicitly, one has to show that the coefficients in (7.5) in the appendix are uniformly continuous over the

whole energy axis and one has to take into account that the expressions in (2.19) are generalized functions and thus have to be smeared out with test functions. We give an extended version of the proof of ref. [14] using these insights in the appendix of this work.

2.1.2 Ultrarelativistic approximation

In this section we derive the asymptotic properties of the solutions of the Klein-Gordon equation for large energies in the over barrier regime. The comparison with the WKB solutions of equation (2.1) in the same limit shows equivalence up to a phase and a normalization constant.

The WKB solution of (2.1) can be found with the help of ref. [17]. We restrict our considerations to the lowest order and neglect all reflection terms. For an in-propagating state from the left we find

$$\phi_{WKB}(z) = \frac{\sqrt{p(-)}}{\sqrt{\kappa_p(z)}} e^{\frac{i}{\hbar}\int_{-z_0}^{z} d\sigma \kappa_p(\sigma)} e^{-ip(-)z_0} \tag{2.20}$$

where $\kappa_p(x_3) = \sqrt{(\bar{p}_0 - \frac{z}{2})^2 - \mu_\perp^2}$. There is clearly an unspecified phase in this wave function due to the starting point of the integral in the argument of the exponential function. It can be fixed by asymptotic connecting conditions. Here we require the coincedence of the wave function with a plane wave moving from left to the right at the boundary of the acceleration region $z = -z_0$. This corresponds to the identification scheme of ref. [14]. In section II of the z-axis and for large values of p_0 equation (2.20) can be approximated by

$$\phi_{WKB}(z) \approx \frac{\sqrt{p(-)}}{\sqrt{2\bar{p}_0 - z}} \sqrt{2} e^{-\frac{i}{4}(2\bar{p}_0 - z)^2} e^{i\mu_\perp^2 \ln(2\bar{p}_0 - z)} e^{\frac{i}{4}(\bar{p}_0 + z_0)^2} e^{-i\mu_\perp^2 \ln(2\bar{p}_0 + z_0)} e^{-\frac{i}{2} z_0 (2\bar{p}_0 + z_0)}. \tag{2.21}$$

We now investigate the same limit for the exact solutions we constructed in the last chapter with the identification scheme of ref. [14]. Up to a constant factor we get the same result with the identification scheme of ref. [15]. From equation (7.5), (7.2) and (7.1) in Appendix B we obtain that $B(c_L) \approx \frac{n}{k} c_2(c_L) e^{ip(+)z_0} D_{n-1}[-\gamma(2\bar{p}_0 - z_0)] \propto (2\bar{p}_0 - z_0)^{-\frac{3}{2}}$ is strongly decreasing if $\bar{p}_0 \to \infty$ and

$A(c_L) \approx \frac{1}{k} c_2(c_L) e^{ip(+)z_0} D_{n-1}[\gamma(2\bar{p}_0 - z_0)] \propto (2\bar{p}_0 - z_0)^{\frac{1}{2}}$ increases. Thus we only have to calculate $A(b_1)$. For large $\bar{p}_0$ we get with equation (7.1) in the appendix up to the normalization constant b_1 again equation (2.21). This shows directly the correspondence between the semiclassical approximation and the identification schemes of ref. [14] and ref. [15] and all of their linear combinations. The complex phase can be adjusted by changing the starting point of the integration in the exponent in equation (2.20).

2.1.3 Propagation of wave packets

In this section we investigate the propagation of a wave packet in the causal identification scheme of ref. [14]. In what follows we present the results of numerical simulations computed with *Mathematica 6*. In figure 2.4 we have plotted the logarithm ot the wave functions absolute value of in-propagating wave packets in the pair creation and over barrier regime. The system parameters lie above a critical value for pair creation; the Schwinger limit[18]. At this value the interaction with electron-positron field results in a quantum correction term for the energy momentum tensor of the electromagnetic field in the order $\frac{1}{10}$ with respect to the classical value. It is given by

$$E_{crit} = \sqrt{\frac{45}{20} \frac{m^4 c^5}{\hbar^3} \frac{1}{\alpha^2 \epsilon_0}} \approx 10^{19} \frac{\mathrm{V}}{\mathrm{m}}. \tag{2.22}$$

In figure 2.4 one can clearly see the in-propagating packet and the two out-propagating packets; one of the latter with enhanced amplitude. Further interesting features are the small packets on either side of the main packets. These features seem to form at the kinks of the potential located at $\pm z_0$, i.e. they are results of an additional reflection. In contrast to the reflection effect known from optics, which arises from a discontinuity in the particle momentum, the effect caused by the kinks here arises from a discontinuity in the derivative of the particle momentum and therefore is a second order effect.

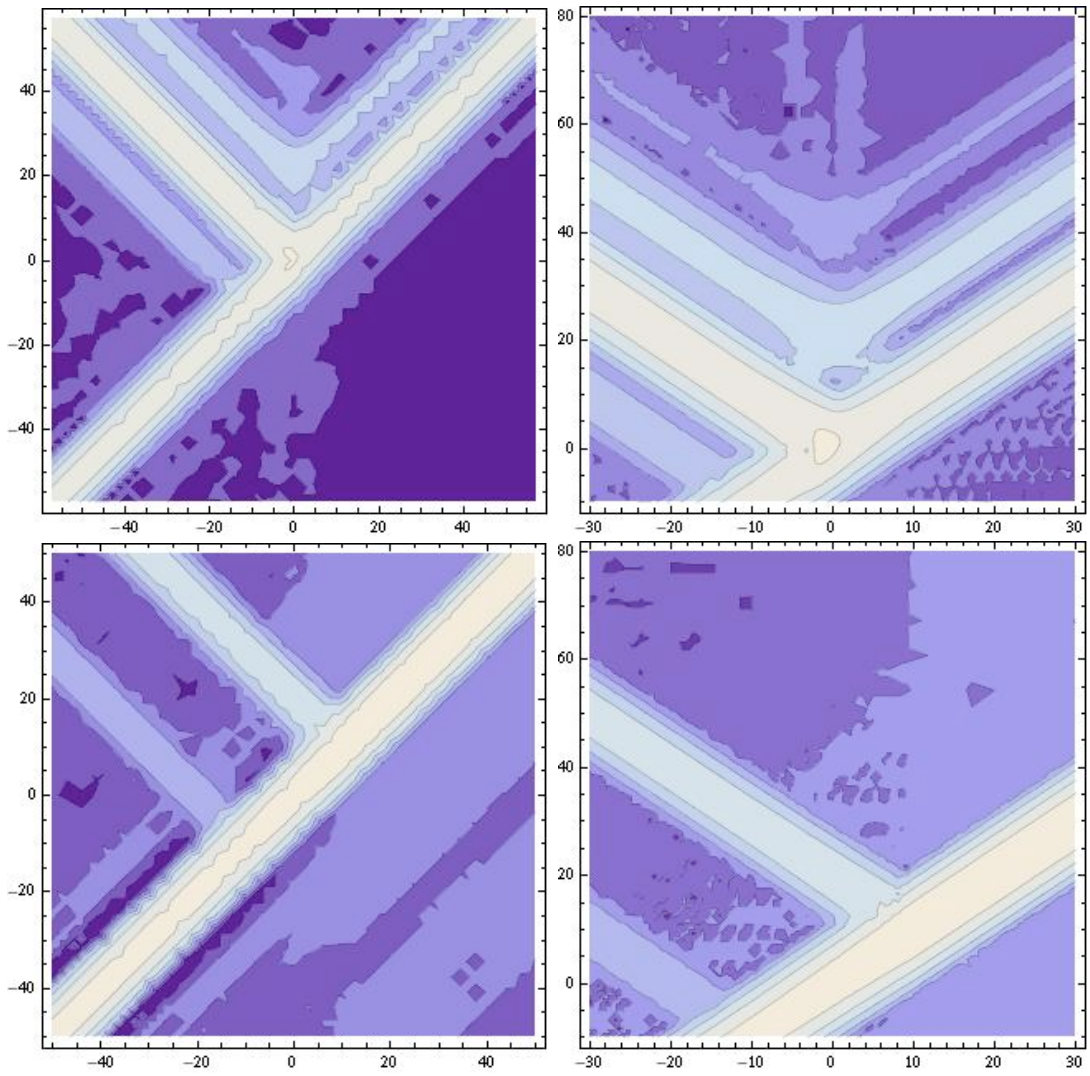

Figure 2.4: Logarithmic contour plot of the absolute value $|\Phi|$ of the wave function of an in-propagating particle wave packet propagating from the left to the right in the pair creation regime (upper left and upper right plot) and in the over barrier regime (lower left and lower right plot) where the left plots differ from the right plots only by the scaling of the axes. The horizontal axis shows the spatial direction z and the vertical axis shows the time t' where z and t' are the dimensionless variables defined in (2.7). The system parameters are $z_0 = 10$ and $\mu = 0.04$. In the pair creation regime we see clearly the antiparticle wave packet propagating to the right. This can be interpreted as the antiparticle part of a pair created at the classical turning point. In all four diagramms one can see the additional wave packets propagating to the right and to the left. The origin of these additional packets are the kinks at $\pm z_0$.

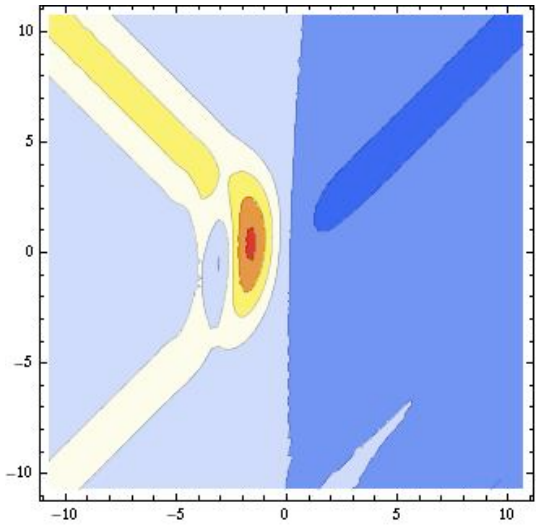

Figure 2.5: Plot of the charge density ρ for the wave function of an in-propagating wave packet propagating from left to right in the pair creation regime. The system parameters are again $z_0 = 10$ and $\mu = 0.04$. Since, in contrast to figure 2.4, this plot's scale is linear the additional reflections at the kinks are not visible.

Despite the fact that one can investigate additional reflection effects effectively, the amplitude we considered in the last passage is not suitable to investigate the pair creation behaviour; it does not consider the charge of the particles and its spatial integral is not a conserved quantity. To get better insight into the pair creation one has to investigate the Klein-Gordon charge density (2.16). In figure 2.5 one can see the charge density for in-propagating particle states from the left in different regimes. The enhanced out-propagating negatively charged wave packet and the additional positively charged wave packet propagating to the right are a manifestation of the pair creation. The quantitative calculation of the pair creation rate is the aim of the next chapter.

2.2 Spinor particles

The Dirac equation is

$$\left[iD_\mu \gamma^\mu - \frac{mc}{\hbar}\right] \Psi = 0 \tag{2.23}$$

As we did for the solution space of the Klein-Gordon equation we use the charge, up to the factor e, as an inner product.

$$(\Psi_1, \Psi_2)_D = -i \int d^3x \Psi_1^\dagger \Psi_2. \tag{2.24}$$

Again $D_\mu = \partial_\mu + i\frac{q}{\hbar}A_\mu$ and A_0 is given by (2.3). Sauter already calculated the solutions of this equation in [19]. To get clearer insight into the solutions we use a slightly different and much simpler ansatz: we calculate the solutions of a quadratic spinor wave equation with a spin transport term and get the solutions of the dirac equation by using a projection operator (see ref. [9], [20] and [21]). We define

$$\Psi =: \left[iD_\mu \gamma^\mu + \frac{mc}{\hbar} \right] Z \tag{2.25}$$

and get the quadratic equation

$$\left[D^\mu D_\mu - i\frac{1}{2}\frac{e}{\hbar c}\gamma^\mu\gamma^\nu F_{\mu\nu} + \frac{m^2c^2}{\hbar^2} \right] Z = 0 \tag{2.26}$$

where $F_{\mu\nu}$ is the field strength tensor of the external electromagnetic field. Equation (2.26) differs from the Klein-Gordon equation (2.1) for each spinor component only by the spin transport term $-i\frac{e}{2}\gamma^\mu\gamma^\nu F_{\mu\nu}$. For a general external electromagnetic field these equations can be decoupled by diagonalization of the spin transport term. To distinguish different spin states we consider the finite extended electric field corresponding to the potential (2.3) superimposed by a magnetic field in x_3-direction. Thus we get

$$-i\frac{1}{2}\gamma^\mu\gamma^\nu F_{\mu\nu} = \begin{pmatrix} B\sigma_3 & -iE\sigma_3 \\ -iE\sigma_3 & B\sigma_3 \end{pmatrix} \tag{2.27}$$

where $\sigma_3 = \begin{pmatrix} 1 & 0 \\ 0 & -1 \end{pmatrix}$ is the third Pauli matrix in the standard representation.

The matrix (2.27) has four eigenvalues $\lambda_{\rho,s} = \rho iE - sB$ where $\rho, s \in \{-1, +1\}$. $\lambda_{\pm 1,+1}$ and $\lambda_{\pm 1,-1}$ correspond to spin up and spin down states in x_3-direction respectively. The corresponding eigenvectors are

$$\Gamma_{-1,-1} = \tfrac{1}{\sqrt{2}} \begin{pmatrix} 1 \\ 0 \\ 1 \\ 0 \end{pmatrix} \qquad \Gamma_{+1,-1} = \tfrac{1}{\sqrt{2}} \begin{pmatrix} 1 \\ 0 \\ -1 \\ 0 \end{pmatrix}$$
$$\Gamma_{-1,+1} = \tfrac{1}{\sqrt{2}} \begin{pmatrix} 0 \\ 1 \\ 0 \\ 1 \end{pmatrix} \qquad \Gamma_{+1,+1} = \tfrac{1}{\sqrt{2}} \begin{pmatrix} 0 \\ 1 \\ 0 \\ -1 \end{pmatrix}. \tag{2.28}$$

Thus, with $Z_{\rho,s} = \phi_{\rho,s}\Gamma_{\rho,s}$ and equation (2.26), we get four independent second order differential equations

$$\left[D^\mu D_\mu + \frac{e}{\hbar c}\lambda_{\rho,s} + \frac{m^2c^2}{\hbar^2} \right] \phi_{\rho,s} = 0. \tag{2.29}$$

We can solve each of these equations in the same way as we did for the Klein-Gordon equation in section 2.1.1. Since we only need the magnetic field for the identification of spin states we set $B = 0$. In section II of diagramm 2.1 we then get an additional ρ-dependent term for the parameter n of the parabolic cylinder function. We define $n(\rho) := i\mu^2 - \frac{1}{2} - \frac{\rho}{2}$. For the identification of in- and out-propagating states we again use their asymptotic properties and the identification scheme of ref. [14]. Thus we obtain solutions like in equation (7.5) and (7.6) where n is replaced by $n(\rho)$ and

$$c^{\,L}_{\,R} = \frac{1}{\sqrt{2\pi_0(\pm)(\pi_0(\pm) + \mu)}} \quad \text{and} \quad c^{\,L}_{\,R} = \frac{1}{\sqrt{2\pi_0(\pm)(\pi_0(\pm) - \mu)}}$$

for particle and antiparticle states respectively.

We get the corresponding solutions of equation (2.23) by using equation (2.25) in the form

$$\tilde{\Psi}_{\rho,s} = \left[iD_\mu \gamma^\mu + \frac{mc}{\hbar} \right] \phi_{\rho,s} \Gamma_{\rho,s}. \tag{2.30}$$

The rank of this projection is two and thus the $4 \times \infty$-dimensional solution space of equation (2.26) is projected onto the $2 \times \infty$-dimensional solution space of equation (2.23). For every pair of values for energy and transversal momentum we get four different solutions, i.e. two for each spin direction and we have to use an additional asymptotic condition to determine our solutions uniquely. In the absence of any background field, i.e. in Minkovski space, we can construct the different spin states by applying the irreducible standard representation of the Lorentz group on the four dimensional vector space of spinors generated by $\sigma^{\mu\nu} = \frac{1}{2}[\gamma^\mu, \gamma^\nu]$ and the solutions of the equations $[\pm\gamma^0 - 1]\,\Psi = 0$ given by

$$\Psi^{(p)}_{-\sigma} = N^{(p)}_{p=0} \begin{pmatrix} u_\sigma \\ \begin{pmatrix} 0 \\ 0 \end{pmatrix} \end{pmatrix} \qquad \Psi^{(a)}_{-\sigma} = N^{(a)}_{p=0} \begin{pmatrix} \begin{pmatrix} 0 \\ 0 \end{pmatrix} \\ u_\sigma \end{pmatrix} \tag{2.31}$$

where $^{(p)}$ denotes a particle and $^{(a)}$ an antiparticle, $N^{(p,a)}_p$ is a normalization constant and

$$u_{+1} = \begin{pmatrix} 1 \\ 0 \end{pmatrix} \qquad u_{-1} = \begin{pmatrix} 0 \\ 1 \end{pmatrix} \tag{2.32}$$

are the eigenvectors of the Pauli matrix σ_3 to the eigenvalue $\sigma = +1$ and $\sigma = -1$ respectively in the standard representation.

We find

$$\Psi^{(p)}_{-\sigma} = N^{(p)}_p \begin{pmatrix} (\tilde{\pi}_0 + \mu) u_\sigma \\ (\vec{\sigma} \cdot \tilde{p}) u_\sigma \end{pmatrix} \qquad \Psi^{(a)}_{-\sigma} = N^{(a)}_p \begin{pmatrix} (\vec{\sigma} \cdot \tilde{p}) u_\sigma \\ (\tilde{\pi}_0 - \mu) u_\sigma \end{pmatrix} \tag{2.33}$$

where $\vec{\sigma} = (\sigma_1, \sigma_2, \sigma_3)$ is the vector of Pauli matrices [1].

[1] For a more detailed presentation of the one particle Dirac theory in Minkovski space see ref. [22] and ref. [23].

As mentioned above for every pair of values for energy and transversal momentum the corresponding subspace of the solution space of the Dirac equation is two dimensional. Thus, in the asymptotic section I and III of the domain, the particle and antiparticle states can be written as linear combinations of the Minkovski space spinor solutions. For particle states we can write

$$\begin{aligned}\tilde{\Psi}_s^{(p)} \begin{pmatrix} z \in I \\ z \in III \end{pmatrix} = \sum_\sigma \Bigg(\begin{pmatrix} (\tilde{\pi}_0(\mp) + \mu) u_\sigma \\ (\sigma \cdot \tilde{p}_-(\mp)) u_\sigma \end{pmatrix} A^{(p)}_{\mp,s,\sigma} e^{-i\tilde{p}(\mp)z} \\ + \begin{pmatrix} (\tilde{\pi}_0(\mp) + \mu) u_\sigma \\ (\sigma \cdot \tilde{p}_+(\mp)) u_\sigma \end{pmatrix} B^{(p)}_{\mp,s,\sigma} e^{i\tilde{p}(\mp)z} \Bigg)\end{aligned} \tag{2.34}$$

and for antiparticle states

$$\begin{aligned}\tilde{\Psi}_s^{(a)} \begin{pmatrix} z \in I \\ z \in III \end{pmatrix} = \sum_\sigma \Bigg(\begin{pmatrix} (\sigma \cdot \tilde{p}_-(\mp)) u_\sigma \\ (\tilde{\pi}_0(\mp) - \mu) u_\sigma \end{pmatrix} A^{(a)}_{\mp,s,\sigma} e^{-i\tilde{p}(\mp)z} \\ + \begin{pmatrix} (\sigma \cdot \tilde{p}_+(\mp)) u_\sigma \\ (\tilde{\pi}_0(\mp) - \mu) u_\sigma \end{pmatrix} B^{(a)}_{\mp,s,\sigma} e^{i\tilde{p}(\mp)z} \Bigg)\end{aligned} \tag{2.35}$$

where $\tilde{p}_\pm(\mp) = (\tilde{p}_1, \tilde{p}_2, \pm\tilde{p}(\mp))$.

Now the missing asymptotic condition can be formulated as the statement that an in-propagating state is represented by a wave function with an in-propagating part with defined spin, that is in the asymptotic regime the in-propagating part of the wave function has to be equivalent to one of the Minkovski space solutions of the Dirac equation with defined spin and defined particle or antiparticle character. We handle the out-propagating states analogously. Using this asymptotic condition the coeffizients $A_{s,\sigma}$ and $B_{s,\sigma}$ can be fixed and, for particle and antiparticle states, we obtain the following

expression:

$$\tilde{\Psi}_s^{(p)} = \frac{1}{2}\left(\tilde{\Psi}_{1,s} + \tilde{\Psi}_{-1,s}\right) \qquad \tilde{\Psi}_s^{(a)} = \frac{1}{2}\left(\tilde{\Psi}_{1,s} - \tilde{\Psi}_{-1,s}\right). \tag{2.36}$$

Full expressions for some of these solutions are given exemplarily in the appendix 7.4. Finally with the inner product (2.24) and after some cumbersome calculations that are mainly equivalent to those for the solutions of the Klein-Gordon equation in Appendix I we get the following orthogonality relations:

$$(\Psi^{(p,a)}_{in,out,(p(\pm),s)}, \Psi^{(p,a)}_{in,out,(p'(\pm),s')})_D = 2\pi\hbar\delta(p(\pm) - p'(\pm))(2\pi\hbar)^2\delta^{(2)}(p_\perp - p'_\perp)\delta_{ss'}$$

$$(\Psi^{(p,a)}_{in,out,p(-)}, \Psi^{(p,a)}_{in,out,p'(+)})_D = 0. \tag{2.37}$$

Chapter 3

Field quantization

The next step on the way to quantum electrodynamics is to go from a one particle to an n-particle theory allowing particle creation and annihilation, with other word we must construct a quantum field theory from the one particle theory. We start with the case of scalar particles. The first task when constructing a quantum field theory is to specify the one particle Hilbert space and construct the Fock space from this. Our construction is closely orientated on the field theory construction outlined in ref. [24] and [25]. Since it is invariant under time evolution and, from a physical point of view, very natural we use the Klein Gordon inner product (2.18) as the inner product for our one particle Hilbert space. It must be mentioned, however, that the term "inner product" is misleading, since it is not positive definite. We must first split the solution space S of the Klein Gordon equation (2.1) to construct a positive definite inner product. The normalization in chapter 2 gives us the required splitting condition. We define $A_{in,out}$ as the set of in- and out-propagating functions respectively which we constructed in chapter 2 and perform the split

$$\mathcal{A}^{\pm}_{in,out} := \{f \in \mathcal{A}_{in,out} : (f,f)_{KG} \gtrless 0\}. \tag{3.1}$$

As outlined in chapter 2 this is equivalent to the decomposition into particle and antiparticle states.

The next step is to construct two separate inner product spaces from $\mathcal{A}^{\pm}_{in,out}$. We define the linear

space

$$\tilde{\mathcal{S}}^{\pm}_{in,out} := \{ \sum_{n}^{finite} \lambda_n f_n : f_n \in \mathcal{A}^{\pm}_{in,out}, \lambda_n \in \mathbb{C}\} \tag{3.2}$$

and a scalar product on it by the definition

$$\langle f, g\rangle_{\pm} := \pm(f, g)_{KG} \quad \text{for} \quad f, g \in \tilde{\mathcal{S}}^{\pm}_{in,out}. \tag{3.3}$$

Since this is positive definite we get a pre-Hilbert, or inner product, space.

$$\tilde{\mathcal{H}}^{\pm}_{in,out} := \left(\tilde{\mathcal{S}}^{\pm}_{in,out}, \langle\cdot,\cdot\rangle_{\pm}\right) \tag{3.4}$$

Now we need a metric on $\tilde{\mathcal{S}}^{\pm}_{in,out}$ to complete the pre-Hilbert space to a Hilbert space. One usually uses the metric induced by

$$g(f, g) := \langle f - g, f - g\rangle. \tag{3.5}$$

Unfortunately our inner product is not finite for every element of $\tilde{\mathcal{S}}^{\pm}_{in,out}$. Since these unnormalizable states cannot exist in quantum mechnics we have to smear out the elements of $\tilde{\mathcal{S}}^{\pm}_{in,out}$ with appropriate smearing functions to get physical states. Due to this physical argument we go on with our construction assuming that the elements of $\tilde{\mathcal{S}}^{\pm}_{in,out}$ are normalizable[1].

By cauchy completion we get a complete space $\mathcal{H}^{\pm}_{in,out} := \left(\mathcal{S}^{\pm}_{in,out}, \langle\cdot,\cdot\rangle\right)$ and by factorizing out the kernel of the product $\langle\cdot,\cdot\rangle$ we get a Hilbert space, that is a complete inner product space with positive definite inner product, with $\tilde{\mathcal{S}}^{\pm}_{in,out}$ as a dense subset. $\mathcal{H}^{\pm}_{in,out}$ is the one particle Hilbert that we require to define a Fock space. With the help of the symmetrization operators $P^{+}_{n}\phi_n = \frac{1}{n!}\sum_{\pi}\phi_n(x_{\pi 1}, ..., x_{\pi n})$ with $\phi_n \in (\mathcal{H}^{\pm})^{\otimes n}$ we define

$$\mathcal{F}^{\pm}_{B} := \{\alpha\Omega : \alpha \in \mathbb{C}\} \oplus_{n=1}^{\infty} P^{+}_{n}\left((\mathcal{H}^{\pm})^{\otimes n}\right) \tag{3.6}$$

[1]It should be possible to give a mathematically clear construction by using the theory of generalized functions [26]

where Ω is the vacuum state. We call $\mathcal{F}_B^+$ the particle Fock space and $\mathcal{F}_B^-$ the antiparticle Fock space.

The next step on the way to a quantum field theory is to define creation and annihilation operators. We define the creation operator $c^\dagger_{in,out}$ as a linear map from the one particle Hilbert space to the space of linear operators on the Hilbert space, i.e.

$$\begin{aligned} c^\dagger_{in,out}: \quad \mathcal{H}_{in,out} &\to \mathcal{L}(\mathcal{F}_B) \\ f &\mapsto c^\dagger_{in,out}(f) \end{aligned} \quad \text{where} \quad c^\dagger(f)\Omega = f$$

$$\text{with} \quad (c^\dagger(f)\Phi)_n(x_1,...,x_n) = \sqrt{n}P_n^+(f(x_1)\phi_{n-1}(x_2,...,x_n)),\ n=1,2,... \quad \text{and} \tag{3.7}$$

$$\begin{aligned} c_{in,out}: \quad \mathcal{H}_{in,out} &\to \mathcal{L}(\mathcal{F}_B) \\ f &\mapsto c_{in,out}(f) \end{aligned} \quad \text{where} \quad c^\dagger(f)\Omega = 0$$

$$\text{with} \quad (c(f)\Phi)_n(x_1,...,x_n) = \sqrt{n+1}\int d^3x f^*(x)\phi_{n+1}(x,x_1,...,x_n),\ n=1,2,...$$

With these definitions we get, after some calculations [25], the commutation relations

$$\begin{aligned} [c_{in,out}(f), c^\dagger_{in,out}(g)] &= \langle f,g\rangle, \\ [c_{in,out}(f), c_{in,out}(g)] &= 0. \end{aligned} \tag{3.8}$$

In [25] the author proves that every irreducible representation of the commutation relations (3.8) with vacuum Ω is unitary equivalent to the Fock representation constructed in (3.6). Thus by defining creation and annihilation operators for the particle and antiparticle Fock space and by defining the total Fock space $\mathcal{F}_B := \mathcal{F}_B^+ \otimes \mathcal{F}_B^-$ we get a well defined many particle theory. Finally we define the

field operator

$$\begin{aligned}\Psi(x) &= \int \tfrac{d^2p_\perp}{4\pi^2\hbar^2} \sum_{d\in\{+,-\}} \int_0^\infty \tfrac{dp(d)}{2\pi\hbar} \left(a_{in}(p(d),p_\perp)\Phi^{(p)}_{in,p(d)} + b^\dagger_{in}(p(d),p_\perp)\Phi^{(a)}_{in,p(d)} \right) \\ &= \int \tfrac{d^2p_\perp}{4\pi^2\hbar^2} \sum_{d\in\{+,-\}} \int_0^\infty \tfrac{dp(d)}{2\pi\hbar} \left(a_{out}(p(d),p_\perp)\Phi^{(p)}_{out,p(d)} + b^\dagger_{out}(p(d),p_\perp)\Phi^{(a)}_{out,p(d)} \right)\end{aligned} \tag{3.9}$$

where the $a_{in}(p(-),p\perp) = a(\Phi^{(p)}_{in,p(d)})$ and the $b^\dagger_{in}(p(-),p\perp) = b^\dagger(\Phi^{(a)}_{in,p(d)})$ are the particle annihilation and antiparticle creation operators respectively.

To argue that this is the correct form of the field operator and to get the unitary, dynamic time evolution operator we use the decomposed field operator to expand the Hamiltonian in terms of creation and annihilation operators. The Lagrangian density for the charged Klein-Gordon field is given by

$$\mathcal{L} = \hbar c \left((D_\mu \Psi)^* D^\mu \Psi - \frac{m^2c^2}{\hbar^2} \Psi^* \Psi \right). \tag{3.10}$$

After some rearrangements we find

$$H = \hbar c \int d^3x \left(\partial_0 \Psi^* \partial_0 \Psi - e^2 A_0^2 \Psi^* \Psi + \frac{m^2c^2}{\hbar^2} \Psi^* \Psi + (D_i \Psi)^* D_i \Psi \right). \tag{3.11}$$

Since we do not want to vary this Hamiltonian to get some equations of motion we are free to confine Ψ as a linear combination of solutions of the Klein-Gordon equation (2.1). By using the Klein-Gordon equation, partial integration and the definition of the Klein-Gordon inner product (2.18) we get for the Hamiltonian

$$H = \frac{i\hbar}{2}((\dot{\Psi}, \Psi)_{KG} - (\Psi, \dot{\Psi})_{KG}). \tag{3.12}$$

Using equation (3.9) we arrive at

$$
\begin{aligned}
: H := c \int \tfrac{d^2 p_\perp}{(2\pi\hbar)^2} \sum_{d\in\{+,-\}} \int_0^\infty \tfrac{dp(d)}{2\pi\hbar} \quad \Big(& p_0^{(p)} a_{in}^\dagger(p(d), p_\perp) a_{in}(p(d), p_\perp) \\
& - p_0^{(a)} b_{in}^\dagger(p(d), p_\perp) b_{in}(p(d), p_\perp) \Big)
\end{aligned}
\tag{3.13}
$$

where : : denotes normal ordering.

With the commutation relation for the creation and annihilation operators $[a_p, a_{p'}^\dagger] = [b_p, b_{p'}^\dagger] = (2\pi\hbar)^3 \delta(p - p')$ the Hamiltonian (3.13) gives the correct time evolution for the field operator, that is it fulfills Heisenberg's equation of motion.

$$
\left.\frac{\Psi(\mathbf{x}, t)}{dt}\right|_{t=0} = \frac{i}{\hbar}[H, \Psi(\mathbf{x}, 0)] \tag{3.14}
$$

Another way of constructing the Hamiltonian (3.13) is to use the one particle Hamiltonian. For a time independent potential A_μ we get from the Klein-Gordon equation (2.1)

$$
i\hbar \frac{\partial}{\partial t}\varphi = \left[c\sqrt{D_i D^i + m^2 c^2} - ecA_0 \right] \varphi =: H_{KG}\varphi \tag{3.15}
$$

where i runs from one to three. Obviously this Hamiltonian is diagonal in the basis of solutions of the Klein-Gordon equation with defined momentum p_i, i.e. $\phi_{p(\pm),p_\perp}$ is a eigenstate of H to the eigenvalue

$$
p_0 = c\sqrt{(p(\pm) - eA_3(\pm))^2 + (p_\perp - eA_\perp)^2 + m^2 c^2} - ecA_0(\pm) \tag{3.16}
$$

where $(-)$ denotes left states and $(+)$ denotes right states and the corresponding asymptotic values of momentum and potential. By using n copies of the Hamiltonian H_{KG} we get the time evolution of each n particle sector of the Fock space. By summing these sector Hamiltonians we find the

Hamiltonian for the whole Fock space as

$$(\mathbf{H}_F\Phi)_n = \sum_{j=1}^{n} 1 \otimes ... \otimes \underset{j}{H} \otimes ... \otimes 1\phi_n.$$

The effect of this operator on an element of the Fock space is the same as the effect of the Hamiltonian (3.13) and thus they represent the same operator.

The construction of the second quantized theory for the spinor particles is mostly the same up to some facts: firstly the natural inner product (2.24) is positive definite and can be used directly and secondly we have a Hamiltonian for the one particle theory and thus can use n copies of it for the time evolution in every n particle sector of the Fock space. The main difference in the results is that we have anticommutation relations instead of commutation relations for the creation and annihilation operators (see ref. [25]). We obtain

$$\begin{aligned}
\{a_{in,out}(f), a^{\dagger}_{in,out}(g)\} &= (P_+ f, P_+ g)_D \\
\{b_{in,out}(f), b^{\dagger}_{in,out}(g)\} &= (P_- f, P_- g)_D \\
\{b_{in,out}(f), b_{in,out}(g)\} &= \{a_{in,out}(f), a_{in,out}(g)\} = 0 \\
\{a_{in,out}(f), b_{in,out}(g)\} &= 0
\end{aligned} \tag{3.17}$$

where P_+ and P_- are the projectors on the particle and antiparticle subspace of the one particle Hilbert space respectively. For the field operator we simply obtain equation (3.9) extended by the spin degree of freedom and summed over the two spin directions.

Chapter 4

Electron-positron pair creation

In the last chapter we outlined the construction of a quantum field theory from a one particle quantum theory. Since the definition of states in chapter II was ambiguous in the sense that we had in- and out-propagating states we get an ambiguous definition of the vacuum state. This fact can be interpreted as an instability of the vacuum; the state associated with the vacuum before the external potential is turned on differs from the state associated with the vacuum after the external potential is turned off. There are particles and antiparticles created by the action of the external potential. Obviously this description of pair creation contains no dynamics. While the interpretation of the Fock space element representing the state of the system changes the Fock space element itself stays the same. Hence we can conclude that the total charge which is given by the inner product, up to a factor e, is a conserved quantity and thus the particles and antiparticles are created in pairs with a zero total charge. Deriving the corresponding pair creation rate is the task of this chapter.

In the first subsection we derive and investigate the pair creation rate for scalar particles. We show that it is the same for both indentification schemes presented in the diagrams 2.2 and 2.3, show a numerical calculation for the momentum distribution of the produced particles and calculate exact expressions for some limiting cases. In the second subsection we derive the pair creation rate for spinor particles and again show plots of the numerically calculated momentum distribution.

4.1 Scalar particles

To find the pair creation rate we have to derive relations between the creation and annihilation operators of the Fock space of in- and out-propagating states constructed in the last chapter. These relations are called Bogoliubov transformations. To derive them we project the field operator, expanded in terms of the out-propagating states, onto the in-propagating states by using the Klein-Gordon inner product. In other words $(\Phi^{(p,a)}_{in,p(\pm)}, \Psi)_{KG}$ gives us the wanted relations. As an example by projecting onto $\Phi^{(p)}_{in,p(\pm)} = \phi^{(p)}_{in,p(\pm)} e^{ip_\perp x_\perp - ip_0^{(p)}(p(\pm),p_\perp)t}$ we obtain

$$\begin{aligned} a_{in}(p(\pm),p_\perp) = \int \tfrac{d^2p_\perp}{4\pi^2\hbar^2} \textstyle\sum_{d\in\{+,-\}} \int_0^\infty \tfrac{dp(d)}{2\pi\hbar} \Big(a_{out}(p(d),p_\perp) \left(\Phi^{(p)}_{in,p(\pm)}, \Phi^{(p)}_{out,p(d)}\right)_{KG} \\ + b^\dagger_{out}(p(d),p_\perp) \left(\Phi^{(p)}_{in,p(\pm)}, \Phi^{(a)}_{out,p(d)}\right)_{KG} \Big) . \end{aligned} \tag{4.1}$$

From the definition of the wave functions in chapter II, especially from the diagrams in figure 2.2 and following Nikishov [14], we come to the conclusion that functions $\alpha(p_0,p_\perp)$ and $\beta(p_0,p_\perp)$ exist such that

$$\phi_{in,p(-)(p_0)} = -\alpha(p_0,p_\perp)\phi_{out,p(-)(p_0)} + \beta(p_0,p_\perp)\phi_{out,p(+)(p_0)} \tag{4.2}$$

where it depends on the energy range whether the states are particle or antiparticle states. From now on we write α_p and β_p instead of $\alpha(p_0,p_\perp)$ and $\beta(p_0,p_\perp)$ to keep the notation as clean as possible. By complex conjugation of eqation (4.2) we find

$$\phi_{out,p(-)(p_0)} = -\alpha^*_p\phi_{in,p(-)(p_0)} + \beta^*_p\phi_{in,p(+)(p_0)} \tag{4.3}$$

From the normalization conditions (2.19) and equation (4.2) we conclude

$$|\alpha|^2 + \epsilon|\beta|^2 = 1 \tag{4.4}$$

where ϵ is $+1$ for domain 1 and domain 3 and -1 for domain 2 of the energy axis. This gives us, with equations (4.2) and (4.3), the following transformation rules:

$$\begin{aligned}
\phi_{in,p(-)(p_0)} &= -\alpha_p \phi_{out,p(-)(p_0)} + \beta_p \phi_{out,p(+)(p_0)}, \\
\phi_{in,p(+)(p_0)} &= \epsilon \beta_p \phi_{out,p(-)(p_0)} + \tfrac{\alpha_p^* \beta_p}{\beta_p^*} \phi_{out,p(+)(p_0)}, \\
\phi_{out,p(-)(p_0)} &= -\alpha_p^* \phi_{in,p(-)(p_0)} + \beta_p \phi_{in,p(+)(p_0)}, \\
\phi_{out,p(+)(p_0)} &= \epsilon \beta_p^* \phi_{in,p(-)(p_0)} + \tfrac{\alpha_p \beta_p^*}{\beta_p} \phi_{in,p(+)(p_0)}.
\end{aligned} \tag{4.5}$$

Hence the transformation between in and out states is confined to a subspace given by p_0. We can now use this insight to simplify equation (4.1) and derive the remaining transformations. Again it is necessary to investigate the three energy domains seperately. Like mentioned earlier the transformations are between creation and annihilation operators at the same energy p_0, that is $p(+)$ and $p(-)$ belong to the same p_0.

Section 1 ($p_0 < -\frac{z_0}{2}$)**:** **under barrier regime**

$$\begin{aligned}
b^\dagger_{out}(p(-), p_\perp) &= -\alpha_p b^\dagger_{in}(p(-), p_\perp) + \beta_p b^\dagger_{in}(p(+), p_\perp) \\
b^\dagger_{out}(p(+), p_\perp) &= \beta_p b^\dagger_{in}(p(-), p_\perp) + \tfrac{\alpha_p^* \beta_p}{\beta_p^*} b^\dagger_{in}(p(+), p_\perp)
\end{aligned} \tag{4.6}$$

Section 2 ($-\frac{z_0}{2} \leq p_0 \leq \frac{z_0}{2}$)**:** **pair creation regime**

$$\begin{aligned}
a_{out}(p(-), p_\perp) &= -\alpha_p a_{in}(p(-), p_\perp) - \beta_p b^\dagger_{in}(p(+), p_\perp) \\
b^\dagger_{out}(p(+), p_\perp) &= \beta_p a_{in}(p(-), p_\perp) + \tfrac{\alpha_p^* \beta_p}{\beta_p^*} b^\dagger_{in}(p(+), p_\perp)
\end{aligned} \tag{4.7}$$

Section 3 ($\frac{z_0}{2} < p_0$)**:** **over barrier regime**

$$\begin{aligned}
a_{out}(p(-), p_\perp) &= -\alpha_p a_{in}(p(-), p_\perp) + \beta_p a_{in}(p(+), p_\perp) \\
a_{out}(p(+), p_\perp) &= \beta_p a_{in}(p(-), p_\perp) + \tfrac{\alpha_p^* \beta_p}{\beta_p^*} a_{in}(p(+), p_\perp)
\end{aligned} \tag{4.8}$$

With these expressions we can derive a relation between the in and the out vacua and give an

expression for the pair creation rate by transforming the particle number operator $N = \int d\mu(p)\, a_p^\dagger a_p$ and calculating its expectation value in the vacuum state. Obviously there are no pairs created in sections 1 and 3. For the out vacuum we get [12]

$$|vac\rangle_{out} = Z^{-1/2} e^{\int \frac{d^3p}{(2\pi\hbar)^3} \left(-\frac{\beta_p}{\alpha_p}\right) a_{in}^\dagger(p) b_{in}^\dagger(p)} |vac\rangle_{in} \tag{4.9}$$

where the integral in the exponent runs over the pair creation regime and Z is a normalization constant. To get an expression for the pair creation rate we only have to consider section 2. We obtain with equation (4.7)

$$\begin{aligned} \langle \Omega \mid N^{(p)} \mid \Omega \rangle &= \langle \Omega \mid \int d\mu(p)\, a_{out}^\dagger(p(-), p_\perp) a_{out}(p(-), p_\perp) \mid \Omega \rangle \\ &= \langle \Omega \mid \int d\mu(p)\, |\beta_p|^2 b_{in}(p(+), p_\perp) b_{in}^\dagger(p(+), p_\perp) \mid \Omega \rangle \\ &= \int d\mu(p)\, |\beta_p|^2 (2\pi\hbar)^3 \delta^{(3)}(p - p) \end{aligned} \tag{4.10}$$

where the sum in equation (4.10) runs over domain 2 of the energy axis. To get the pair creation rate, that is the number of created particles per unit time and area in the x_1-x_2-plane, we have to

make the following rearrangements:

$$\begin{aligned} d\mu(p)\,(2\pi\hbar)^3\delta^{(3)}(p-p) &= \tfrac{dp_\perp}{(2\pi\hbar)^2}\tfrac{dp(-)}{2\pi\hbar}(2\pi\hbar)^3\delta^{(2)}(p_\perp-p_\perp)\delta(p(-)-p(-)) \\ &= \tfrac{dp_\perp}{(2\pi\hbar)^2}\tfrac{dp_0}{2\pi\hbar}(2\pi\hbar)^3\delta^{(2)}(p_\perp-p_\perp)\delta(p_0-p_0) \\ &= \tfrac{dp_\perp}{(2\pi\hbar)^2}\tfrac{dp_0}{2\pi\hbar}\lim_{L\to\infty}\lim_{\Delta p_\perp\to 0}\textstyle\int_{-\frac{L}{2}}^{\frac{L}{2}} dx_1\times \\ &\quad \times\textstyle\int_{-\frac{L}{2}}^{\frac{L}{2}} dx_2 e^{i\frac{\Delta p_\perp}{\hbar}x_\perp}\lim_{T\to\infty}\lim_{\Delta p_0\to 0} c\int_{-\frac{T}{2}}^{\frac{T}{2}} dt\, e^{i\frac{c\Delta p_0}{\hbar}t} \\ &= \lim_{L\to\infty}\lim_{T\to\infty} cTL^2\tfrac{dp_\perp}{(2\pi\hbar)^2}\tfrac{dp_0}{2\pi\hbar} \end{aligned} \tag{4.11}$$

We obtain for the pair creation rate

$$R := c\int\frac{dp_\perp}{(2\pi\hbar)^2}\int\frac{dp_0}{2\pi\hbar}\,|\beta_p|^2. \tag{4.12}$$

This expression gives the number of antiparticles emitted to the right and the number of particles emitted to the left per unit time.

An expression for the coefficient β_p can be calculated from the wave functions constructed in chapter one and the relations (4.5). In section III of the z-axis we find

$$\tfrac{1}{\beta_p}\phi_{in,p(-)(p_0)} + \tfrac{\alpha_p}{\beta_p}\phi_{out,p(-)(p_0)} = \phi_{out,p(+)(p_0)}$$

$$\begin{aligned} lhs &= \tfrac{1}{\beta_p}c_2^p(c_L^p)e^{-ip(+)z} + \tfrac{\alpha_p}{\beta_p}c_2^{p*}(c_L^p)e^{ip(+)z} \\ rhs &= c_R^p e^{-ip(+)z} + c_2^{p*}(c_R^p)e^{ip(+)z} \end{aligned} \tag{4.13}$$

Since the connection conditions and the coefficients in section III uniquely determine the wave func-

tion in its entire domain we get with (7.5) and (7.6) and with $sgn\, p(-) = 1$ and $sgn\, p(+) = -1$ the expression

$$\beta_p = \frac{c_2^p(c_L^p)}{c_R^p} = \sqrt{\frac{\pi_0(+)}{\pi_0(-)}} \frac{2ip(-)ke^{-i(p(-)-p(+))z_0}}{A - ip(+)B + ip(-)C + p(+)p(-)D} \tag{4.14}$$

Now in order to compare 4.14 with equation (4.12) we must derive the pair creation rate for the identification scheme of ref. [15]. From the digrams in figure 2.2 and 2.3 we find simple relations between the wave functions constructed with the identification scheme of ref. [14] and ref. [15]. We denote the latter with a prime.

$$\begin{aligned} \phi'_{in,p(-)(p_0)} &= \phi_{out,p(+)(p_0)} \qquad & \phi'_{out,p(-)(p_0)} &= \phi_{in,p(+)(p_0)} \\ \phi'_{in,p(+)(p_0)} &= \phi_{out,p(-)(p_0)} \qquad & \phi'_{out,p(+)(p_0)} &= \phi_{in,p(-)(p_0)} \end{aligned}$$

Thus in the pair creation regime domain 2 we arrive at

$$\begin{aligned} a_{in}(p(-),p_\perp)' &= b^\dagger_{out}(p(+),p_\perp) \qquad & a_{out}(p(-),p_\perp)' &= b^\dagger_{in}(p(+),p_\perp) \\ b^\dagger_{in}(p(+),p_\perp)' &= a_{out}(p(-),p_\perp) \qquad & b^\dagger_{out}(p(+),p_\perp)' &= a_{in}(p(-),p_\perp). \end{aligned} \tag{4.15}$$

With the relations (4.7) we derive

$$a_{out}(p(-),p_\perp)' = \tfrac{\alpha_p\beta_p^*}{\beta_p} a_{in}(p(-),p_\perp)' + \beta_p^* b^\dagger_{out}(p(+),p_\perp)'. \tag{4.16}$$

Obviously the number of particles in the vacuum is $\langle \Omega \mid N^{(p)} \mid \Omega \rangle = \sum_p |\beta_p|^2$. Therefore the pair creation rate is the same for both identification schemes.

With equations (4.12) and (4.14) we are able to evaluate the pair creation rate. In figure 4.1 we plotted the distribution of pairs for special values of the system parameters above the Schwinger limit (2.22). One can see that there are maxima near the interval boundary of possible values for the longitudinal momentum p_3 and that the distribution clearly shows oszillations. These effects are caused by the finite size of the pair creation regime and thus by the finite extension of the electric

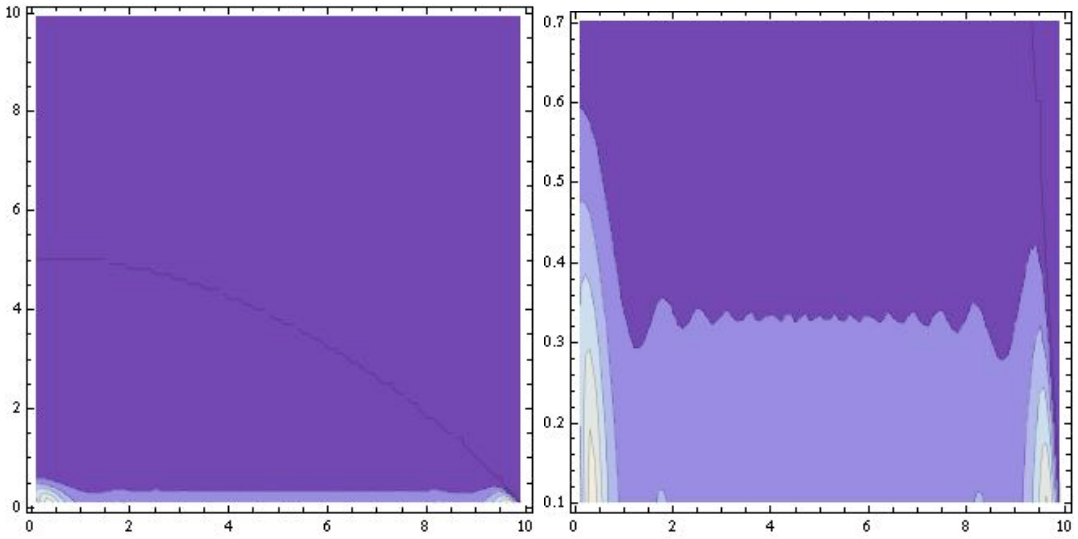

Figure 4.1: Contour plot of the absolute value $|\beta|$. The horizontal axis shows the momentum transversal to the direction of the electric field $\tilde{p}_\perp$. The vertical axis shows the longitudinal momentum $\tilde{p}_3$. $\tilde{p}_\perp$ and $\tilde{p}_3$ are the dimensionless variables defined in (2.7). The system parameters are $z_0 = 10$ and $\mu = 0.04$. Pair creation is possible only in the domain under the dark blue line since for the potential difference the condition $z_0 > 2\mu_\perp^2 = 2(\mu^2 + \tilde{p}_\perp^2)$ must be fulfilled. There are maxima near the margin of the interval of possible values for the longitudinal momentum $\tilde{p}_3$. The flow of created particles is formed like a beam in x_3-direction.

field. Since the extension of the electric field was chosen to be very small for the numerical calculation illustrated in figure 4.1 these oszillations are strongly enhanced. Furthermore, we obtain that, since the pair creation rate strongly decreases for increasing transversal momentum, the flow of created particles is formed like a beam in x_3-direction.

For analytical results we must restrict our investigations to certain limits as the expressions for β are very cumbersome and cannot be presented in a useful closed form. Here we consider the limiting case of the potential step ($x_{3,0} \to 0$, $eEx_{3,0} = const.$), the infinitely extended uniform potential ($x_{3,0} \to \infty$) and the limit of a massless Klein-Gordon field.

We start with the limit of a potential step, that is $x_{3,0} \to 0$, $eEx_{3,0} = const.$ From (4.18) and an expansion of $D_n[z]$ at $z = 0$ [27] we find

$$|\beta_p|^2 = \frac{4p(-)^2}{(p(-) - p(+))^2} \frac{\pi_0(+)}{\pi_0(-)}. \tag{4.17}$$

This expression is, up to the factor $\frac{\pi_0(+)}{\pi_0(-)}$, equivalent to the result calculated by Hund [28] and reinvestigated by ref. [15]. This factor arises from the normalization of the wave modes. The autors of [28] and [15] normalize the current along the x_3 axis to one whereas we instead normalize the charge to one. This dependence on the normalization is to be expected since the pair creation rate obviously depends on how we define a particle. To get a unique, and much more meaningful, result we have to use wave packet states with charge $\pm e$ instead of momentum eigenstates $|p\rangle$. We present such wave packet states in chapter 5.

The next limit we investigate is the infinite extention of the potential. Here we use asymptotic expansions of the parabolic cylinder functions in equation (7.1) in section 7.1 in the appendix which can be found in [10] and [27]. For a very large z_0 in comparison to $\mu_\perp$ we arrive at

$$R = c \int \frac{d^2p_\perp}{4\pi\hbar^2} \int_{-\frac{eE}{c}x_{3,0}}^{\frac{eE}{c}x_{3,0}} \frac{dp_0}{2\pi\hbar} e^{-2\pi \frac{m_\perp^2 c^4}{2eE\hbar c}} = \frac{(eE)^2 x_{3,0}}{2\pi^3 c\hbar^2} e^{-2\pi \frac{m^2 c^4}{2eE\hbar c}}. \tag{4.18}$$

A classical particle in an infinitely extended uniform electric field would be uniformly accelerated by

$a = \frac{-eE}{m}$. Hence the result (4.18) seems to be closely related to the Unruh Effect [29].

The last limit we investigate is that of the massless case. From (4.18) we obtain that in the limit $z_0 \to \infty$ the pair creation rate becomes $R = \frac{(eE)^2 x_{3,0}}{2\pi^3 c\hbar^2}$.

We see that the finite size effects emerging in figure 4.1 vanish in all these limiting cases.

4.2 Spinor particles

By projecting the field operator with the inner product (2.24) onto an in-propagating state we can work out some relations like equation (4.7). First of all we have to state some relations similar to the equations in (4.5). In the spinor case for every value of momentum and energy there are two different spin states and thus the equations are slightly inflated. We write

$$\begin{aligned}\tilde{\Psi}^{(a)}_{-1,out,p(+)(p_0)} &= \alpha_{p,-1,-1}\tilde{\Psi}^{(p)}_{-1,in,p(-)(p_0)} + \beta_{p,-1,-1}\tilde{\Psi}^{(p)}_{-1,out,p(-)(p_0)} \\ &+\alpha_{p,+1,-1}\tilde{\Psi}^{(p)}_{+1,in,p(-)(p_0)} + \beta_{p,+1,-1}\tilde{\Psi}^{(p)}_{+1,out,p(-)(p_0)} \\ \tilde{\Psi}^{(a)}_{+1,out,p(+)(p_0)} &= \alpha_{p,-1,+1}\tilde{\Psi}^{(p)}_{-1,in,p(-)(p_0)} + \beta_{p,-1,+1}\tilde{\Psi}^{(p)}_{-1,out,p(-)(p_0)} \\ &+\alpha_{p,+1,+1}\tilde{\Psi}^{(p)}_{+1,in,p(-)(p_0)} + \beta_{p,+1,+1}\tilde{\Psi}^{(p)}_{+1,out,p(-)(p_0)}.\end{aligned} \tag{4.19}$$

After some rearrangements and by projection with the inner product we find

$$\begin{aligned}b^{\dagger}_{-1,out}(p(+),p_\perp) &= \alpha'_{-1,-1}a_{-1,in}(p(-),p_\perp) + \alpha'_{-1,+1}a_{+1,in}(p(-),p_\perp) \\ &+\beta'_{-1,-1}b^{\dagger}_{-1,in}(p(+),p_\perp) + \beta'_{-1,+1}b^{\dagger}_{+1,in}(p(+),p_\perp),\end{aligned} \tag{4.20}$$

$$\begin{aligned}\alpha'_{-1,-1} &= \frac{-\alpha_{p,-1,+1}}{\alpha_{p,+1,+1}\alpha_{p,-1,-1} - \alpha_{p,-1,+1}\alpha_{p,+1,-1}} \\ \alpha'_{-1,+1} &= \frac{\alpha_{p,+1,+1}}{\alpha_{p,+1,+1}\alpha_{p,-1,-1} - \alpha_{p,-1,+1}\alpha_{p,+1,-1}}\end{aligned} \tag{4.21}$$

and $\beta'_{-1,\pm1}$ can be disregarded since terms with $b^\dagger_{\pm1,in}(p(+),p_\perp)$ obviously do not contribute to the expectation value of the particle number operator.

Thus for the pair creation rate of spinor particles with spin antiparallel to the electric field we obtain

$$R_{-1} = c\int \frac{dp_\perp}{(2\pi\hbar)^2}\int \frac{dp_0}{2\pi\hbar}\left(|\alpha'_{-1,-1}|^2 + |\alpha'_{-1,+1}|^2\right). \tag{4.22}$$

Analogously we get for the other spin orientation

$$R_{+1} = c\int \frac{dp_\perp}{(2\pi\hbar)^2}\int \frac{dp_0}{2\pi\hbar}\left(|\alpha'_{+1,-1}|^2 + |\alpha'_{+1,+1}|^2\right). \tag{4.23}$$

and

$$\begin{aligned}\alpha'_{+1,-1} &= \frac{-\alpha_{p,+1,-1}}{\alpha_{p,+1,+1}\alpha_{p,-1,-1}-\alpha_{p,-1,+1}\alpha_{p,+1,-1}}\\ \alpha'_{+1,+1} &= \frac{\alpha_{p,-1,-1}}{\alpha_{p,+1,+1}\alpha_{p,-1,-1}-\alpha_{p,-1,+1}\alpha_{p,+1,-1}}.\end{aligned} \tag{4.24}$$

As in the scalar case the coefficients in equation (4.19) can be calculated directly from the representation of the wave functions. We give explicit expressions in section 7.5 in the appendix.

We obtain that the pair creation rate is the same for both spin orientations. Figure 4.2 is a plot of the resulting distribution of created pairs for system parameters above the Schwinger limit (2.22). It significantly differs from the corresponding distribution in the scalar case, here the pair creation rate increases for a small and decreasing momentum p_3 and decreases for a large and increasing momentum. Thus the oscillations are hardly apparent although they are present as in the scalar case.

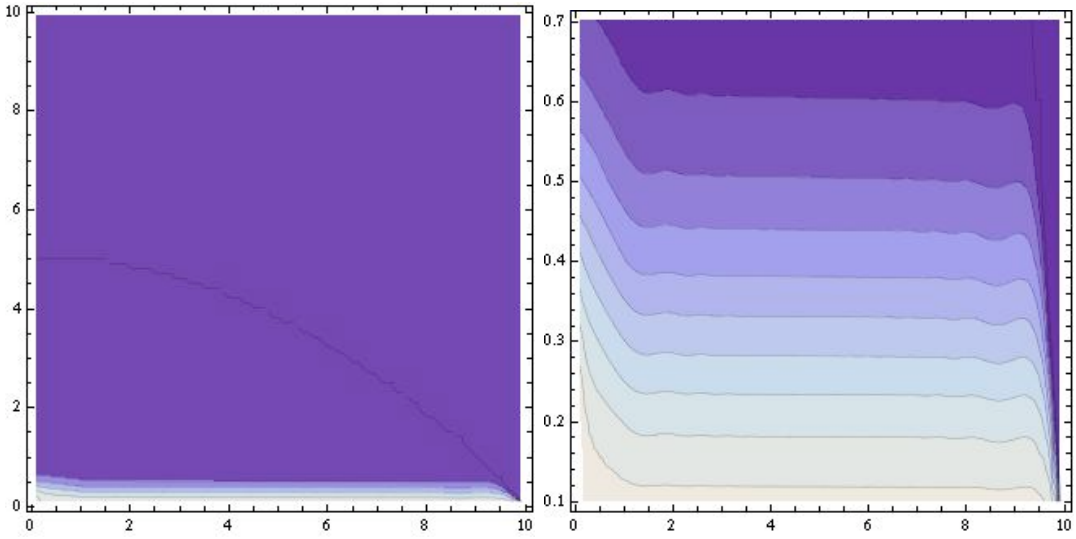

Figure 4.2: Contour plot of the absolute value $|\beta|$. The horizontal axis shows the momentum transversal to the direction of the electric field $\tilde{p}_\perp$. The vertical axis shows the longitudinal momentum $\tilde{p}_3$. $\tilde{p}_\perp$ and $\tilde{p}_3$ are the dimensionless variables defined in (2.7). The system parameters are $z_0 = 10$ and $\mu = 0.04$. Pair creation is possible in the domain under the dark blue line only since for the potential difference the condition $z0 > 2\mu_\perp^2 = 2(\mu^2 + \tilde{p}_\perp^2)$ must be fulfilled.

Chapter 5

Quantum Electrodynamics

The following chapter is the heart of this thesis. To investigate the emission of photons from accelerated charges we have to couple the particle field to the second quantized electromagnetic field, assume this coupling to be small and then derive the corresponding perturbative expressions for the differential cross sections of the relevant processes. This is the task of the first part of this chapter. In the second part we evaluate these cross sections with numerical and approximative methods and discuss the results. Due to the reasonable interpretability, in the context of wave packets discussed in section 2.1.3, in the rest of this thesis we solely use the solutions constructed with the identification scheme of ref. [14]. However, in the parameter domain used for the numerical calculation the differences in the results of both identification schemes are vanishingly small.

We start the development of the QED theory by splitting the electromagnetic field into a classical part and a second quantized field operator part $A_\mu = \tilde{A}_\mu + \hat{A}_\mu$ where the classical part is given by the potential (2.3) and models the acceleration of the charged particles and the quantized part corresponds to the radiation field. The quantization of a charged massive scalar field in an electromagnetic background field was outlined in chapter 2 and 3. We obtained that the time evolution of the second quantized field is totally governed by the Hamiltonian (3.12) and Heisenberg's equation of motion (3.14). However, in the coupled theory, the time evolution of the matter field depends

additionally on the interaction with the second quantized part $\hat{A}_\mu$ of the electromagnetic field and thus on the evolution of the radiation field itself. Since we consider minimal coupling the matter field is directly coupled to the vector potential $\hat{A}_\mu$ in a gauge invariant form. This gauge invariance has to be considered in the quantization of the electromagnetic field (for an extensive presentation of this issue see [30]). Here we use the established form of the theory as it is presented in textbooks such as [31] and [25], with other words we fix the gauge with an appropriate gauge condition and quantize the field $\hat{A}_\mu$ as a linear combination of independent uncharged scalar fields. We have

$$\hat{A}_\mu = \sum_\lambda \int \frac{d^3k}{(2\pi\hbar)^3} \left(a_\lambda \Phi_{\lambda,\mu} + a_\lambda^\dagger \Phi_{\lambda,\mu}^* \right) \tag{5.1}$$

and $\phi_{\lambda,\mu} = \varepsilon_{\lambda,\mu} \sqrt{\frac{\hbar^2}{2\epsilon_0 c k_0}} e^{-\frac{i}{\hbar} k_\nu x^\nu}$.

Since we want to investigate the interaction of one particle with the radiation field and restrict our considerations to tree graphs it is appropriate to use the radiation gauge for $\hat{A}_\mu$ in our calculations. The corresponding gauge conditions are $\partial^i \hat{A}_i = 0$ and $\hat{A}_0 = 0$ where i runs from one to three. We thus have for the total electromagnetic field the coulomb gauge $\partial^i A_i = 0$ with additional gauge fixing condition $A_0 = \tilde{A}_0$. In this gauge the radiation field is transversal, that is $\hat{A}_\mu k^\mu = 0$, and thus only two scalar fields remain. These two components of $\hat{A}_\mu$ can be interpreted in a physically meaningful way as photons with orthogonal polarization vector $\varepsilon_{\lambda,\mu}$.

The time evolution of the total system is governed by the total Hamiltonian $H := H_{RF} + H_I + H_{MF}$ where H_{RF} is the Hamiltonian of the radiation field, H_I the interaction Hamiltonian and H_{MF} the Hamiltonian of the matter field. The coupled system of the electromagnetic and particle field cannot be solved directly, at least not in our framework. We therefore use scattering theory to derive the system's evolution. In the following we shortly outline the foundations of scattering theory.

From the Schrödinger equation we get the following formal expression for the time evolution of a

state ψ in the one particle theory:

$$\psi(t) = e^{-\frac{i}{\hbar}\int_{t_0}^{t} dt' H(t')}\psi(t_0) = U(t,t_0)\psi(t_0) \tag{5.2}$$

The basis of scattering theory is that we can split the Hamiltonian H in a time independent diagonalized free part and a time dependent interaction part with offdiagonal elements like $H = H_0 + H_I$. We define the scattering matrix

$$S := \lim_{s\to-\infty}\lim_{t\to+\infty} e^{\frac{i}{\hbar}H_0 t}U(t,s)e^{-\frac{i}{\hbar}H_0 t} \tag{5.3}$$

This operator evolves a state from $t = 0$ to $t = -\infty$ with the free Hamiltonian, from $t = -\infty$ to $t = +\infty$ with the full Hamiltonian and back to $t = 0$ with the free Hamiltonian. Thus we get, for the probability of the transition from the time independent initial state φ to the state ψ, the expression $P(\varphi \to \psi) = |(\psi, S\varphi)|^2$. By defining $\tilde{\varphi}(t) = e^{\frac{i}{\hbar}H_0 t}\varphi(t)$ and $\tilde{H}_I(t) := e^{\frac{i}{\hbar}H_0 t}H_I(t)e^{-\frac{i}{\hbar}H_0 t}$ we get

$$i\frac{d}{dt}\tilde{\varphi}(t) = \tilde{H}_I(t)\tilde{\varphi}(t)$$

and thus

$$S = \lim_{s\to-\infty}\lim_{t\to+\infty}\tilde{U}(t,s). \tag{5.4}$$

This is the so-called interaction picture and for the free theory, that is for $H_I = 0$, it coincides with the Heisenberg picture. This framework can be carried over to quantum field theory as it is shown in chapter 2.4-2.5 of ref. [25], in ref. [32] and in standard textbooks like ref. [33]. Since H_{RF} and H_{MF} are diagonal and time independent in the basis of the states of the free theories, scattering theory should work perfectly for quantum electrodyamics. However, we cannot find a closed solution for the full scattering matrix. We have to restrict our considerations to perturbation theory assuming

that the effect of the operator H_I is small in comparison with the effect of H_0. Since the coupling constant is the elementary charge e this assumption is fulfilled in quantum electrodynamics.

5.1 Perturbation theory

An important technical aspect in QED is renormalization: every physical theory contains parameters that must be fixed by comparing the outcomes of experiments with the predictions of this theory. In QED these parameters are e, m and Z where Z is the normalization constant of the fields. The determination of these quantities contains some subtle difficulties. Due to the perturbative treatment of the interaction between the electromagnetic and matter field, in every order of perturbation theory it is necessary to fix the parameters to the amount of accuracy corresponding to the perturbative order. In every order of this perturbative treatment so-called loops arise. These loops correspond to virtual particles which only exist as intermediate states during the quantum mechanical processes. To define the system's parameters we have to predict values for measurable quantities such as cross sections. Thus we have to sum over all possible processes which contribute to this measurable quantity. By considering all possible momenta of the virtual particles infinite expressions arise and, since obviously measurable quantities are finite, the system's parameters have to be infinite. This method of giving the system's parameters an infinite value in order to achieve finite outcomes of the theory is called renormalization (see ref. [34]). For QED in a classical electromagnetic background field the renormalization functions that relate the system's parameters with measurable quantities obviously depend on the background field.

To deal with these problems we use a framework called causal perturbation theory as it is presented in ref. [25]. Beside its mathematical and conceptual clarity, its major attribute is that the process of renormalization is inherent; finite renormalized expressions for the S-matrix elements are constructed order by order, taking care of potential sources of infinities in every step of the construction. In this subsection we want to outline this theory following ref. [25].

We begin by writing the scattering matrix as a series in powers of the coupling constant e. Since the scattering matrix is not a function but a generalized function (also-called distribution) we have to regularize it by using a smearing function g and considering the limit $g \to 1$ at the end. We assume that the occuring distributions are tempered and thus g is in $\mathcal{S}(\mathbb{R}^4)$, the Schwartz space of fast decaying functions. We write

$$S(g) = 1 + \sum_{n=1}^{\infty} \frac{1}{n!} \int d^4x_1 ... d^4x_n T_n(x_1, ..., x_n) g(x_1) ... g(x_n) := 1 + T. \tag{5.5}$$

We do not need to worry about the convergency properties of the series (5.5); since we use it only up to a finite order we can treat it simply as an approximative tool with finite accuracy. The most important ingredient of causal perturbation theory is the causality condition: for two smearing functions g_1 and g_2 with disjoined support in time e.g. $\operatorname{supp} g_1 \subset \{ x \in \mathbb{R}^4 \,|\, x_0 \in (-\infty, r) \}$ and $\operatorname{supp} g_2 \subset \{ x \in \mathbb{R}^4 \,|\, x_0 \in (r, \infty) \}$ we postulate $S(g_1 + g_2) = S(g_1)S(g_2)$. This causality condition is a generalization of a causality condition for the interaction of a classical external electromagnetic field with a quantum particle. In the one particle theory we postulate that, if an external electromagnetic field is turned on and off again and some time later another electromagnetic field is turned on and off again, the effects of these fields on a quantum particle can be considered seperately. In Fock space this results in the following statement: For $A^\mu = A_1^\mu + A_2^\mu$ where A_1^μ and A_2^μ have disjoined support in time we have $S = e^{i\psi} S_2 S_1$ where $S_j = S[A_j]$. The transitions probability is independent of the phase ψ and, by requirering $\psi = 0$, we get the causality condition as the generalization of the foregoing statement. In addition to equation (5.5) we can write the inverse of the scattering matrix as a power series in e

$$S^{-1}(g) = 1 + \sum_{n=1}^{\infty} \frac{1}{n!} \int d^4x_1 ... d^4x_n \tilde{T}_n(x_1, ..., x_n) g(x_1) ... g(x_n) \tag{5.6}$$

and define the distributions

$$A'_n(x_1,...,x_n) = \sum_{P_2} \tilde{T}_{n_1}(X) T_{n-n_1}(Y, x_n) \tag{5.7}$$

$$R'_n(x_1,...,x_n) = \sum_{P_2} T_{n-n_1}(Y, x_n) \tilde{T}_{n_1}(X). \tag{5.8}$$

The sums run over all partitions P_2 of $x_1, ..., x_{n-1}$ into disjoined subsets X and Y where $|X| = n_1 \geq 1$. We further define the distributions $A_n = A'_n + T_n$ and $R_n = R'_n + T_n$. We only know $D_n = R_n - A_n = R'_n - A'_n$ the differences between these distributions. We define the closed forward and backward lightcone as

$$\bar{V^+}(x) = \{y | \eta_{\mu\nu}(y-x)^\mu (y-x)^\nu \geq 0, y^0 \geq x^0\}$$

$$\bar{V^-}(x) = \{y | \eta_{\mu\nu}(y-x)^\mu (y-x)^\nu \geq 0, y^0 \leq x^0\}$$

respectively and their generalizations

$$\Gamma^\pm_n(x) = \{(x_1,...,x_n) | x_j \in \bar{V^\pm}(x) \, \forall j = 1,...,n\}.$$

By investigating the support properties of D_n, A_n and R_n we obtain that

$$\operatorname{supp} D_n(x_1,...,x_{n-1},x_n) \subseteq \Gamma^+_n(x_n) \cup \Gamma^-_n(x_n)$$

whereas

$$\operatorname{supp} A_n(x_1,...,x_{n-1},x_n) \subseteq \Gamma^-_{n-1}(x_n)$$

$$\operatorname{supp} R_n(x_1,...,x_{n-1},x_n) \subseteq \Gamma^+_{n-1}(x_n).$$

A_n and R_n can be constructed by splitting D_n into an advanced and a retarded part respectively. This

procedure is called causal splitting, and for tempered distributions $d \in \mathcal{S}(\mathbb{R}^{4n})$, it is well defined by asymptotic conditions (see section 3.2. of ref. [25]). In the widely used standard perturbation theory, such as it is developed in textbooks like [35], the causal split corresponds to the construction of the retarded and the advanced part of Green's functions. In contrast to the mathematically well defined procedure in causal perturbation theory in standard perturbation theory the causal split is done trivially by multiplication with Heaviside functions, that is with objects such as $\chi_n(x) = \prod_{j=1}^{n-1} \Theta(x_j^0 - x_n^0)$. This sloppy multiplication of distributions in standard perturbation theory leads to ultraviolett and infrared divergencies which must subsequently be removed. In causal perturbation theory these devergencies are avoided from the beginning by performing the causal split in a mathematically well difined way. During this procedure factors arise which have to be fixed by physical conditions. This replaces the process of renormalization (see chapter 4.3. of ref. [25]).

In [24] the authors show that causal perturbation theory can also be developed for quantum electrodynamics with an external electromagnetic background field. Thus we can use it for our purposes.

5.2 Scalar QED

As outlined above the first step from a free theory to an interacting theory is the derivation of the appropriate interaction Hamiltonian. To achieve this goal for scalar quantum electrodynamics we have to investigate the action

$$\mathcal{L} = \hbar c \left((D_\mu \Psi)^* D^\mu \Psi - \frac{m^2 c^2}{\hbar^2} \Psi^* \Psi \right)$$

where $D_\mu = \partial_\mu - i\frac{e}{\hbar c}A_\mu$. By splitting the electromagnetic field into a classical part and a second quantized field operator part $A_\mu = \tilde{A}_\mu + \hat{A}_\mu$ we get

$$\begin{aligned} \mathcal{L} &= \hbar c \left(\underbrace{(\tilde{D}_\mu \Psi)^* \tilde{D}^\mu \Psi - \frac{m^2 c^2}{\hbar^2} \Psi^* \Psi}_{\mathcal{L}_0} + \underbrace{i\frac{e}{\hbar} \hat{A}_\mu \Psi^* \overset{\leftrightarrow}{\tilde{D}}_\mu \Psi}_{\mathcal{L}_3} + \underbrace{\frac{e^2}{\hbar^2} \hat{A}_\mu \hat{A}^\mu \Psi^* \Psi}_{\mathcal{L}_4} \right) \\ &=: \mathcal{L}_0 + \mathcal{L}_3 + \mathcal{L}_4 \end{aligned} \tag{5.9}$$

where $\tilde{D}_\mu = \partial_\mu + i\frac{q}{\hbar}\tilde{A}_\mu$ and $\Psi^* \overset{\leftrightarrow}{\tilde{D}}_i \Psi := \Psi^* \tilde{D}_i \Psi - (\tilde{D}_i \Psi)^* \Psi$. By applying a Legendre transformation with the canonical momenta $\Pi_1 = (\partial_0 + i\frac{e}{\hbar}A_0)\Psi^*$ and $\Pi_2 = (\partial_0 - i\frac{e}{\hbar}A_0)\Psi$ we obtain the hamiltonian density. It can be split into a part containing the classical background field $\tilde{A}_\mu$ only and a part containing the background field and the quantum field $\hat{A}_\mu$, that is the interaction hamiltonian density $\mathcal{H}_I$, which can be written as,

$$\begin{aligned} \mathcal{H}_I &= -ec\hat{A}_\mu \left[2\tfrac{e}{\hbar}\eta^{\mu 0}\tilde{A}_0 \Psi^* \Psi + i\eta^{\mu i}(\Psi^* \overset{\leftrightarrow}{\tilde{D}}_i \Psi)^* \Psi) + \tfrac{e}{\hbar}\hat{A}^\mu \Psi^* \Psi \right] \\ &=: -ec\hat{A}_\mu (j_3^\mu + j_4^\mu) =: \mathcal{H}_3 + \mathcal{H}_4 \end{aligned}$$

where the greek indices run from zero to three and the latin indices run from one to three.

Since we use the radiation gauge $\hat{A}_0 = 0$ and we get

$$\mathcal{H}_3 = iec\hat{A}_i(\Psi^* \overset{\leftrightarrow}{\tilde{D}}_i \Psi) \tag{5.10}$$

$$\mathcal{H}_4 = -c\frac{e^2}{\hbar}\hat{A}_\mu \hat{A}^\mu \Psi^* \Psi. \tag{5.11}$$

We find that $\mathcal{H}_3$ acts on three particles, i.e. two scalar particles and one photon, and $\mathcal{H}_4$ acts on four particles, i.e. two scalar particles and two photons. This can be illustrated with diagrams like those in figure 5.1 and 5.2.

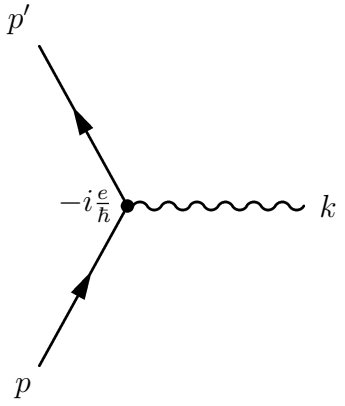

Figure 5.1: $\mathcal{H}_3$ vertex

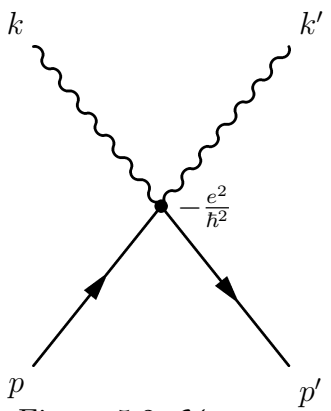

Figure 5.2: $\mathcal{H}_4$ vertex

In the following we want to investigate the corresponding scattering matrix elements in first and second order perturbation theory. To get expressions with the correct dimensions in every step of our calculations we need to impose periodic boundary conditions, introduce a parameter V for the volume of the periodic cell and then take the limit $V \to \infty$. We skip this rather technical detail in our calculations since the intermediate expressions are not of physical interest; they are not even measurable.

To keep the notation as clean as possible we do not distinguish between dimensionless variables and physical variables in our calculations; we drop the tilde above the dimensionless variables defined in (2.7). However, we do give all expressions for measurable quantities, such as emission probabilities, in terms of physical variables.

5.2.1 First order

The second part of the interaction Hamiltonian $\mathcal{H}_4$ is already of second order in the coupling constant e. It thus has to be treated as a part of the second order scattering matrix element in the next subsection. Since the system Hamiltonian has to be normally ordered to allow the normalization of the ground state energy, $\mathcal{H}_3$ must also be normally ordered. We get $T_1(x) = -\frac{i}{\hbar c} : \mathcal{H}_3 :$. It is easy to see that $\mathcal{H}_3$ is not covariant and thus, the perturbative expansion of the scattering matrix is not covariant either. However, since we are dealing with a background field our system is, by no means,

covariant. To get a covariant interaction term one can use the approach of ref. [36]. The authors use the normally ordered, first order part of the covariant interaction Lagrangian (5.9) as $-T_1(x)$. Since we use the radiation gauge and thus $\hat{A}_0 = 0$ both approaches give the same result and we do not need to struggle with the difficult question how to derive $T_1(x)$ from first principles.

The main task of this section is to calculate the S-matrix element for the following process: an in-propagating scalar particle comes from the right, emits a photon and is then either transmitted to the left or reflected to the right. Therefore we have to evaluate the S-matrix elements

$$\begin{aligned} & S_3(k, \lambda, p'_\perp, p'(\pm), p, l_1, ..., l_N, m_1, ..., m_N) \\ & = \int d^4x \, {}_{out}\langle k, p', l_1, ..., l_N, m_1, ..., m_N | T_1(x) | p \rangle_{in} \\ & = \tfrac{e}{\hbar} \int d^4x \, {}_{out}\langle k, \lambda, p'_\perp, p'(\pm), l_1, ..., l_N, m_1, ..., m_N | \hat{A}_i : (\Psi^* \overset{\leftrightarrow}{\tilde{D}}_i \Psi) : | p_\perp, p(+) \rangle_{in} \end{aligned} \tag{5.12}$$

for $N \in \mathbb{N}$. The indices *in* and *out* denotes in- and out-propagating states respectively. The momenta l_n and m_n correspond to particles and antipaticles which are created in pairs by the electric background field. In the beginning we restrict our attention to the case of $N = 0$; it is the leading term if the pair creation rate is small, that is when the electrical field strength is sufficiently small in comparision with the Schwinger limit. To enable normal ordering the scalar field operators must be expanded in the same basis. We choose the basis of out-propagating states, and with equation

(3.9), we arrive at the expression

$$
\begin{aligned}
&S_3(k,\lambda,p'_\perp,p'(\pm),p) = \\
&\tfrac{e}{\hbar}\int d^4x\, {}_{out}\langle\Omega|a_\lambda(k)a_{out}(p'(\pm),p'_\perp)\textstyle\sum_{\lambda'}\int\frac{d^3k}{(2\pi\hbar)^3}\left(a_{\lambda'}\Phi_{\lambda',\mu}+a^\dagger_{\lambda'}\Phi^*_{\lambda',\mu}\right)\times \\
&\times :\int\tfrac{d^2q'_\perp}{4\pi^2\hbar^2}\textstyle\sum_{d\in\{+,-\}}\int_0^\infty\frac{dq'(d)}{2\pi\hbar}\left(a^\dagger_{out}(q'(d),q'_\perp)\Phi^{(p)*}_{out,q'(d)}+b_{out}(q'(d),q'_\perp)\Phi^{(a)*}_{out,q'(d)}\right)\times \\
&\times\overset{\leftrightarrow}{\tilde{D}}_i\int\tfrac{d^2q_\perp}{4\pi^2\hbar^2}\textstyle\sum_{d\in\{+,-\}}\int_0^\infty\frac{dq(d)}{2\pi\hbar}\left(a_{out}(q(d),q_\perp)\Phi^{(p)}_{out,q(d)}+b^\dagger_{out}(q(d),q_\perp)\Phi^{(a)}_{out,q(d)}\right):\times \\
&\times a^\dagger_{in}(p(+),p_\perp)|\Omega\rangle_{in}
\end{aligned}
\tag{5.13}
$$

By using the normal ordering and the commutation relations $[c_{in,out}(f),c^\dagger_{in,out}(g)]=\langle f,g\rangle$ and $[a_p,a^\dagger_{p'}]=[b_p,b^\dagger_{p'}]=(2\pi\hbar)^3\delta(p-p')$ we find

$$
\begin{aligned}
&S_3(k,\lambda,p'_\perp,p'(\pm),p) = \tfrac{e}{\hbar}\int d^4x\Big({}_{out}\langle\Omega|\Omega\rangle_{in}\Phi^*_{\lambda,\mu}\times \\
&\times\Phi^{(p)*}_{out,p'(\pm)}\overset{\leftrightarrow}{\tilde{D}}_i\textstyle\sum_{d\in\{+,-\}}\left(\Phi^{(p)}_{out,p(d)},\Phi^{(p)}_{in,p(+)}\right)_{KG}\Phi^{(p)}_{out,p(d)} \\
&+\int\tfrac{d^2q'_\perp}{4\pi^2\hbar^2}\int\tfrac{d^2q_\perp}{4\pi^2\hbar^2}\int_0^\infty\tfrac{dq'(+)}{2\pi\hbar}\int_0^\infty\tfrac{dq(-)}{2\pi\hbar}\Phi^*_{k,\lambda,\mu}\Phi^{(a)*}_{out,q'(+)}\overset{\leftrightarrow}{\tilde{D}}_i\,\Phi^{(p)}_{out,q(-)}\times \\
&\times\ {}_{out}\langle\Omega|b_{out}(q'(+),q'_\perp)a_{out}(q(-),q_\perp)|\Omega\rangle_{in}\left(\Phi^{(p)}_{out,p(\pm)},\Phi^{(p)}_{in,p(+)}\right)_{KG}\Big)
\end{aligned}
\tag{5.14}
$$

where ${}_{out}\langle\Omega|\Omega\rangle_{in}$ is directly related to the instability of the vacuum induced by the background field and the accompanying pair creation and can be evaluated by investigating equation (4.9).

Furthermore, by using equation (4.9), it can easily be seen that the integrand in the second term in equation (5.14) is nonzero and thus there is an additional process that contributes to the S-matrix

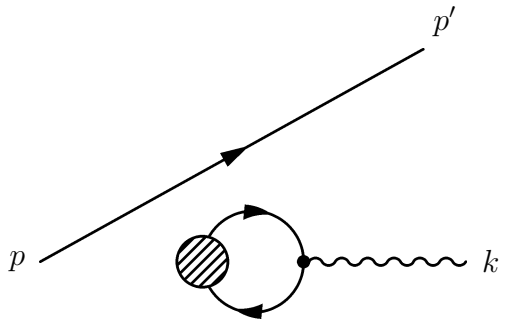

Figure 5.3: Electron-positron pair creation and subsequent annihilation accompanied by the emission of a photon.

element due to pair creation. This is illustrated in figure 5.3; a pair is created from the vacuum and subsequently annihilated, this is accompanied by the emission of a photon [32]. The contribution of this process to the value of the S-matrix element depends on the pair creation rate we investigated in chapter 4 due to the term ${}_{out}\langle\Omega|b_{out}(q'(+),q'_\perp)a_{out}(q(-),q_\perp)|\Omega\rangle_{in}$. Thus this process could have significant effects on the values of the electric field strength close to the Schwinger limit. However, we learned in chapter 4 that the electrons and positrons that are created as pairs by the background field have the same energy q_0 and transversal momentum $q_\perp$. We obtain

$$ {}_{out}\langle\Omega|b_{out}(q'(+),q'_\perp)a_{out}(q(-),q_\perp)|\Omega\rangle_{in} = g(q_0,q_\perp)\delta(q_0-q'_0)\delta(q_\perp-q'_\perp) \tag{5.15} $$

$$ \begin{aligned} &S_3(k,\lambda,p'_\perp,p'(\pm),p) \\ &= \tfrac{e}{\hbar}\int d^4x \Phi^*_{\lambda,\mu}\Phi^{(p)*}_{out,p'(\pm)} \overset{\leftrightarrow}{\tilde{D}}_i \Phi^{(p)}_{in,p(+)}\, {}_{out}\langle\Omega|\Omega\rangle_{in}. \end{aligned} \tag{5.16} $$

Since all the wave functions in equation (5.16) factorize with respect to the space and time coordi-

nates and the factors depending on $x_\perp$ and x_0 are simple exponential functions we can evaluate the integration over these coordinates and use the dimensionless variables defined in (2.7). We find

$$\begin{aligned} S_3(k,\lambda,p'_\perp,p'(\pm),p) &= \sqrt{\tfrac{e^2}{2\epsilon_0 c k_0}}\ {}_{out}\langle\Omega|\Omega\rangle_{in}\times \\ &\times\int dz\, e^{\frac{i}{\hbar}\tilde{k}_3 z}\left(\varepsilon_{\lambda,3}\left(\phi^{(p)*}_{out,p'(\pm)}(z)\tfrac{\partial}{\partial z}\phi^{(p)}_{in,p(+)}(z)-\tfrac{\partial}{\partial z}\phi^{(p)*}_{out,p'(\pm)}(z)\phi^{(p)}_{in,p(+)}(z)\right)\right. \\ &\left.+\varepsilon_{\lambda,i_\perp} i(\tilde{p}_{i_\perp}+\tilde{p}'_{i_\perp})\phi^{(p)*}_{out,p'(\pm)}(z)\phi^{(p)}_{in,p(+)}(z)\right) 2\pi\hbar\delta(p_0-p'_0-k_0)(2\pi\hbar)^2\delta^{(2)}(p_\perp-p'_\perp-k_\perp) \\ &=: I(k,\lambda,p'_\perp,p'(\pm),p)2\pi\hbar\delta(p_0-p'_0-k_0)(2\pi\hbar)^2\delta^{(2)}(p_\perp-p'_\perp-k_\perp) \end{aligned} \tag{5.17}$$

where $i_\perp\in\{1,2\}$. To get the emission probability we have to calculate the squared absolute value of S_3 integrated over all momenta p'. As can be seen in equation (5.17) in this procedure squares of delta functions would appear. To make sence of such expressions we introduce normalized wave packet states.

$$|\varphi^\sigma_{p_m}\rangle = \int \frac{d^3p}{(2\pi\hbar)^3}\varphi^\sigma_{p_m}(p)|p\rangle \tag{5.18}$$

where

$$\varphi^\sigma_{p_m}(p) = \prod_{i=1}^{3}\frac{(2\pi\hbar)^{1/2}}{(2\pi\sigma^2)^{1/4}}e^{-\frac{(p_i-p_{m,i})^2}{4\sigma^2}} \tag{5.19}$$

We define the charge operator as $Q := \int \frac{d^3p}{(2\pi\hbar)^3}\left(a^\dagger_p a_p - b^\dagger_p b_p\right)$. In a particle wave packet state its expectation value is $\langle\varphi^\sigma_{p_m}|Q|\varphi^\sigma_{p_m}\rangle = e$. Thus $|\varphi^\sigma_{p_m}\rangle$ represents a particle of charge e moving with momentum p_m.

Using a wave packet state for the in-propagating particle we obtain for the corresponding S-matrix

element integrated over every external state

$$M_3(k,\lambda,p_m) := \sum_{d\in\{+,-\}} \int \frac{d^3p'(d)}{(2\pi\hbar)^3} |S_3(k,\lambda,p'_\perp,p'(d),p_m)|^2 = \\ \sum_{d\in\{+,-\}} \int \frac{d^3p'(d)}{(2\pi\hbar)^3} \left(\varphi^\sigma_{p_m}(p_{in}(p'))\right)^2 \left|\frac{\partial p_3}{\partial p_0}\Big|_{p=p_{in}(p')} I(k,\lambda,p'_\perp,p'(d),p_{in}(p'))\right|^2 \tag{5.20}$$

where $d \in \{+,-\}$ denotes the propagation direction of the out-propagating particle and $p_{in}(p') = ((p'_0 + k_0 - \frac{z_0}{2})^2 - \mu^2 - (p'_\perp + k_\perp)^2)^{1/2}$. The next step is to change the intergration variable from $p'(d)$ to $p(+)$. For a narrow wave packet, i.e. for large σ, we can now evaluate the integrand up to the Gaussian function φ at the maximium of the wave packet and take it out of the integral. Due to the normalization condition of the wave packet states the remaining Gaussian integral can be performed and we arrive at

$$M_3(k,\lambda,p_m) = \sum_{d\in\{+,-\}} \frac{p(+)}{p'(d)(p_m)} \left|\frac{\pi'(d)(p_m)}{\pi(+)}\right| \\ \left|\frac{\partial p_3}{\partial p_0}\Big|_{p=p_m} I(k,\lambda,p'_\perp(p_m),p'(d)(p_m),p_m)\right|^2 \tag{5.21}$$

where $p'(\pm)(p_m) = ((p_0 - k_0 \mp \frac{z_0}{2})^2 - \mu^2 - (p'_\perp)^2)^{1/2}$, $\pi(\pm) = p_0 - k_0 \mp \frac{z_0}{2}$ and $p'_\perp = p_\perp - k_\perp$. We find for the differential cross section

$$\frac{d\sigma_\lambda}{d\Omega}\Big|_{\Omega(k)} = \int \frac{dk_0}{(2\pi\hbar)^3} k_0^2 M_3(k,\lambda,p_m) \tag{5.22}$$

where $d\Omega = \sin\theta d\theta d\phi$ is a differential solid angle element. In what follows we study $M_3(k,\lambda,p_m)$ using numerical and analytical methods.

First of all we split the integration over dz into three parts, corresponding to the three sections of the potential (2.3). Section I and III are integrations over exponential functions which we perform analytically and get a product of several distributions. We outline an example of the mathematical

treatment of these products in section 7.6 in the appendix. We obtain

$$
\begin{aligned}
I(k,\lambda,p'_\perp,p'(\pm),p) \propto \Big(& (\pi\delta(p'(\mp)-p(\mp)-k_3) \mp i\mathcal{P}\tfrac{1}{p'(\mp)-p(\mp)-k_3}) f_{{}^{I}_{II},aa'} \\
& +(\pi\delta(-p'(\mp)+p(\mp)-k_3) \mp i\mathcal{P}\tfrac{1}{-p'(\mp)+p(\mp)-k_3}) f_{{}^{I}_{II},bb'} \\
& +(\pi\delta(-p'(\mp)-p(\mp)-k_3) \mp i\mathcal{P}\tfrac{1}{-p'(\mp)-p(\mp)-k_3}) f_{{}^{I}_{II},ab'} \\
& +(\pi\delta(p'(\mp)+p(\mp)-k_3) \mp i\mathcal{P}\tfrac{1}{p'(\mp)+p(\mp)-k_3}) f_{{}^{I}_{II},ba'} \Big)
\end{aligned}
\tag{5.23}
$$

where $\mathcal{P}\frac{1}{x}$ is the generalized function called Cauchy principal value. $p'(\pm)$ and $p(\pm)$ are functions of p_m and the indices a, b and a', b' refer to the coefficients of the in- and out-propagating wave functions respectively. Since from the time integration we get $p'_0 - p_0 + k_0 = 0$ and the scalar field is massive it can easily be seen that $p'(\pm) - p(\pm)(p', k) - k_3 \neq 0 \quad \forall p'(\pm)$ and thus the first two delta functions do not contribute. The last two delta functions and Cauchy principal value intergrals have arguments which are only zero for values of the photon energy in the order of the electron rest mass. We therefore restrict our considerations to photon energies sufficiently small in comparison to the electron rest mass and neglect these terms. The sole remaining terms are the first two Cauchy principal value integrals. After some calculations we obtain that these terms cannot be neglected for small photon energies in general. For very large values of $x_{3,0}$ the remaining terms do not contribute since they become strongly oscillatory and thus average to zero due to the integration over the momentum of the out-propagating particle. We see that the remaining terms in (5.23) are a result of the finite extension of the interaction region and of the kinks at the end of this region. Due to a lack of time we do not investigate these terms in this thesis.

Section II corresponds to the acceleration region and we have to integrate over products of exponential functions and parabolic cylinder functions. Since we have full azimuthal symmetry around the k_3-axis we restrict our calculation to the k_1-k_3-plane and make the following definitions for the

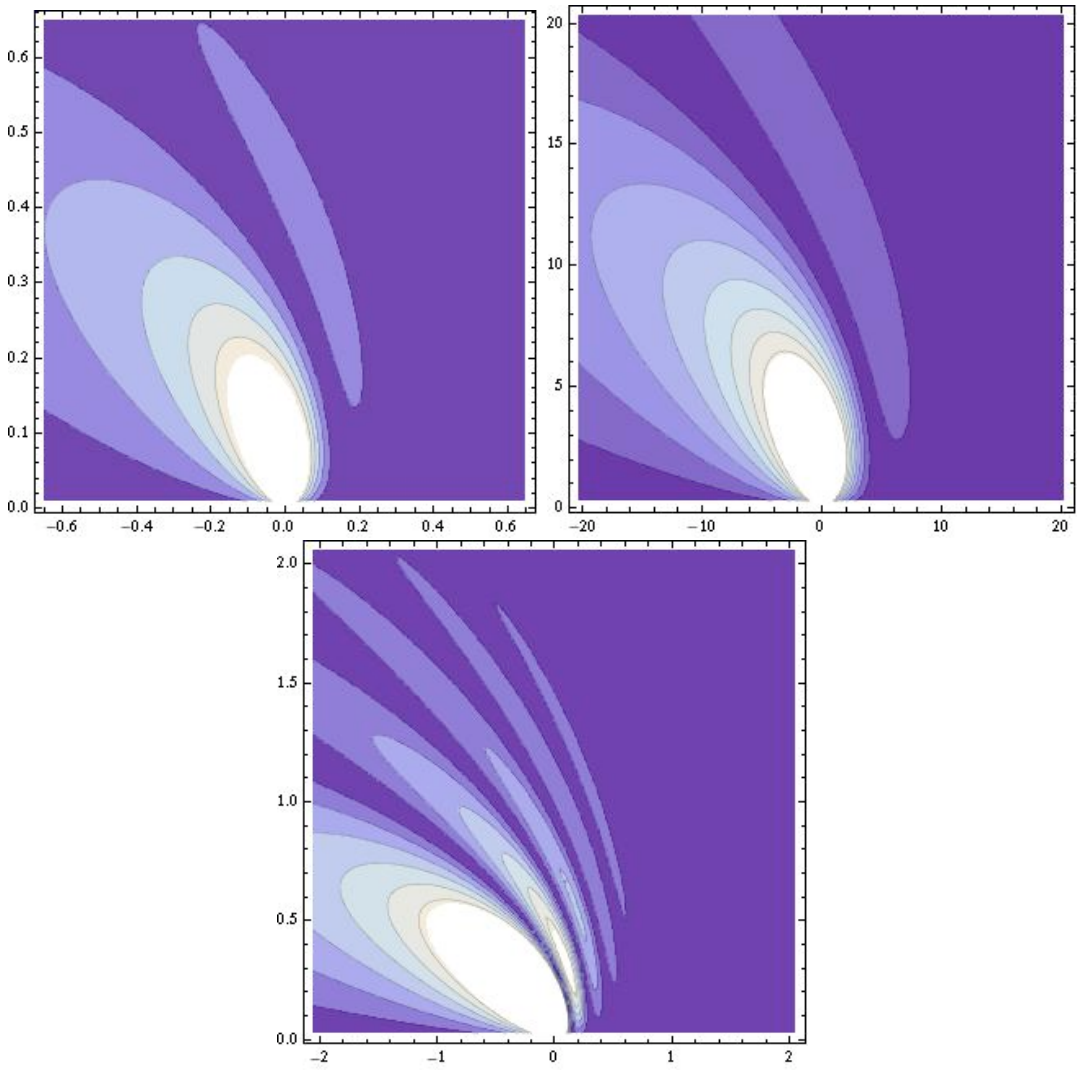

Figure 5.4: Contour plot of $|I(k, 1, p_m)|$. The horizontal axis shows the momentum transversal to the direction of the electric field $\tilde{k}_1$. The vertical axis shows the longitudinal momentum $\tilde{k}_3$. $\tilde{k}_1$ and $\tilde{k}_3$ are dimensionless momentum variables like those defined in (2.7). For the upper left plot $\tilde{p}_{m,3}$ is in order of z_0 and the system parameters are $z_0 = 10$ and $\mu = 0.04$ and for the upper right plot $\tilde{p}_{m,3}$ is in the order of 200μ and the system parameters are $z_0 = 0.3$ and $\mu = 1.3$. In both plots the value of the momentum of the incident particle in SI-units is $p_{m,3} = \sqrt{\frac{2eE\hbar}{c}}\tilde{p}_{m,3} = 200 m_e c$. For the lower plot the system parameters are the same as for the upper left plot but the momentum $p_{m,3}$ is a factor $10^{3/2}$ larger. The characteristics of the Larmor radiation can clealy be seen in all plots. For values of the system parameters and the scalar particle energy used for these numerical calculations the reflection term is neglegible.

transversal polarization vectors:

$$\varepsilon_{1,\mu} = (0, \tfrac{k_3}{k0}, 0, -\tfrac{k_1}{k0})$$
$$\varepsilon_{2,\mu} = (0, 0, 1, 0) \tag{5.24}$$

Moreover, we restrict our calculations to the case of an incident particle with momentum vector solely in x_3-direction, i.e. $p_1 = 0 = p_2$. With these restrictions we get, for the polarization $\varepsilon_{2,\mu}$ perpendicular to the k_1-k_3-plane, the analytical exact result $M_3 = 0$. This is due to the fact that the derivative with respect to x_2 gives a term with a facor $p_2' = p_2 - k_2 = -k_2$ which is zero in the k_1-k_3-plane. For the polarization $\varepsilon_{1,\mu}$ numerical results can be seen in figure 5.4. These graphics where calculated and plotted with *Mathematica 6* for system parameters near the Schwinger limit and energies of the incident particle in the order of 10^2 times the electron rest mass. We use these values for the parameters in order to achieve acceptable computation times being aware, however, that in this regime the effect of pair creation cannot be neglected. The additional possible processes are discussed in the last part of this subsection. In figure 5.4 we can see that the maximum of the photon energy is in the order of 10^{-1} times the energy of the incident particle in the corresponding parameter domain. We calculated only the transmission part of M_3, that is the part with the out-propagating state propagating to the left, since other numerical results show that the reflection part is extremely suppressed. All contour plots in 5.4 show the well-known characteristic of Larmor radiation. The upper two contour plots are for the same energy of the incident particle but differ in the value of M_3, that is in the magnitude of the differential radiation probability, and in the electric field stregth by a factor $10^{3/2}$. Hence the dependency of the radiation probability on the electric field strength in this parameter domain is linear. The lower contour plot shows M_3 for the same values of the electric field strength as the upper right plot but for an $10^{3/2}$ times larger energy of the incident particle.

Now we want to discuss the effect of electron-positron pair creation on the S-matrix elements in equation (5.12) for $N \neq 0$. By using equation (4.9) we get all the addition processes that occur. In

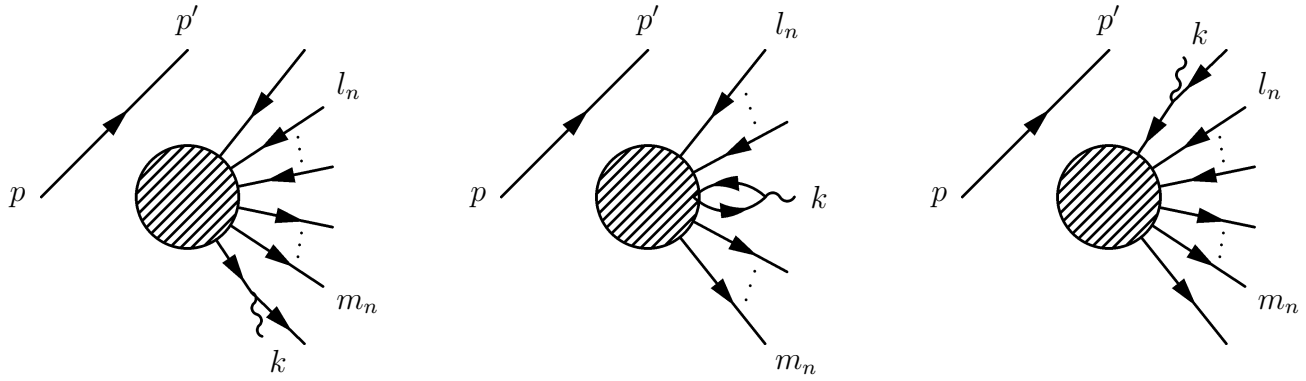

Figure 5.5: Additional possible processes induced by pair creation in first order perturbation theory.

figure 5.5 we see illustrations of these processes. In contrast to the process in figure 5.3 these processes cannot be excluded by energy conservation. There are two possible ways that allow us to neglect them. Firstly we can restrict our considerations to field strength sufficiently below the Schwinger limit. Secondly we can state a measurement of the number of antiparticles produced in the process and restrict our consideration to processes where no antiparticles are produced. The additional processes correspond to the emission of photons with a broad bandwidth of energies. Thus the emitted radiation can be seen as a background noise that reduces the accuracy of detection schemes. In all our considerations we must, therefore, be aware that close to the Schwinger limit the accuracy of the detection of acceleration radiation from an incident particle will be significantly reduced due to pair creation if we cannot exclude processes which correspond to the creation of positrons. To give estimates for the detectability of the acceleration radiation, especially for the photon pair radiation for electric field strengths close to the Schwinger limit, we must give estimates for the background noise by computing the cross section for the correspondig processes. Such calculations for an infinite extended external field can be found in ref. [32] for spinor QED. We postpone the calculations for a finite extended background field to further work.

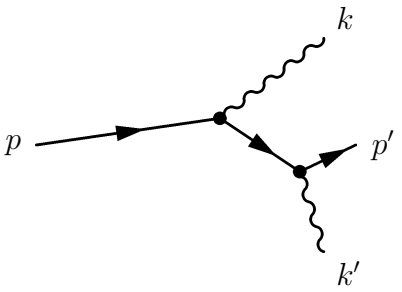

Figure 5.6: Photon pair creation tree-graph with an internal particle line

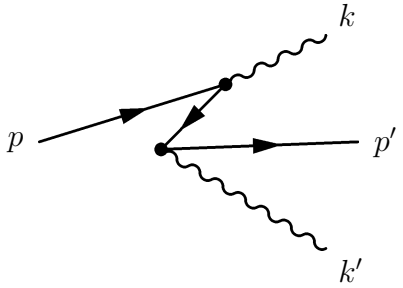

Figure 5.7: Photon pair creation tree-graph with an internal antiparticle line

5.2.2 Second order

In ref. [36] the authors show that, in the framework of causal perturbation theory, the construction of the second order for the calculation of cross sections for processes like those illustrated in figure 5.6 and 5.7 cannot be performed naively. Due to the derivative in the coupling term ultraviolett devergencies appear if one did so. Thus distributional terms have to be added. In [36] the authors show that if one starts with $T_1(x) = \mathcal{L}_3$, in absence of any electromagnetic field, this additional term is exactly the term $\mathcal{L}_4$. However, we cannot take for granted that this result can be carried over to scalar QED with an external background field; we do not know which method is correct to split the fermionic propagator. In contrast, for spinor QED - which is supposed to be much more complicated, it is shown in [24] that in second order perturbation theory no additional terms are needed when calculating the S-matrix elements of the emission processes we consider in this thesis. In addition this spinor QED obviously describes electrons much more accurately than scalar QED. Thus we postpone the investigation of second order tree graphs to the next subsection where we consider spinor particles.

Nonetheless, since it shows interesting parallels to other results in quantum optics we want to investigate $\mathcal{H}_4$, the second part of the interaction Hamiltonian, in the rest of this subsection. Since $\mathcal{H}_4$ is of the same order in the Klein-Gordon field operator as $\mathcal{H}_3$, the regularization of the S-matrix

elements with wave packets and the calculations of the differential emission probabilities work in the same way as for the first order perturbation theory in the last chapter. We obtain

$$\frac{d\sigma_\lambda}{d\Omega d\Omega'}\Big|_{\Omega(k),\Omega(k')} = \int \frac{dk_0}{(2\pi\hbar)^3} \int \frac{dk_0'}{(2\pi\hbar)^3} (k_0 + k_0')^2 M_4(k', \lambda', k, \lambda, p_m), \tag{5.25}$$

$$\begin{aligned} M_4(k, \lambda, k', \lambda', p_m) &= \textstyle\sum_{d\in\{+,-\}} \frac{p(+)}{p'(d)(p_m)} \times \\ &\times \left| \frac{\pi'(d)(p_m)}{\pi(+)} \right| \left| \frac{\partial p_3}{\partial p_0}\Big|_{p=p_m} I(k, \lambda, k', \lambda', p'_\perp(p_m), p'(d)(p_m), p_m) \right|^2 \end{aligned} \tag{5.26}$$

and

$$\begin{aligned} I(k, \lambda, k', \lambda', p'_\perp, p'(\pm), p) &= \langle k, \lambda, k', \lambda', p'|S_4|p\rangle \\ &= \frac{ie^2}{2\epsilon_0 c\sqrt{k_0 k_0'}} \, {}_{out}\langle\Omega|\Omega\rangle_{in} \int dz e^{\frac{i}{\hbar}(\tilde{k}_3 + \tilde{k}_3')z} \phi^{(p)*}_{out,p'(\pm)}(z) \phi^{(p)}_{in,p(+)}(z) \times \\ &\times 2\pi\hbar\delta(p_0 - p_0' - k_0 - k_0')(2\pi\hbar)^2 \delta^{(2)}(p_\perp - p'_\perp - k_\perp - k'_\perp)\delta_{\lambda,\lambda'}. \end{aligned} \tag{5.27}$$

It can easily be seen that the emission probability is the same for both polarizations and that the emitted photons have the same polarization; they are maximally entangled in their polarization degree of freedom.

Figure 5.8 shows a plot of $|I(k, \lambda, k', \lambda', p_m)|$. The six dimensional momentum space of the two-photon-system is reduced to two dimensions because we have used the restriction $k = k'$ and the resulting rotational invariance around the k_3 axis. We obtain that the maximum of the emission probability lies in the acceleration direction and thus in the blind spot of the emission probability in first order perturbation theory, as shown in figure 5.4.

In the following we derive an analytical result for the emission probability resulting from $\mathcal{H}_4$ using

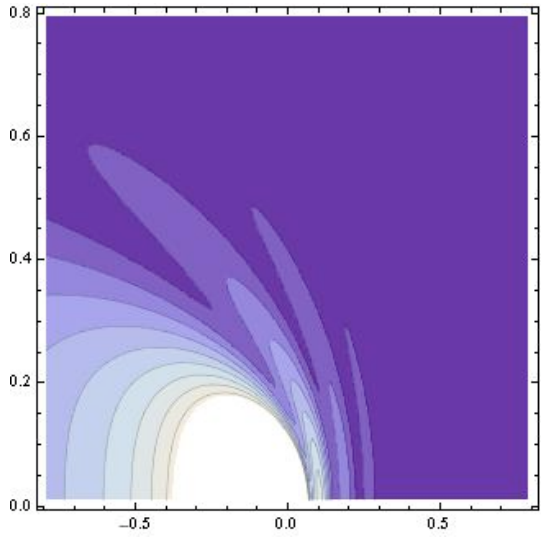

Figure 5.8: Contour plot of $|I(k,\lambda,k,\lambda,p_m)|$. The horizontal axis shows the momentum transversal to the direction of the electric field $\tilde{k}_1$. The vertical axis shows the longitudinal momentum $\tilde{k}_3$. $\tilde{k}_1$ and $\tilde{k}_3$ are dimensionless momentum variables as defined in (2.7). The momentum $\tilde{p}_{m,3}$ of the incident scalar particle is of the order of z_0 and the system parameters are $z_0 = 10$ and $\mu = 0.04$.

approximative methods. In ref. [37] the authors derive the Larmor formula (1.1) from scalar quantum electrodynamics in first order perturbation theory by using the WKB solutions of the Klein-Gordon equation with minimal coupling to a classical linear electric field. They consider the first part of the interaction Lagrangian $\mathcal{L}_3$ only. As we suggested in section 2.1.2, for the case of the ultrarelativistic limit, the solutions of the Klein-Gordon equation are equivalent to the WKB solutions. We therefore want to adopt some of the calculation in [37] to the second order term $\mathcal{L}_4$ in the following. The WKB solution of the Klein-Gordon equation in a linear electric field in x_3-direction is given by

$$\phi_{WKB}(x_3) = \frac{1}{\sqrt{2\pi(\pm)}} \frac{\sqrt{p(\pm)}}{\sqrt{\kappa_p(x_3)}} e^{\frac{i}{\hbar}\int_0^{x_3} d\sigma \kappa_p(\sigma)}. \tag{5.28}$$

where $\kappa_p(x_3) = \sqrt{(p_0 - \frac{eEx_3}{c})^2 - m^2c^2 - p_\perp^2}$. This wave function is correctly normalized in sence of the construction of the wave function as outlined in chapter 2. We neglect contributions of the electron positron pair creation and get for the photon-pair-emission S-matrix element in first order

perturbation theory

$$\langle k,\lambda,k',\lambda',p'|S_4|p\rangle = \\ ie^2\frac{\hbar}{2\epsilon_0 c\sqrt{k_0k_0'}}\int dx_3 e^{-\frac{i}{\hbar}(k_3+k_3')x_3}\phi^*_{WKB,p'}(x_3)\phi_{WKB,p}(x_3)\delta_{\lambda,\lambda'}. \tag{5.29}$$

We assume that the photon energies are much smaller than the energy of the incident particle and define the transversal momentum of the incident particle to be zero. Hence we get for the momentum of the out-propagating particle in first approximation

$$\kappa_{p'}(x_3) = \kappa_p(x_3) - (k_0+k_0')\frac{p_0-\frac{eEx_3}{c}}{\kappa_p(x_3)}. \tag{5.30}$$

We define

$$ct := \int_0^{x_3} d\sigma \frac{p_0-\frac{eE\sigma}{c}}{\kappa_p(\sigma)}. \tag{5.31}$$

We assume that the potential diffence between the right and left side is small and set $p(-) = p(+)$. In first approximation for energies of the involved scalar particles that are large in comparison with that of the electron rest mass and small photon energies we obtain

$$\langle k,\lambda,k',\lambda',p'|S_4|p\rangle = ie^2\frac{\hbar}{2\epsilon_0 c\sqrt{k_0k_0'}}\int dx_3 \frac{1}{\kappa_p(x_3)}e^{-\frac{i}{\hbar}(k_3+k_3')x_3+\frac{i}{\hbar}(k_0+k_0')ct}\delta_{\lambda,\lambda'}. \tag{5.32}$$

With the definitions $\omega := \frac{c(k_0+k_0')}{\hbar}$ and $\tau := t - \frac{x_3}{c}\cos\theta$, where $\cos\theta = \frac{|k_3+k_3'|}{k_0+k_0'}$, we find

$$\langle k,\lambda,k',\lambda',p'|S_4|p\rangle = ie^2\frac{\hbar}{2\epsilon_0 ck_0}\int dx_3 \frac{1}{\kappa_p(x_3)}e^{i\omega\tau}\delta_{\lambda,\lambda'} \tag{5.33}$$

For a classical relativistic particle we have $\dot{x}_3 = \frac{p}{E} = \frac{\kappa_p(x_3)}{p_0-eEx_3}$ where $c=1$ and thus $(1-\dot{x}_3^2) = \frac{m}{p_0-\frac{eEx_3}{c}}$.

After some rearrangements and with $\frac{dx_3}{d\tau} = \frac{\dot{x}_3}{1-\dot{x}_3\cos\theta}$ the S-matrix element becomes

$$\langle k,\lambda,k',\lambda',p'|S_4|p\rangle = ig\frac{\varepsilon_{k,\lambda}\cdot\varepsilon_{k',\lambda}}{2\epsilon_0\sqrt{\omega_k\omega_{k'}}}\int d\tau \frac{\sqrt{1-\dot{x}_3^2}}{1-\dot{x}_3^{\parallel}} e^{i\omega\tau} \tag{5.34}$$

where $g = \frac{e^2}{m}$ and $\dot{x}_3^{\parallel} = \dot{x}_3\cos\theta$. This result is equivalent to equation (7) in ref. [3]. As it can be seen in equation (5.34) and even in the interaction Lagrangian density $\mathcal{L}_4$, the emitted photons are maximally entangled in their polarization degree of freedom. From numerical calculations we find the maximum of the emission probability in the acceleration direction whereas the emission probability corresponding to $\mathcal{L}_3$ is zero in this direction. In ref. [3] and [4] the authors suggest that, due to the blind spot of the Larmor radiation in the acceleration direction, these photon pairs could be detected. They claim further that these photon pairs, like those produced by parametric down conversion in nonlinear cristals, could be used in experimental quantum optics. In the next subsection we show that the existence of a blind spot in the acceleration direction in first order perturbation theory of scalar QED is due to the insufficiency of this theory when describing accelerated electrons; this blind spot does not exist in spinor QED.

5.3 Spinor QED

Spinor QED accurately describes the interaction of electrons with the electromagnetic field. In contrast to the fast decaying particles, for which scalar QED gives a rather inaccurate description, electrons are cheap and easy to handle. Therefore spinor QED is obviously much more useful than scalar QED when searching for experimental set-ups for the detection of new effect concerning the radiation from accelerated charges. Furthermore, as we suggested in the last subsection, the second order of perturbation theory for spinor QED can be constructed naively. We can thus investigate the emission of photon pairs with the knowledge that we are on a well defined path. However, even in the first order the results differ significantly from those we get from scalar QED, Quantum Optics and classical electrodynamics. Hence the task of this section is the investigation of photon emission

in first and second order perturbation theory. Moreover, we compare the results with those from theories that do not contain spin as a particle property. We start by investigating the Lagrangian density for a spinor field

$$\mathcal{L}_D = i\hbar c\bar{\Psi}\gamma^\mu \overset{\leftrightarrow}{\tilde{D}}_\mu \Psi - mc^2\bar{\Psi}\Psi \tag{5.35}$$

where $\bar{\Psi} = \Psi^\dagger\gamma^0$, $\tilde{D}_\mu = \partial_\mu - i\frac{e}{\hbar}A_\mu$ and $A_\mu = \tilde{A}_\mu + \hat{A}_\mu$. Since the Lagrangian density is linear in A_μ the classical background field and the radiation field do not couple as in scalar QED and we get the interaction Lagrangian

$$\mathcal{L}_I = ec\bar{\Psi}\gamma^\mu\Psi\hat{A}_\mu. \tag{5.36}$$

Since there are no time derivatives in the interaction Lagrangian we have, for the interaction Hamiltonian, $\mathcal{H}_I = -\mathcal{L}_I$ and we have no difficulty in defining the first order term for the perturbation expansion of the S-matrix.

5.3.1 First order

We find

$$T_1(x) = i\frac{ec}{\hbar} : \bar{\Psi}\gamma^\mu\Psi : \hat{A}_\mu \tag{5.37}$$

and start with the investigation of the differential cross section for the emission of one photon, with momentum k, from an incident spinor particle, with momentum p and spin s, in first order

perturbation theory. For this purpose we have to calculate the S-matrix element

$$\begin{aligned} &S(k,\lambda,p'_\perp,p'(\pm),s',p,s,\bar{l}_1,...,\bar{l}_N,\bar{m}_1,...,\bar{m}_N) \\ &= \int d^4x \, {}_{out}\langle k,p',\bar{l}_1,...,\bar{l}_N,\bar{m}_1,...,\bar{m}_N|T_1(x)|p\rangle_{in}. \end{aligned} \tag{5.38}$$

where $\bar{l} = (l, s_l)$. The procedure used to calculate the matrix element is mainly analogous to the corresponding procedure in scalar QED, outlined in the last section. We use again the Coulomb gauge with $\hat{A}_0 = 0$ and $\partial_\mu A^\mu = 0$. In order to simplify the expressions we use the commutation relations between the creation and annihilation operators originating from the external particle states and those originating from the normal ordered product of the field operators in figure (5.37). Again we get the additional processes illustrated in 5.5 due to the electron-positron pair creation. We neglect these processes but must be aware that our results are then only reliable for electrical field strengths sufficiently below the Schwinger limit. Additionally we get the process illustrated in 5.3, here the same arguementation applies as in section 5.2.1 and we can neglect this term. For the remaining term the integration over $x_\perp$ and x_0 can be performed and the resulting generalized functions in momentum space can be treated mathematically by using a wave packet state for the incident particle. By assuming narrow wavepackets we can average over the momentum of the out-propagating particle and we arrive at the expression

$$\begin{aligned} M_3(k,\lambda,p_m,s) = \; & \textstyle\sum_{s'} \sum_{d\in\{+,-\}} \frac{p(+)}{p'(d)(p_m)} \left|\frac{\pi'(d)(p_m)}{\pi(+)}\right| \times \\ & \times \left| \left.\frac{\partial p_3}{\partial p_0}\right|_{p=p_m} I(k,\lambda,p'_\perp(p_m),p'(d)(p_m),s',p_m,s) \right|^2 \end{aligned} \tag{5.39}$$

where

$$I(k,\lambda,p'_{\perp}(p_m),p'(d)(p_m),s',p_m,s) = \tag{5.40}$$

$$\sqrt{\tfrac{e^2}{2\epsilon_0 c k_0}}\ {}_{out}\langle\Omega|\Omega\rangle_{in}\sqrt{\tfrac{\hbar c}{2eE}}\int dz\, e^{\frac{i}{\hbar}\tilde{k}_3 z}\varepsilon_{\lambda,i}\psi^{(p)*}_{out,p'(\pm),s'}(z)\gamma^0\gamma^i\psi^{(p)}_{in,p(+),s}(z)$$

In section I and III of the x_3-domain the same delta functions and Cauchy principal value integrals appear as in equation (5.23), only the factors differ. The same argumentation as for the scalar case applies to the spinor case. Due to a lack of time we do not investigate these terms in this thesis.

In spinor QED there are two alternatives for the emission process illustrated in figure 5.1: the spin of the incident particle is conserved or flipped. These processes give different differential emission probabilities. Examples for parameters in the order of Schwinger's critical value are shown in figure 5.9. Due to the azimuthal symmetry around the x_3-axis we again show only the results for the k_1-k_3-plane. We find that the upper plots show all characteristics of Larmor radiation. On the other hand, the lower plots, illustrating the spin-flip process, show no blind spot for photon emission in the acceleration direction $-x_3$; both lower plots show a non zero emission probability in $-x_3$ direction. In the considered parameter domain the magnitude of the spin-flip radiation is five orders smaller than the magnitude of the classical Larmor radiation. Further numerical results show that, for decreasing electrical field strength, the ratio of the probability of the spin-flip and the spin-conserving process decreases. Thus the spin-flip process is strongly suppressed and does not emerge in standard experiments with, for example, particle accelerators. However, clever experimental set-ups could reveal the spin-flip radiation.

In the next subsection we shall see that the first order spin-flip process is of strong relevance for discussions about the detectability of two photon pair acceleration radiation. An additional difference between the emission from scalar and spinor particles is the contribution of both polarization directions in the spinor case.

In the following we want to derive some analytical results. By taking the ultrarelativistic limit

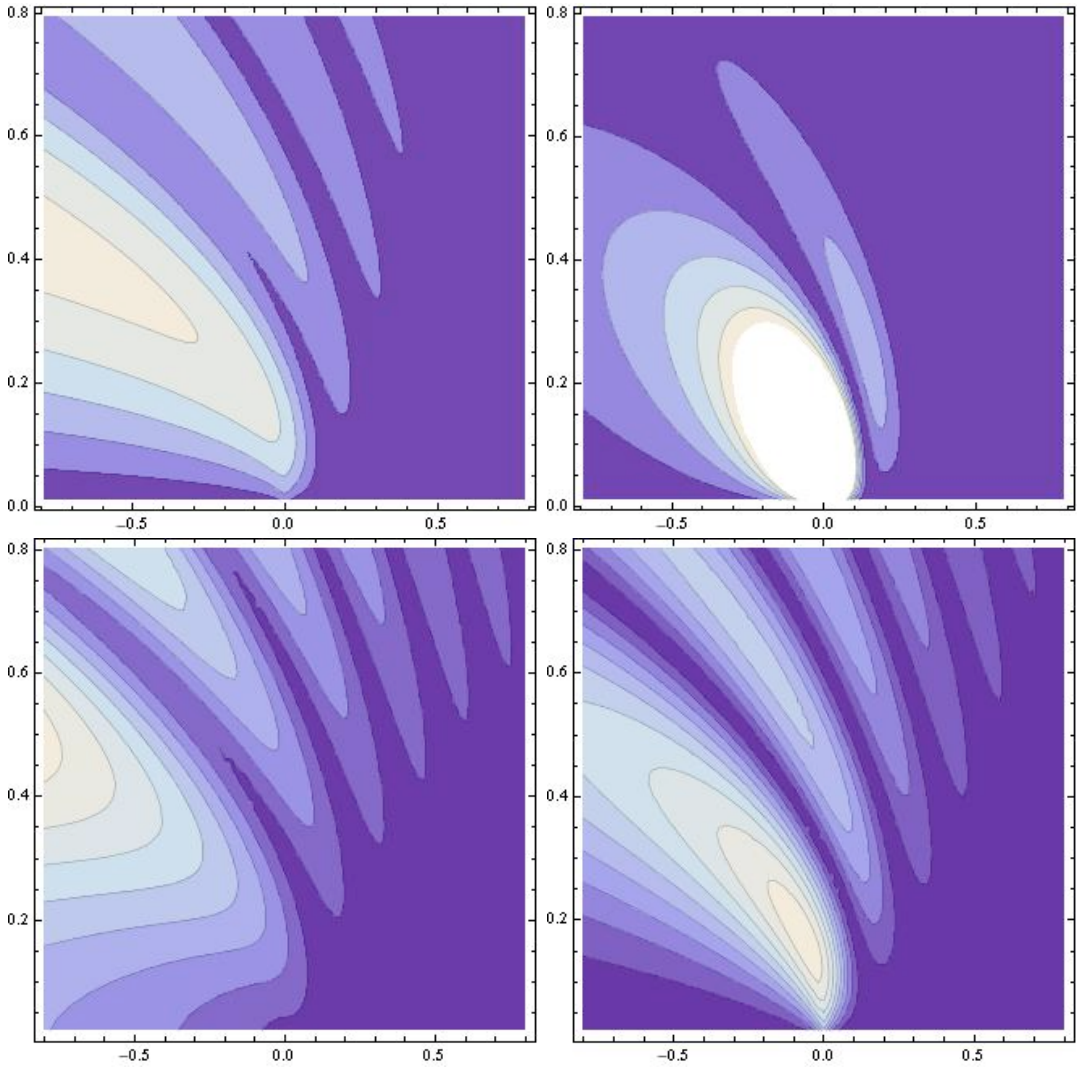

Figure 5.9: Contour plot of $|I(k, \lambda, p_m, s)|$. The horizontal axis shows the momentum transversal to the direction of the electric field $\tilde{k}_1$. The vertical axis shows the longitudinal momentum $\tilde{k}_3$. $\tilde{k}_1$ and $\tilde{k}_3$ are dimensionless momentum variables like those defined in (2.7). The system parameters are $z_0 = 10$ and $\mu = 0.04$. The momentum of the incident particle is in the order of $2z_0$ and the maximum of the photon energy is in the order of $z_0/5$. The upper two contour plots are for the spin-conserving process and the lower two for the spin-flip process. The two left plots show the results for the polarization direction perpendicular to the k_1-k_3-plane and the two right plots show the results for the polarization direction lying in this plane. The relative magnitude of the maximum of the contour plot is: for the upper left 10^{-3}, upper right 1, lower left 10^{-5} and for the lower right plot 10^{-4}. One can clearly see that the upper plots show all characteristics of Larmor radiation. On the other hand, the lower plots, illustrating the spin-flip process, show no blind spot for photon emission in the acceleration direction $-x_3$; both lower plots show a non zero emission probability in $-x_3$ direction. In contrast to the scalar case we get a non zero emission probability for both polarization directions. As in the scalar case, for the chosen values of the system parameters and the particle energy, the reflection term is neglegible.

as in section I we can derive approximate expressions for the S-matrix elements. For an incident particle with spin antiparallel to the x_3-direction we find for the spin-conserving process

$$I(k,\lambda,p'_\perp(p_m),p'(d)(p_m),-1,p_m,-1) = B(z_0)\sqrt{\tfrac{e^2}{2\epsilon_0 c k_0}}\,{}_{out}\langle\Omega|\Omega\rangle_{in}$$
$$\sqrt{\tfrac{\hbar c}{2eE}}\int dz\, G(\lambda)_{SC} e^{i\mu^2 \ln\frac{2\bar{p}'_0 - z}{2\bar{p}_0 - z}} e^{\frac{i}{4}((2\bar{p}_0-z)^2-(2\bar{p}'_0-z)^2)} e^{ip'^2_1 \ln(2\bar{p}'_0-z)} e^{-ik_3 z} \tag{5.41}$$

and factors for the different polarization of the emitted photon

$$G(\lambda=1)_{SC} = \tfrac{k_1}{k_0}\left(1 - \tfrac{k_3}{2p'_0 - z}\right)$$
$$G(\lambda=2)_{SC} = -i\tfrac{k_1}{2p'_0 - z} \tag{5.42}$$

and a phase factor dependent on z_0

$$B(z_0) = e^{i\mu^2 \ln\frac{2\bar{p}_0 - z_0}{2\bar{p}'_0 + z_0}} e^{\frac{i}{4}((2\bar{p}'_0+z_0)^2-(2\bar{p}_0-z_0)^2)} e^{-ip'^2_1 \ln 2\bar{p}'_0 + z_0} e^{-\frac{i}{2}((2p'_0+z_0)z_0+(2p_0-z_0)z_0)}. \tag{5.43}$$

In the following we restrict our considerations to $k_\perp = 0$. To derive useable expressions for the general case would require a much greater effort, we postpone this to further work. We obtain in first approximation

$$I(k,\lambda,p'_\perp(p_m),p'(d)(p_m),-1,p_m,-1) = B(z_0)\sqrt{\tfrac{e^2}{2\epsilon_0 c k_0}}\,{}_{out}\langle\Omega|\Omega\rangle_{in}$$
$$\sqrt{\tfrac{\hbar c}{2eE}}\int dz\, G(\lambda)_{SF} e^{i\mu^2 \ln\frac{2\bar{p}'_0 - z}{2\bar{p}_0 - z}} e^{\frac{i}{4}((2\bar{p}_0-z)^2-(2\bar{p}'_0-z)^2)} e^{-ik_3 z} \tag{5.44}$$

and the polarization dependend factors are

$$G(\lambda=1)_{SF} = i\frac{k_0\mu}{(2p_0-z)(2p_0'-z)}$$
$$G(\lambda=2)_{SF} = \frac{k_0\mu}{(2p_0-z)(2p_0'-z)}. \tag{5.45}$$

For higher values of $k_\perp$ additional terms from the expansion of the parabolic cylinder functions have to be considered and after further calculations the expression (5.44) would be a sum of several terms each with different amplitude and phase. This expression would be very clumsy to use. However, for very small $k_\perp$ we can compare the magnitude of the differential radiation probability of purely Larmor-like, spin-conserving radiation with that of spin-flip radiation.

For large values of p_0 and small $k_\perp$ the term with $p_1^{'2}$ in expression (5.41) can be neglected and for small photon energies $k_0 \ll p_0$ the integration can be performed. At least for $\frac{m^2c^2}{p_0}\frac{\omega_k}{2eE} \ll 1$ we get the differential emission probability

$$\frac{d\sigma}{d\Omega}\Big|_{SC} = \frac{e^2}{2\epsilon_0\hbar}(2x_{3,0}\sin\theta)^2 \int \frac{d\omega_k}{(2\pi c)^3}\omega_k \tag{5.46}$$

where ω_k is the angular frequency of the emitted photon. From equation (5.44) we obtain for $k_0 \ll p_0$ and $\frac{m^2c^2}{4p_0^2-(\frac{2eE}{c}x_{3,0})^2}\frac{\omega_k x_{3,0}}{c} \ll 1$

$$\frac{d\sigma}{d\Omega}\Big|_{SF} = \frac{e^2}{2\epsilon_0\hbar}\left(\frac{2m\hbar x_{3,0}}{4p_0^2-(\frac{2eE}{c}x_{3,0})^2}\right)^2 \int \frac{d\omega_k}{(2\pi c)^3}\omega_k^3. \tag{5.47}$$

For $E = 10^{12}\frac{\mathrm{V}}{\mathrm{m}}$, $x_{3,0} = 10^{-6}\mathrm{m}$, $p_0 = 20mc$ and $\omega_k = 10^{16}\frac{1}{\mathrm{s}}$ in the ultraviolett region of the spectrum the requirements above are fulfilled and we find for the differential emission probability in a small

frequency range $\Delta\omega_k$

$$\begin{aligned} \tfrac{d\sigma}{d\Omega}\big|_{SC} &\approx \Delta\omega_k 10^{-16}\mathrm{s} \\ \tfrac{d\sigma}{d\Omega}\big|_{SF} &\approx \Delta\omega_k 10^{-31}\mathrm{s}. \end{aligned} \tag{5.48}$$

Numerical results show that this is true for values of E between $10^{12}\frac{\mathrm{V}}{\mathrm{m}}$ and $E = 10^{9}\frac{\mathrm{V}}{\mathrm{m}}$. The ratio of the probability of the spin-flip process and the probability of the spin-conserving process decreases for decreasing E [1]. Moreover, this ratio decreases for increasing $x_{3,0}$ and decreasing ω_k. $10^{16}\frac{1}{\mathrm{s}}$ is the maximal value of ω_k for which the restrictions on the parameters for the validity of the approximations are fulfilled. Values of the extension of the interaction region much smaller than $x_{3,0} = 10^{-6}\mathrm{m}$ are experimentally unrealisable. These results show that the spin-flip radiation is mainly suppressed in all experimentally accessible cases and thus it is hardly detectable even for very large electrical field strengths. Hence a blind spot in the acceleration direction is a very good approximation. We discuss in the next subsection why this does not give us an advantage when we want to detect second order effects.

An interesting task would be the derivation of an effective point particle radiation theory such as that in the last subsection and that in ref. [37]. To achieve this we need WKB like semiclassical solutions for the Dirac equation. The ultrarelativistic approximation cannot be used for this task since we take the limits $\pi_0(z) \to (2p_0 - z)$ and $p_0(z) \to (2p_0 - z)$ and thus $\dot{x}_3 \to c$. Techniques to derive semiclassical solutions of the Dirac equation are controversely discussed and, due to the spin transport, contain some subtleties that do not emerge in the theory of semiclassical solutions of the Klein-Gordon equation. Examples can be found in ref. [38] and [39]. We postpone the derivation of such an effective radiation theory to further work.

[1] An analogous result can be found in [9] for the case of an electron in an infinitely extended classical electric field.

5.3.2 Second order

The task of this section is to derive expressions for the differential probability for the processes illustrated in 5.6 and 5.7. In ref. [24] the authors showed that in spinor QED these processes can be calculated directly from the interaction Lagrangian without adding any regularizing terms, with other words the causal splitting of the propagator depicted by the inner line in 5.6 and 5.7 can be performed trivially by multiplication with Heaviside functions. We neglect all contributions from the electron-positron pair creation[2] and obtain the following expression for the S-matrix element:

$$S_2(k,\lambda,k',\lambda',p'(\pm),p'_\perp,s',p,s) = -i\tfrac{e^2}{2}\int d^4x_1 \int d^4x_2 \left(\Phi^*_{k,\lambda,\mu}(x_1)\Phi^*_{k',\lambda',\nu}(x_2)\right. \\ \left. +\Phi^*_{k',\lambda',\mu}(x_1)\Phi^*_{k,\lambda,\nu}(x_2)\right) \bar{\Phi}^{(p)}_{out,p'(\pm),s'}(x_1)\gamma^\mu S^F_{out}(x_1,x_2)\gamma^\nu \Phi^{(p)}_{in,p(+),s}(x_2)\, {}_{out}\langle\Omega|\Omega\rangle_{in} \tag{5.49}$$

and

$$S^F_{out}(x_1,x_2) = i\sum_s \int \tfrac{d^3q}{(2\pi\hbar)^3}\left(\Theta(x_{2,0}-x_{1,0})\Phi^{(a)}_{out,q,s}(x_1)\bar{\Phi}^{(a)}_{out,q,s}(x_2)\right. \\ \left. -\Theta(x_{1,0}-x_{2,0})\Phi^{(p)}_{out,q,s}(x_1)\bar{\Phi}^{(p)}_{out,q,s}(x_2)\right) \tag{5.50}$$

the out-propagating causal, or Feynman, propagator in the background field. This expression corresponds to an in-propagating spinor particle from the right and an out-propagating spinor particle with energy in the over barrier regime and two emitted photons in second order perturbation theory. Due to the sum in the expression (5.49) the resulting two-photon-state is symmetric as expected for a bosonic state. The particle and antiparticle part of the causal propagator (5.50) corresponds to the two processes 5.6 and 5.7 respectively. Investigating the arguments of the Heaviside functions in the causal propagator (5.50) we obtain the well-known fact that an antiparticle can be, apart from its charge, interpretated as a particle moving backwards in time. Due to these Heaviside functions

[2]There are many of these processes since, as in the first order, positrons and electrons created by the background field can annihilate or create photons in the same processes as the incident particle. The investigation of their contributions must be postponed to further work.

the energy conservation we got in previous calculations will not be obtained for (5.49). This fact will cause some trouble in further calculations.

To regularize the expression (5.49) we have to use wave packet states for the incident and the out-propagating spinor particle. In order to sum over all possible momenta of the external particle we must use an appropriate measure over the wave packet space. With the requirement

$$\int d\mu(p_m)|\varphi_{p_m}\rangle\langle\varphi_{p_m}| \stackrel{!}{=} 1 \tag{5.51}$$

and the definition of the wave packet states (5.18) we obtain, in the limit of small wave packets, $d\mu(p_m) = \frac{d^3p'_m}{(4\pi\sigma)^3}$. The rest of the calculations is almost analogous to the calculations in scalar QED. In the following we outline the calculations for one of the "addends" in the symmetrizing sum for the particle part of the propagator.

$$\begin{aligned}
&S_2(k,\lambda,k',\lambda',p'(\pm),p'_\perp,s',p,s) = -\tfrac{e^2}{2}\int dx_{1,3}\int dx_{2,3}\phi^*_{k,\lambda,\mu}(x_{1,3})\phi^*_{k',\lambda',\nu}(x_{2,3})\times \\
&\times\sum\nolimits_{s_q}\int \tfrac{d^3q}{(2\pi\hbar)^3}\bar{\phi}^{(p)}_{out,p'(\pm),s'}(x_{1,3})\gamma^\mu\phi^{(p)}_{out,q,s_q}(x_{1,3})\bar{\phi}^{(p)}_{out,q,s_q}(x_{2,3})\gamma^\nu\phi^{(p)}_{in,p(+),s}(x_{2,3})\times \\
&\times(2\pi\hbar)^3\delta^{(2)}\left(k_\perp+p'_\perp+k'_\perp-p_\perp\right)\delta\left(k_0+p'_0+k'_0-p_0\right)\times \\
&\times(2\pi\hbar)^2\delta^{(2)}\left(\tfrac{1}{2}(k_\perp+p'_\perp-(k'_\perp-p_\perp))-q_\perp\right)\hbar\Big(\pi\delta\left(\tfrac{1}{2}(k_0+p'_0-(k'_0-p_0))-q_0\right) \\
&+i\mathcal{P}\tfrac{1}{\frac{1}{2}(k_0+p'_0-(k'_0-p_0))-q_0}\Big)\ {}_{out}\langle\Omega|\Omega\rangle_{in}
\end{aligned} \tag{5.52}$$

This expression can be separated into a part with energy conservation at both vertices, from the last delta function and a part contradicting this conservation, from the Cauchy principal value. Using arguments like those taking us from equation (5.17) to (5.21) in the first order perturbation theory, the first three delta functions can easily be evaluated for the limitting case of small wave packets.

We find, after some rearrangements and with the definition $p_2 := p' + p$,

$$\begin{aligned} M_2(k,\lambda,k',\lambda',p'(\pm)_m,s',p_m,s) = -\tfrac{e^2}{2}\tfrac{c}{2\epsilon_0\hbar\sqrt{k_0k_0'}}\int dz_1 \int dz_2 \tfrac{\hbar c}{2eE}\times \\ \times \textstyle\sum_{s_q}\int \frac{dq_3}{2\pi\hbar}\frac{1}{2}\int \frac{dp_{2,0}}{2\pi\hbar}\frac{dp_3}{dp_0}\frac{dp_3'}{dp_0'}\varphi_{p'_{m,3}}(p_3')\varphi_{p_{m,3}}(p_3)\phi^*_{k,\lambda,\mu}(z_1)\phi^*_{k',\lambda',\nu}(z_2)\times \\ \times \bar{\phi}^{(p)}_{out,p'_{m,\perp},p'(\pm),s'}(z_1)\gamma^\mu\phi^{(p)}_{out,q_\perp,q_3,s_q}(z_1)\bar{\phi}^{(p)}_{out,q_\perp,q_3,s_q}(z_2)\gamma^\nu\phi^{(p)}_{in,p_{m,\perp},p(+),s}(z_2)\times \\ \times\hbar\left(\pi\delta\left(\tfrac{1}{2}(p_{2,0}+k_0-k_0')-q_0\right)+i\mathcal{P}\tfrac{1}{\frac{1}{2}(p_{2,0}+k_0-k_0')-q_0}\right)\ {}_{out}\langle\Omega|\Omega\rangle_{in} \end{aligned} \tag{5.53}$$

where $p_0 - p_0' = k_0 + k_0'$, $p_{m,\perp} - p'_{m,\perp} = k_\perp + k'_\perp$ and $q_\perp = p_{m,\perp} - k_\perp$ and

$$\begin{aligned} \tfrac{d\sigma}{d\Omega_k d\Omega_{k'}}\Big|_{\hat{k},\lambda,\hat{k}',\lambda',p_m,s} &= \int \tfrac{dk_0}{(2\pi\hbar)^3}k_0^2\int\tfrac{dk_0'}{(2\pi\hbar)^3}k_0'^2\times \\ &\quad\times\textstyle\sum_{s'}\int\frac{dp'(\pm)_m}{4\pi\sigma}M_2(k,\lambda,k',\lambda',p'(\pm),s',p_m,s) \end{aligned} \tag{5.54}$$

where $\hat{k} = \frac{k}{k_0}$.

Now the energy conservation part could be evaluated like the other delta functions simply by assuming small wave packet states. Thus the results for this part do not depend on the form of the wave packets. In contrast, the Cauchy principal value term must be evaluated by integration over the momentum space distribution, $\varphi_{p_m}(p)$, of the wave packets. This can be done numerically by expending a large amount of computation time. We postpone the computation of probability distributions in the momentum space of the emitted photons to further work.

From equation (5.53) and from the solutions of the Dirac equation we obtain that, for $p_\perp = 0$ and $k_\perp = k'_\perp = 0$, only processes with two spin-flips contribute to the differential emission probability. This can easily be seen when we take into account that the second order process is just an evarage over the iteration of two first order processes where the transversal momentum of the intermediate state $q_\perp$ is fixed by momentum conservation and $p_\perp = 0$ and $k_\perp = k'_\perp = 0$ give $q_\perp = 0$ and $p'_\perp = 0$.

The computation of several selected values for the momenta of the emitted photons show that, in the parameter domain used for the computation illustrated in figure 5.9, the Cauchy principal value term is of the order of the delta function term. Thus the probability of the emission of a photon pair in forward direction is in the order of the square of the probability of the first order spin-flip process given in equation (5.47). Hence gor electrons there is no blind spot for photon pairs when both photons are emitted exactly in the acceleration direction. However, the finite accuracy of photon detection devices makes it impossible to implement such strong restrictions on the photon momenta in real experimental situations. We must therefore consider a distribution for the transversal momenta of the emitted photons appropriate to the detection device. This could be done numerically for the respective experimental situation using the formulas given above. If the uncertainty in the transversal momenta is large enough the spin-conserving process will take over and give a larger contribution than the spin-flip process, even if the averaged photon momenta are parallel to the acceleration direction. Obviously, even in this situation, there is no blind spot that could simplify the detection of two photon radiation. To quantify the ratio between the probability of the second order and that of the first order process we have to compute the probability of these processes in the six dimensional momentum space of the two emitted photons. However, for single electron experiments, the application of two photon coincidence detection devices could be used to blank out the first order processes. The efficiency of the two photon coincidence measurement depends on the correlations of the two emitted photons in the continious space variables and thus on the ratio of second order processes where the emitted two photons really can be denoted as a photon pair. Therefore we would have to compute the differential emission probability for the whole six dimensional momentum space of the two emitted photons and use the methods outlined in ref. [40] to quantify the degree of entanglement. Unfortunately, using the current version of our framework a huge amount of computation time must be expended to compute the differential irradiation propability of the second order process for more than a few points in momentum space. This can hardly be provided by a desktop pc. Hence we have to postpone the investigation of the

corresponding questions to further work.

5.4 Polarization entanglement of photon pairs in second order perturbation theory

In the following we discuss conclusions about the entanglement of the emitted photon pairs in their polarization degree of freedom. Due to the difficulties discussed above we restrict our considerations to statements which can be extracted from the structure of the expression for M_2 in equation (5.53) and from numerical results of this expression for several selected values of the photon momenta. First of all we investigate the expression

$$\bar{\phi}^{(p)}_{out,p'_{m,\perp},p'(\pm),s'}(z_1)\gamma^\mu\phi^{(p)}_{out,q_\perp,q_3,s_q}(z_1) \tag{5.55}$$

for $\nu = 1$ and $\nu = 2$ and obtain, from the solutions of the Dirac equation, that for $k_\perp = k'_\perp = 0$ they only differ by a factor i. From equation (5.20) and its counterpart, where the photon momenta have been swaped, we conclude that emitted photon pairs with momenta in the acceleration direction are in the following polarization state:

$$|pol\rangle = \frac{1}{2^{3/2}}\left((|1\rangle + i|2\rangle)(|1\rangle - i|2\rangle) + (|1\rangle - i|2\rangle)(|1\rangle + i|2\rangle)\right) \tag{5.56}$$

where the states $|1\rangle$ and $|2\rangle$ correspond to polarization in x_1 and x_2 direction respectively. Hence the emitted photon pair is circularly polarized and maximally entangled in the polarization degree of freedom. Numerical investigations show that for $|k_\perp| = |k'_\perp| = k_0$ the probability of the emission of photon pairs with polarization vector lying in the k_3-$k_\perp$-plane is a factor 10^5 larger than the probability of the emission of pairs with polarization perpendicular to this plane. Thus for these values of the photon momenta the photon pair is almost in a product state and therefore barely entangled. With some effort, one could compute numerically the degree of entanglement for the

whole domain of interest of the photon pair's momentum space. However, even this qualitative result differs strongly from the results found in [3] and [4] where the photon pairs are maximally entangled in the polarization degree of freedom for all emission directions. This should be of interest when discussing the detectability of the photon pairs; a photon pair consisting of wave packet states in the transversal momentum $k_\perp$ will clearly not be maximally entangled in its polarization degree of freedom. Further investigation could give information on the degree of entanglement of the photon pairs. We could than contemplate the usefulness of this entanglement for the detection and the useability of acceleration emission processes as sources of entangled photons in quantum optical experiments.

Chapter 6

Conclusions and options for further work

We have seen that the emission of entangled photon pairs from transiently accelerated charges can be derived in the framework of Quantum Electrodynamics in a classical electromagnetic background field. We have obtained that the second order perturbation theory for a background field QED can be derived using the techniques of causal perturbation theory. In ref. [36] the authors show that, in scalar QED, counterterms have to be added to the second order term to achieve a regularized expression. In [24] the authors show that for tree graph processes as in figure 5.6 and 5.7 no counterterms are needed and the construction of the second order can be performed naively simply by multiplication of the fermionic propagator with Heaviside step functions. These results and the fact that spinor QED applies to particles that actually exist, namely electrons, have encouraged us to look at the full second order theory for spinor QED only. However, we have shown that in scalar QED one part of the interaction Hamiltonian, $\mathcal{H}_4$, - which is of second order in the interaction constant e - gives, in the semiclassical approximation, an effective theory for emission of photon pairs from an accelerated spinless point particle that is equivalent to the results of ref. [3].

For spinor QED we have derived an expression for the S-matrix elements of the processes illustrated in figure 5.1 and 5.6 in first and second order perturbation theory respectively, neglecting the effects of pair creation by confining the electric background field to be significantly below the

Schwinger limit (2.22). The investigation of the additional terms that arise for field strengths close to the Schwinger limit would be an interesting task for further investigations. By considering the processes 5.1 and 5.6 we have obtained that, in the first order, the differential emission probability looks, for the most part, like the angular distribution of classical Larmor radiation emitted by an accelerated point charge. However, in contrast to classical theory and first order of scalar QED, in spinor QED, due to the spin-flip process, there is no blind spot in the acceleration direction (see figure 5.9). We have seen that, in experimentally realisable situations far below the Schwinger limit, this spin-flip process is strongly suppressed. Even then there is no blind spot for the detection of second order photon pair radiation in the acceleration direction since the only process giving a nonzero result in the acceleration direction is a combination of two spin-flip processes. Obviously we do not get a blind spot by easing the restriction on the emission direction to a larger solid angle around the acceleration direction; there is then first order spin-conserving radiation emitted by the photon. There could be a certain solid angle domain around the acceleration direction where the ratio between the total probability of the detection of second order emission and that for the detection of first order emission has a maximum. To investigate this we have to calculate the mentioned ratio in the corresponding domain of the six dimensional momentum space of the two photons. We have argued that, in order to solve the problem of the detection of two-photon-emission, it could be usefull to know the correlation properties of these photons. We have obtained that photon pairs emitted in the acceleration direction are maximally entangled in their polarization degrees of freedom and that those emitted perpendicular to the acceleration direction are barely entangled. It would be valuable to compute the degree of entanglement for the whole domain of interest in the momentum space of the photon pairs. A further interesting task would be to derive the entanglement of the photon pairs in the continous momentum and space variables. The results would be of use when discussing the applicability of two photon coincidence measurements for the detection of two photon radiation and when quantifying the usefulness of the two-photon-emission process as a source of entangled photon pairs for quantum optical experiments. However, using the current analytic version of our framework

to carry out all these tasks would take an amount of numerical computation time that can hardly be provided by a desktop pc.

Vast opportunities lie in the development of an effective theory using semiclassical methods as it is done for scalar QED in ref. [37]. For spinor QED we need semiclassical solutions of the Dirac equation in an electric background field. Approaches for finding these solutions are controversely discussed in literature like ref. [38] and [39] and contain subtleties that are related to the spin transport term which gives a complex contribution in an electric field.

All our results show that Quantum Electrodynamics can be used to describe photon emission phenomena in experimentally realisable situations. QED predicts several interesting effects that are not inherent in Quantum Optics due to the lack of the spin in this theory. Furthermore, the framework developed in this thesis can be adopted to any other background field constellation, including magnetic fields, without considerably more effort. For example it would be interesting to investigate the emission properties of electrons in a strong laser background field modelled by a plane wave. The solutions of the corresponding particle wave equations are the so-called Volkov solutions which are well studied in literature like ref. [33], [41] and [42]. Another interesting approach would be to place the acceleration region in a resonator cavity to enhance the emission in a certain domain of the spectrum. For an accelerated two level atom such a setting was investigated in ref. [43] with quantum optical techniques.

All these opportunities encourage further investigations in the direction we tried to shed light onto in this thesis. We believe the results show the value of the description of photon emission processes from charged particles in the framework of QED that we would call QED Optics.

Chapter 7

Appendix

7.1 Some relations for parabolic cylinder functions

For the sake of completeness we present here some relations satisfied by the parabolic cylinder functions $D_n[z]$ we used for our calculations. We begin with the asymptotic expansion formulas. They are valid for the arguement of $D_n[z]$ much larger than the parameter n.

$$D_n[z] \approx$$

$$\begin{cases} z^n e^{-\frac{z^2}{4}} \left(1 - \frac{(n-1)n}{2z^2} + \frac{(n-3)(n-2)(n-1)n}{8z^4} + O\left(z^{-6}\right)\right) \\ \qquad : -\frac{\pi}{2} < arg(z) < \frac{\pi}{2} \\ \\ z^n e^{-\frac{z^2}{4}} \left(1 - \frac{(n-1)n}{2z^2} + \frac{(n-3)(n-2)(n-1)n}{8z^4} + O\left(z^{-6}\right)\right) \\ -\frac{\sqrt{2\pi}}{\Gamma[-n]} e^{-i\pi n} z^{-n-1} e^{\frac{z^2}{4}} \left(1 + \frac{(n+1)(n+2)}{2z^2} + \frac{(n+1)(n+2)(n+3)(n+4)}{8z^4} + O\left(z^{-6}\right)\right) \\ \qquad : arg(z) < -\frac{\pi}{2} \end{cases} \tag{7.1}$$

The following relations are algebraic relations between the $D_n[x]$ of different n and the derivative of $D_n[x]$.

$$\begin{aligned} D_n'[z] + \tfrac{1}{2} z D_n[z] &= n D_{n-1}[z] \\ D_n'[z] - \tfrac{1}{2} z D_n[z] &= -D_{n+1}[z] \end{aligned} \tag{7.2}$$

7.2 Solutions of the Klein-Gordon equation

To present the wave functions as compactly as possible we introduce a sign for the momenta $\tilde{p}(+)$ and $\tilde{p}(-)$.

$$\tilde{p}(-) \begin{cases} \leq 0 & for \quad \tilde{p}_0 < -\frac{z_0}{2} \\ \geq 0 & for \quad \tilde{p}_0 > -\frac{z_0}{2} \end{cases} \qquad \tilde{p}(+) \begin{cases} \leq 0 & for \quad \tilde{p}_0 < \frac{z_0}{2} \\ \geq 0 & for \quad \tilde{p}_0 > \frac{z_0}{2} \end{cases} \tag{7.3}$$

Thus we get in the different domains

	Section 1	Section 2	Section 3
$\tilde{p}(-)$	≤ 0	≥ 0	≥ 0
$\tilde{p}(+)$	≤ 0	≤ 0	≥ 0.

(7.4)

We rename the coefficients and make some definitions:

$$\begin{aligned} A &:= \gamma(D_n'[-\gamma(z_0 - 2\tilde{p}_0)]D_n'[-\gamma(z_0 + 2\tilde{p}_0)] - D_n'[\gamma(z_0 - 2\tilde{p}_0)]D_n'[\gamma(z_0 + 2\tilde{p}_0)]), \\ B &:= (D_n[-\gamma(z_0 - 2\tilde{p}_0)]D_n'[-\gamma(z_0 + 2\tilde{p}_0)] + D_n[\gamma(z_0 - 2\tilde{p}_0)]D_n'[\gamma(z_0 + 2\tilde{p}_0)]), \\ C &:= (D_n'[-\gamma(z_0 - 2\tilde{p}_0)]D_n[-\gamma(z_0 + 2\tilde{p}_0)] + D_n'[\gamma(z_0 - 2\tilde{p}_0)]D_n[\gamma(z_0 + 2\tilde{p}_0)]), \\ D &:= \gamma^{-1}(D_n[-\gamma(z_0 - 2\tilde{p}_0)]D_n[-\gamma(z_0 + 2\tilde{p}_0)] - D_n[\gamma(z_0 - 2\tilde{p}_0)]D_n[\gamma(z_0 + 2\tilde{p}_0)]) \end{aligned}$$

where the prime indicates the derivation with respect to the argument of D_n and

$$\text{the Wronskian} \qquad k := D_n[-z]\frac{d}{dz}D_n[z] - D_n[z]\frac{d}{dz}D_n[-z] = -\frac{\sqrt{2\pi}}{\Gamma(-n)}$$

$$\text{and} \qquad \tilde{\pi}_0(-) := \tilde{p}_0 + \frac{z_0}{2} \qquad \tilde{\pi}_0(+) := \tilde{p}_0 - \frac{z_0}{2}$$

With these definitions and the requirements stated above we arrive at the following wave functions for the left side:

$$\phi_{in,p(-)}(z) = \begin{cases} c_1(c_L)e^{-i\tilde{p}(-)z} + c_L e^{i\tilde{p}(-)z} & : \quad x_3 < -x_{3,0} \\ A(c_L)D_n[\gamma(z-2\tilde{p}_0)] & \\ +B(c_L)D_n[-\gamma(z-2\tilde{p}_0)] & : \quad -x_{3,0} \leq x_3 \leq x_{3,0} \\ c_2(c_L)e^{i\tilde{p}(+)z} & : \quad x_{3,0} < x_3 \end{cases} \tag{7.5}$$

where $c_L = \left(\frac{\hbar c}{8eE|\tilde{\pi}_0(-)|^2}\right)^{\frac{1}{4}}$ and

$$\begin{aligned} c_2(c_L) &= \frac{2i\tilde{p}(-)kc_L e^{-i(\tilde{p}(-)+\tilde{p}(+))z_0}}{A + i\tilde{p}(+)B + i\tilde{p}(-)C - \tilde{p}(+)\tilde{p}(-)D} \\ c_1(c_L) &= c_L e^{-2i\tilde{p}(-)z_0}\frac{-A - i\tilde{p}(+)B + i\tilde{p}(-)C - \tilde{p}(+)\tilde{p}(-)D}{A + i\tilde{p}(+)B + i\tilde{p}(-)C - \tilde{p}(+)\tilde{p}(-)D} \\ A(c_L) &= \frac{1}{k}c_2(c_L)e^{i\tilde{p}(+)z_0}(D_n'[-\gamma(z_0-2\tilde{p}_0)] + \gamma\tilde{p}(+)D_n[-\gamma(z_0-2\tilde{p}_0)]) \\ B(c_L) &= \frac{1}{k}c_2(c_L)e^{i\tilde{p}(+)z_0}(D_n'[\gamma(z_0-2\tilde{p}_0)] - \gamma\tilde{p}(+)D_n[\gamma(z_0-2\tilde{p}_0)]). \end{aligned}$$

From these functions we find by the transformations $z \to -z$, $\tilde{p}_0 \to -\tilde{p}_0$, $c_1 \leftrightarrow c_2$, $c_L \to c_R$ and $A \leftrightarrow B$ for the right side

$$\phi_{in,p(+)}(z) = \begin{cases} c_1(c_R)e^{-i\tilde{p}(-)z} & : \quad x_3 < -x_{3,0} \\ A(c_R)D_n[\gamma(z-2\tilde{p}_0)] & \\ +B(c_R)D_n[-\gamma(z-2\tilde{p}_0)] & : \quad -x_{3,0} \leq x_3 \leq x_{3,0} \\ c_R e^{-i\tilde{p}(+)z} + c_2(a_2)e^{i\tilde{p}(+)z} & : \quad x_{3,0} < x_3 \end{cases} \tag{7.6}$$

where $c_R = \left(\frac{\hbar c}{8eE|\tilde{\pi}_0(+)|^2}\right)^{\frac{1}{4}}$ and

$$\begin{aligned}
c_1(c_R) &= \frac{2i\tilde{p}(+)kc_R e^{-i(\tilde{p}(-)+\tilde{p}(+))z_0}}{A + i\tilde{p}(+)B + i\tilde{p}(-)C - \tilde{p}(+)\tilde{p}(-)D} \\
c_2(c_R) &= c_R e^{-2i\tilde{p}(+)z_0} \frac{-A + i\tilde{p}(+)B - i\tilde{p}(-)C - \tilde{p}(+)\tilde{p}(-)D}{A + i\tilde{p}(+)B + i\tilde{p}(-)C - \tilde{p}(+)\tilde{p}(-)D} \\
A(c_R) &= \frac{1}{k} c_1(c_R) e^{i\tilde{p}(-)z_0} (D'_n[\gamma(z_0 + 2\tilde{p}_0)] - \gamma\tilde{p}(-)D_n[\gamma(z_0 + 2\tilde{p}_0)]) \\
B(c_R) &= \frac{1}{k} c_1(c_R) e^{i\tilde{p}(-)z_0} (D'_n[-\gamma(z_0 + 2\tilde{p}_0)] + \gamma\tilde{p}(-)D_n[-\gamma(z_0 + 2\tilde{p}_0)]).
\end{aligned}$$

7.3 Orthonormality of the solution

To prove the orthogonality relations (2.19) we follow closely ref. [14]. To make it mathematically clearer we use explicitly methods from the theory of generalized functions [26]. First we define $\mathcal{D}(\mathbb{R})$ as the space of testfunctions over $\mathbb{R}$ and with $\phi \in \mathcal{D}(\mathbb{R})$ we get from (2.19) the following statement:

$$\begin{aligned}
\int dp(\pm)\varphi(p(\pm))(\Phi^{(p,a)}_{in,out,p(\pm)}, \Phi^{(p,a)}_{in,out,p'(\pm)})_{KG} &= \epsilon_{p,a} 2\pi\hbar\phi(p'(\pm)) 4\pi^2\hbar^2\delta^{(2)}(p_\perp - p'_\perp) \\
\int dp(\pm)\varphi(p(\pm))(\Phi^{(p,a)}_{in,out,p(-)}, \Phi^{(p,a)}_{in,out,p'(+)})_{KG} &= 0
\end{aligned} \tag{7.7}$$

Let us start with the first equation. Since in section 7.2 the wave functions are not very handy we use a trick to restrict our calculations to sections I and III [14]. With the definition of the Klein-Gordon current

$$j_\mu(\phi_{p_0}, \phi_{p'_0}) = -ie(\phi^*_{p_0} D_\mu \phi_{p'_0} - (D_\mu \phi_{p_0})^* \phi_{p'_0}) \tag{7.8}$$

we get, after a derivation and some rearrangements, the relation

$$j_0(\phi_{p_0}, \phi_{p'_0}) = \frac{i\hbar}{p_0 - p'_0} \frac{d}{dx_3} j_3(\phi_{p_0}, \phi_{p'_0}) = \frac{i}{\tilde{p}_0 - \tilde{p}'_0} \frac{d}{dz} j_3(\phi_{p_0}, \phi_{p'_0}) \tag{7.9}$$

Since $j_0(\phi_1,\phi_2) = e(\phi_1,\phi_2)_{KG}$ and by using the dimensionless variables defined in (2.7) we write (7.7) as

$$S(p'(\pm)) := -iN \lim_{\sigma\to\infty} \int d\tilde{p}(\pm)\varphi(\sqrt{\tfrac{2eE\hbar}{c}}\tilde{p}(\pm)) \int_{L_d(\sigma)}^{L_u(\sigma)} dz \tfrac{i}{\tilde{p}_0-\tilde{p}'_0}\times$$

$$\times \tfrac{d}{dz}\left(\phi^{(p,a)*}_{in,out,\tilde{p}(\pm)}(z)\tfrac{d}{dz}\phi^{(p,a)}_{in,out,\tilde{p}'(\pm)}(z) - \tfrac{d}{dz}\phi^{(p,a)*}_{in,out,\tilde{p}(\pm)}(z)\phi^{(p,a)}_{in,out,\tilde{p}'(\pm)}(z)\right)$$

$$= N \lim_{\sigma\to\infty} \int dp(\pm)\tilde{\varphi}(\tilde{p}(\pm))\tfrac{i}{\tilde{p}_0-\tilde{p}'_0}\times \tag{7.10}$$

$$\times \left(\phi^{(p,a)*}_{in,out,\tilde{p}(\pm)}(z)\tfrac{d}{dz}\phi^{(p,a)}_{in,out,\tilde{p}'(\pm)}(z) - \tfrac{d}{dz}\phi^{(p,a)*}_{in,out,\tilde{p}(\pm)}(z)\phi^{(p,a)}_{in,out,\tilde{p}'(\pm)}(z)\right)\Big|_{L_d(\sigma)}^{L_u(\sigma)} \times$$

$$\times\epsilon_{p,a}2\pi N\tilde{\varphi}(\tilde{p}'(\pm)) = \epsilon_{p,a}2\pi\hbar\varphi(p'(\pm))$$

where $L_d(\sigma)$ and $L_u(\sigma)$ are functions, which will be defined later, with the property $L_d(\sigma)\to-\infty$ and $L_u(\sigma)\to\infty$ for $\sigma\to\infty$ and $N = \sqrt{\frac{2eE\hbar}{c}}$. To keep the notation clean we drop the tilde over the momenta and energies and over φ.

We demonstrate the proofe for the in-propagating wave functions from the left only since by the transformations $z\to -z$, $p_0\to -p_0$, $a_1\leftrightarrow b_2$, $b_1\leftrightarrow a_2$ and $A\leftrightarrow B$ we get the proofe for the in-propagating wave functions from the right and by complex conjugation we get the proofe for the out-propagating wave functions. With the definition in (7.5) and the additional definitions

$$b'_2 = \frac{b_2}{b_1} \qquad a'_1 = \frac{a_1}{b_1} \tag{7.11}$$

we obtain

$$S(p'(-)) = iN \lim_{\sigma\to\infty} \int dp(-)\varphi(p(-))\tfrac{1}{p_0-p_0'}\times$$

$$\times\left(\tfrac{b_2'^*(p(-))b_2'(p'(-))}{\sqrt{4|\pi_0(-)\pi_0'(-)|}}(p'(+)+p(+))e^{i(p'(+)-p(+))L_u(\sigma)}\right.$$

$$-\tfrac{1}{\sqrt{4|\pi_0(-)\pi_0'(-)|}}\left(-a_1'^*(p(-))a_1'(p'(-))(p'(-)+p(-))e^{-i(p'(-)-p(-))L_d(\sigma)}\right. \tag{7.12}$$

$$+(p'(-)+p(-))e^{i(p'(-)-p(-))L_d(\sigma)} - a_1'(p'(-))(p'(-)-p(-))e^{-i(p'(-)+p(-))L_d(\sigma)}$$

$$\left.\left.+a_1'^*(p(-))(p'(-)-p(-))e^{i(p'(-)-p(-))L_d(\sigma)}\right)\right)$$

With some rearrangements we find the relation

$$(p'(-)-p(-))(p'(-)+p(-)) = (\pi_0'(-)+\pi_0(-))(p_0'-p_0) \tag{7.13}$$

Now we investigate the last two terms of (7.12). We denote them as $S^2(p'(-))$ and get after some rearrangements and a partial integration

$$S^2(p'(-)) = -iN \lim_{\sigma\to\infty} \tfrac{1}{iL_d(\sigma)} \int dp(-)\varphi(p(-))\tfrac{\pi_0'(-)+\pi_0(-)}{p'(-)+p(-)}\tfrac{1}{\sqrt{4|\pi_0(-)\pi_0'(-)|}}\times$$

$$\times\left(a_1'(p'(-))(p'(-)-p(-))e^{-i(p'(-)+p(-))L_d(\sigma)}\right. \tag{7.14}$$

$$\left.-a_1'^*(p(-))(p'(-)-p(-))e^{i(p'(-)-p(-))L_d(\sigma)}\right)$$

This expression is zero if the derivative of the integrand is uniformly continuous in its entire domain

since by a partial integration we obtain

$$\lim_{\sigma\to 0}\int dp\, f(p)e^{ip\sigma} = -\lim_{\sigma\to 0}\int dp \frac{d}{dp}(f(p))\frac{1}{i\sigma}e^{ip\sigma} = 0 \tag{7.15}$$

for uniformly continuous f. Thus we have to investigate the coefficient

$$a_1'(p(-)) = e^{-2ip(-)z_0}\frac{-A - ip(+)B + ip(-)C - p(+)p(-)D}{A + ip(+)B + ip(-)C - p(+)p(-)D}. \tag{7.16}$$

We have to ensure that its denominator is unequal to zero in the whole domain. We define

$$G = A + ip(+)B + ip(-)C - p(+)p(-)D. \tag{7.17}$$

For small $p(-)$ we have to investigate G numerically and for large values of $|p(-)|$ we do it with the asymptotic expansions of ref. [10]. In figure 7.1 we plotted G with *Mathematica 6* in the parameter range we used in our simulations in chapter two. For large values of $|p(-)|$ we get

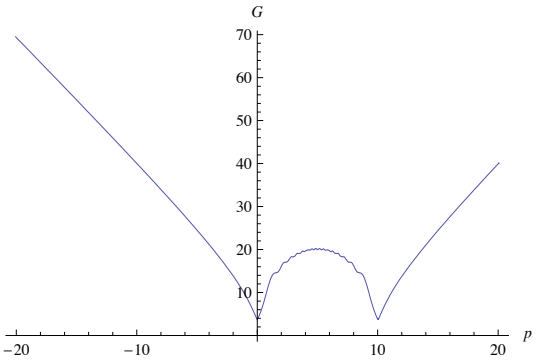

Figure 7.1: Plot of the denominator G of a_1' in dependence of the dimensionless variable $p(-)$. The system parameters are again $x_{3,0} = 10^{-12}$m and $eE = 10\frac{\mathrm{J}}{\mathrm{m}}$ and the mass is the electron mass. Obviously in the depicted interval G is larger than zero.

$$|G| \to \left| n\frac{\sqrt{2\pi}}{\Gamma(-n+1)} \right| 2p_0. \tag{7.18}$$

These investigations show that $|G| \neq 0$ in its whole domain and thus we proved that $S^2(p'(-)) = 0$.

The next step is to investigate the first three terms in (7.12).

$$S^1(p'(-)) = iN \lim_{\sigma\to\infty} \int dp(-)\varphi(p(-)) \tfrac{\pi_0'(-)+\pi_0(-)}{p'(-)-p(-)}$$

$$\left(\tfrac{b_2'^*(p(-))b_2'(p'(-))}{\sqrt{4|\pi_0(-)\pi_0'(-)|}} \tfrac{p'(+)+p(+)}{p'(-)+p(-)} e^{i(p'(-)-p(-))L_u(\sigma)\frac{p'(+)-p(+)}{p'(-)-p(-)}} \right. \tag{7.19}$$

$$\left. - \tfrac{1}{\sqrt{4|\pi_0(-)\pi_0'(-)|}} \left(e^{i(p'(-)-p(-))L_d(\sigma)} - a_1'^*(p(-))a_1'(p'(-))e^{-i(p'(-)-p(-))L_d(\sigma)} \right) \right)$$

Since the coefficient

$$b_2'(p(-)) = \frac{2ip(-)ke^{-i(p(-)+p(+))z_0}}{A + ip(+)B + ip(-)C - p(+)p(-)D} \tag{7.20}$$

has the same denominator as $a_1'(p(-))$ it is uniformly continuous in its whole domain. We obtain that up to the factor $p'(-) - p(-)$ the whole integrand is uniformly continuous. We define

$$L_u(\sigma)\frac{p'(+) - p(+)}{p'(-) - p(-)} := L_d(\sigma) \quad \text{and} \tag{7.21}$$

$$\tilde{\varphi}_1 := (\pi_0'(-) + \pi_0(-) \tfrac{)b_2'^*(p(-))b_2'(p'(-))}{\sqrt{4|\pi_0(-)\pi_0'(-)|}} \tfrac{p'(+)+p(+)}{p'(-)+p(-)}\varphi$$

$$\tilde{\varphi}_2 := (\pi_0'(-) + \pi_0(-)) \tfrac{1}{\sqrt{4|\pi_0(-)\pi_0'(-)|}}\varphi \tag{7.22}$$

$$\tilde{\varphi}_3 := (\pi_0'(-) + \pi_0(-)) \tfrac{a_1'^*(p(-))a_1'(p'(-))}{\sqrt{4|\pi_0(-)\pi_0'(-)|}}\varphi.$$

For further investigations we have to consider the split of the energy axis described in figure 2.1. If we restrict our considerations to wave functions where $p(-)$ and $p'(-)$ are in the same domain of the energy axis we obtain that the denominator of the three functions defined in (7.22) is larger than zero due to the properties of G stated above. Hence the functions in (7.22) are uniformly continuous at least for $p(-)$ and $p'(-)$ in the same domain of the energy axis. However, considering (7.12) we obtain that this is true even for $p(-)$ and $p'(-)$ in different domains. Additionally since

$\varphi \in \mathcal{D}(\mathbb{R})$ we obtain that $\tilde{\varphi}_1$, $\tilde{\varphi}_2$ and $\tilde{\varphi}_3$ have compact support. Now let $N \in \mathbb{R}$ be given such that $supp(\varphi) \subset [-N+p(-), N+p(-)]$. Thus we can use for each of the three terms in (7.19) the following relation which holds for any linear function $\eta(p(-))$ and for any continuous function $\tilde{\varphi}$ with compact support $supp(\tilde{\varphi}) \subset [-N+p(-), N+p(-)]$:

$$\lim_{\sigma\to\infty} \int_{-N+p'(-)}^{N+p'(-)} dp(-) \frac{\tilde{\varphi}(p(-))}{p(-)-p'(-)} e^{(\eta(p(-))\pm\eta(p'(-)))\sigma}$$

$$= \lim_{\sigma\to\infty} \int_{-N+p'(-)}^{N+p'(-)} dp(-) \left(\frac{\tilde{\varphi}(p(-))-\tilde{\varphi}(p'(-))}{p(-)-p'(-)} e^{(\eta(p(-))\pm\eta(p'(-)))\sigma} \right.$$

$$\left. + \frac{\tilde{\varphi}(p'(-))}{p(-)-p'(-)} e^{(\eta(p(-))\pm\eta(p'(-)))\sigma} \right) \tag{7.23}$$

$$= 0 + \tilde{\varphi}(p'(-)) \lim_{\sigma\to\infty} \int_{-\sigma(N-p'(-))}^{\sigma(N+p'(-))} d(\sigma p(-)) \frac{1}{\sigma(p(-)-p'(-))} e^{\eta(\sigma p(-))\pm\eta(\sigma p'(-)))}$$

$$= \tilde{\varphi}(p'(-)) \int_{-\infty}^{\infty} d\tilde{p}(-) \frac{1}{\tilde{p}(-)-\tilde{p}'(-)} e^{\eta(\tilde{p}(-))\pm\eta(\tilde{p}'(-)))}$$

Due to the translation invariance of this integral we find

$$S^1(p'(-)) = N sgn(\pi_0'(-)) i\varphi(p'(-)) \times$$

$$\times \left(\int dy \frac{e^{iy}}{y} - \left(|b_2'(p'(-))|^2 \frac{p'(+)}{p'(-)} + |a_1'(p'(-))|^2 \right) \int dy \frac{e^{-iy}}{y} \right) \tag{7.24}$$

$$= 2iN\, sgn(\pi_0'(-)) i\varphi(p'(-)) \int dy \frac{\sin y}{y} = \epsilon_{p,a} 2\pi N \varphi(p'(-))$$

since $|a_1'|^2 + \frac{p'(+)}{p'(-)}|b_2'|^2 = 1$ because of current conservation. $\square$

Finally we prove the second relation in (2.19). We do it explicitly for the in propating wave functions only since by complex conjugation we get the same statement for the out-propagating wave functions. Using simular rearrangements as we used at the beginning of the proof above we

find

$$S^3(p'(-)) = iN \lim_{\sigma\to\infty} \int dp(-)\varphi(p(-))\tfrac{1}{p_0-p'_0}\tfrac{1}{\sqrt{4|\pi_0(+)\pi'_0(-)|}}\times$$

$$\times \big(a'^*_2(p(+))b'_2(p'(-))(p'(+)-p(+))e^{i(p'(+)+p(+))L_u(\sigma)}$$

$$+b'^*_2(p(+))b'_2(p'(-))(p'(+)+p(+))e^{i(p'(+)-p(+))L_u(\sigma)} \tag{7.25}$$

$$+a'^*_1(p(+))a'_1(p'(-))(p'(-)+p(-))e^{-i(p'(-)-p(-))L_d(\sigma)}$$

$$+\, a'^*_1(p(+))b'_1(p'(-))(p'(-)-p(-))e^{i(p'(-)+p(-))L_d(\sigma)}\big)$$

Since G is the denominator of a'_1, a'_2, b'_1 and b'_2 and $G \leq 0$ the two terms with $p'(+)+p(+)$ in the exponent can be neglected due to the same arguments used for S^1 in the prove above and with the definitions

$$L_u := \frac{p_0-p'_0}{p(+)-p'(+)}\sigma \qquad L_d := \frac{p_0-p'_0}{p(-)-p'(-)}\sigma \tag{7.26}$$

we obtain from (7.25) by rearranging the remaining two terms with the relation (7.23)

$$\begin{aligned} S^3(p'(-)) \;&=\; iN\tfrac{\varphi(p(-))}{\sqrt{|\pi_0(+)\pi'_0(-)|}}\,(b'^*_2(p(+))b'_2(p(-))p(+) \\ &\qquad +a'^*_1(p(+))a'_1(p(-))p(-))\int dy\tfrac{e^{-iy}}{y} \end{aligned} \tag{7.27}$$

By representing $\phi_{in,p(\pm)}$ as a linear combination of $\phi_{in,p(\mp)}$ and $\phi_{out,p(\mp)}$ and by using the fact that for these functions the x_3-component of the four-current is conserved, i.e. $|a'_1|^2+\frac{p'(+)}{p'(-)}|b'_2|^2=1$, we get

$$b'^*_2(p(+))b'_2(p(-))p(+)+a'^*_1(p(+))a'_1(p(-))p(-)=0. \qquad \square$$

7.4 Solutions of the Dirac equation

In this section of the appendix we give explicit expressions for the left out-propagating particle states with spin up and spin down and for the left in-propagating state with spin down in part I and II of the x_3-axis. From the expressions in section 2.2 we get in section I of the x_3-axis

$$\begin{aligned}\tilde{\Psi}^{(p)}_{1,out,L} \overset{z<-z_0}{=} \frac{1}{2}\Bigg(\begin{pmatrix}0\\ \tilde{\pi}_0(-)+\mu\\ \tilde{p}_1-i\tilde{p}_2\\ -\tilde{p}(-)\end{pmatrix}\Big((b_{+1,-1}+b_{+1,+1})+\tfrac{-\tilde{p}(-)}{\tilde{\pi}_0(-)+\mu}(b_{+1,-1}-b_{+1,+1})\Big)\\ +\begin{pmatrix}\tilde{\pi}_0(-)+\mu\\ 0\\ \tilde{p}(-)\\ \tilde{p}_1+i\tilde{p}_2\end{pmatrix}(b_{+1,-1}-b_{+1,+1})\tfrac{\tilde{p}_1-i\tilde{p}_2}{\tilde{\pi}_0(-)+\mu}\Bigg)e^{i\tilde{p}(-)z}\\ +\begin{pmatrix}0\\ \tilde{\pi}_0(-)+\mu\\ \tilde{p}_1-i\tilde{p}_2\\ \tilde{p}(-)\end{pmatrix}\tfrac{1}{(2\tilde{\pi}_0(-)(\tilde{\pi}_0(-)+\mu))^{1/2}}e^{-i\tilde{p}(-)z}\end{aligned} \tag{7.28}$$

$$\tilde{\Psi}^{(p)}_{-1,out,L} \overset{z<-z_0}{=} \frac{1}{2}\left(\begin{pmatrix} \tilde{\pi}_0(-)+\mu \\ 0 \\ \tilde{p}(-) \\ \tilde{p}_1+i\tilde{p}_2 \end{pmatrix}\Big((b_{+1,-1}+b_{+1,+1})+\tfrac{-\tilde{p}(-)}{\tilde{\pi}_0(-)+\mu}(b_{+1,-1}-b_{+1,+1})\Big)\right.$$

$$\left.+\begin{pmatrix} 0 \\ \tilde{\pi}_0(-)+\mu \\ \tilde{p}_1-i\tilde{p}_2 \\ -\tilde{p}(-) \end{pmatrix}(b_{+1,-1}-b_{+1,+1})\tfrac{-(\tilde{p}_1+i\tilde{p}_2)}{\tilde{\pi}_0(-)+\mu}\right) e^{i\tilde{p}(-)z} \tag{7.29}$$

$$+\begin{pmatrix} \tilde{\pi}_0(-)+\mu \\ 0 \\ -\tilde{p}(-) \\ \tilde{p}_1+i\tilde{p}_2 \end{pmatrix}\tfrac{1}{(2\tilde{\pi}_0(-)(\tilde{\pi}_0(-)+\mu))^{1/2}}e^{-i\tilde{p}(-)z}$$

$$\tilde{\Psi}^{(p)}_{-1,in,R} \overset{z<-z_0}{=} \frac{1}{2}\left(\begin{pmatrix} \tilde{\pi}_0(-)+\mu \\ 0 \\ -\tilde{p}(-) \\ \tilde{p}_1+i\tilde{p}_2 \end{pmatrix}\Big((a_{+1,-1}+a_{+1,+1})+\tfrac{\tilde{p}(-)}{\tilde{\pi}_0(-)+\mu}(a_{+1,-1}-a_{+1,+1})\Big)\right. \tag{7.30}$$

$$\left.+\begin{pmatrix} 0 \\ \tilde{\pi}_0(-)+\mu \\ \tilde{p}_1-i\tilde{p}_2 \\ \tilde{p}(-) \end{pmatrix}(a_{+1,-1}-a_{+1,+1})\tfrac{-(\tilde{p}_1+i\tilde{p}_2)}{\tilde{\pi}_0(-)+\mu}\right) e^{-i\tilde{p}(-)z}$$

In the relativistic one particle quantum theory the coefficients in front of the spinors are interpreted as reflection and transmission coefficients. In this interpretation we obtain that for $p_1 = p_2 = 0$ the spin direction is conserved.

In section II of the x_3-axis we find

$$\begin{aligned}
\tilde{\Psi}_1^{(p)}(z) &= \tfrac{1}{2}\left(\begin{pmatrix} \tilde{p}_1 - i\tilde{p}_2 \\ \mu \\ \tilde{p}_1 - i\tilde{p}_2 \\ -\mu \end{pmatrix}\left(A_{-1}D_{n+1/2}[\gamma(z-2\tilde{p}_0)] + B_{-1}D_{n+1/2}[-\gamma(z-2\tilde{p}_0)]\right)\right. \\
&\quad -\tfrac{n+1/2}{\gamma}\begin{pmatrix} 0 \\ 1 \\ 0 \\ 1 \end{pmatrix}\left(A_{-1}D_{n-1/2}[\gamma(z-2\tilde{p}_0)] - B_{-1}D_{n-1/2}[-\gamma(z-2\tilde{p}_0)]\right) \\
&\quad +\begin{pmatrix} -(\tilde{p}_1 - i\tilde{p}_2) \\ \mu \\ \tilde{p}_1 - i\tilde{p}_2 \\ -\mu \end{pmatrix}\left(A_{+1}D_{n-1/2}[\gamma(z-2\tilde{p}_0)] + B_{+1}D_{n-1/2}[-\gamma(z-2\tilde{p}_0)]\right) \\
&\quad \left. -\tfrac{1}{\gamma}\begin{pmatrix} 0 \\ 1 \\ 0 \\ -1 \end{pmatrix}\left(A_{+1}D_{n+1/2}[\gamma(z-2\tilde{p}_0)] - B_{+1}D_{n+1/2}[-\gamma(z-2\tilde{p}_0)]\right)\right)
\end{aligned} \tag{7.31}$$

7.5 Pair creation coefficients

For the coefficients in equation (4.19) we find

$$\alpha_{+1,-1} = f(\tilde{p}_1 + i\tilde{p}_2)(\tilde{\pi}_0(+) + \mu)(c_{2,out,-1}(c_R) + c_{2,out,+1}(c_R))$$

$$\alpha_{-1,+1} = f(\tilde{p}_1 - i\tilde{p}_2)(\tilde{\pi}_0(+) + \mu)(c_{2,out,-1}(c_R) + c_{2,out,+1}(c_R))$$

$$\alpha_{+1,+1} = -\alpha_{-1,-1} = f\,(\tilde{p}_\perp^2(c_{2,out,-1}(c_R) - c_{2,out,+1}(c_R))$$

$$+\tilde{p}(+)((\tilde{\pi}_0(+) + \mu)(c_{2,out,-1}(c_R) + c_{2,out,+1}(c_R)) + \tilde{p}(+)(c_{2,out,-1}(c_R) - c_{2,out,+1}(c_R))))$$

where

$$f = \sqrt{2}(\tilde{\pi}_0(+)(\tilde{\pi}_0(+) - \mu))^{-1/2}(\tilde{p}_\perp^2(c_{2,out,-1}(c_R) - c_{2,out,+1}(c_R))^2$$

$$+((\tilde{\pi}_0(+) + \mu)(c_{2,out,-1}(c_R) + c_{2,out,+1}(c_R)) + \tilde{p}(+)(c_{2,out,-1}(c_R) - c_{2,out,+1}(c_R)))^2)^{-1}$$

7.6 Product of distributions

We want to investigate the generalized function

$$\int \mathcal{P}\delta := \int \frac{dp(+)}{2\pi}\varphi(p(+)) \int_{-\infty}^{z_0} dz e^{i(p'(\pm)-p(\pm)-k_3)z)} \int_{-\infty}^{\infty} e^{i(p'_0-p_0-k_0)x_{3,0)}}$$

$$= \lim_{\sigma\to\infty}\lim_{\eta\to\infty} \int \frac{dp(+)}{2\pi}\varphi(p(+)) \int_{-\sigma}^{0} dz' e^{i(p'(\pm)-p(\pm)-k_3)(z'-z_0)} \int_{-\eta}^{\eta} e^{i(p'_0-p_0-k_0)x_{3,0)}}$$

$$= \lim_{\sigma\to\infty}\lim_{\eta\to\infty} \int \frac{dp(+)}{2\pi}\varphi(p(+)) e^{-i(p'(\pm)-p(\pm)-k_3)z_0} \times$$

$$\times \frac{1 - e^{i(p'(\pm) - p(\pm) - k_3)\sigma}}{i(p'(\pm) - p(\pm) - k_3)} \frac{2\sin\left((p'_0 - p_0 - k_0)\eta\right)}{p'_0 - p_0 - k_0}.$$

To achieve this we have to split the integration over $p(+)$ into two sections.

$$\begin{aligned} I: &\qquad \exists p(+) : p'_0 - p_0 - k_0 = 0, &&\qquad p'(\pm) - p(\pm) - k_3 \neq 0 \quad \forall p(+) \\ II: &\qquad p'(\pm) - p(\pm) - k_3 \neq 0 \quad \forall p(+), \quad \exists p(+) : p'_0 - p_0 - k_0 = 0 \end{aligned} \tag{7.32}$$

For $k_0 \neq 0$ this splitting is possible since the scalar particles are massive and thus the equation $p'(\pm) - p(\pm) - k3 = 0$ has no real solutions.

In section I we define

$$\varphi_\eta(p(+)) := \varphi(p(+)) \frac{2\sin\left((p'_0 - p_0 - k_0)\eta\right)}{p'_0 - p_0 - k_0}.$$

Due to the conditions defined in (7.32), φ_η and all its derivatives are uniformly continuous for every $p(+)$. Thus we obtain

$$\begin{aligned} \left(\int \mathcal{P}\delta\right)_I &= \lim_{\sigma\to\infty}\lim_{\eta\to\infty} \int_a^b \frac{dp(+)}{2\pi} \varphi_\eta(p(+)) e^{-i(p'(\pm) - p(\pm) - k_3)z_0} \times \\ &\times \frac{1 - \cos\left((p'(\pm) - p(\pm) - k_3)\sigma\right) + i\sin\left((p'(\pm) - p(\pm) - k_3)\sigma\right)}{i(p'(\pm) - p(\pm) - k_3)} \\ &= \lim_{\eta\to\infty} \left(\varphi_\eta(p(+)(p', k3)\right) \\ &-i \lim_{\epsilon\to 0} \left(\int_a^{p'(\pm) - k_3 - \epsilon} + \int_{p'(\pm) - k_3 + \epsilon}^b \right) \frac{dp(+)}{2\pi} \frac{\varphi_\eta(p(+))}{p'(\pm) - p(\pm) - k_3} \Bigg). \end{aligned} \tag{7.33}$$

Partial integration delivers, for the second term

$$\begin{aligned}\left(\int \mathcal{P}\delta\right)_I = -i \lim_{\eta\to\infty} \Bigg(& \frac{\varphi(p(+))}{p'(\pm)-p(\pm)-k_3} \frac{2\cos\left((p_0'-p_0-k_0)\eta\right)}{\eta} \times \\ & \times \frac{1}{p_0'-p_0-k_0} \frac{dp(+)}{dp_0}\Big|_{p_0(a)}^{p_0(b)} \\ + \lim_{\epsilon\to 0} \left(\int_a^{p'(\pm)-k_3-\epsilon} + \int_{p'(\pm)-k_3+\epsilon}^{b} \right) & \frac{dp(+)}{2\pi} \frac{d}{dp_0} \left(\frac{\varphi(p(+))}{p'(\pm)-p(\pm)-k_3} \right) \times \\ & \times \frac{2\cos\left((p_0'-p_0-k_0)\eta\right)}{\eta} \frac{1}{p_0'-p_0-k_0} \Bigg).\end{aligned} \tag{7.34}$$

Since the integrand in the second term is uniformly continuous in the whole domain of integration we can take the limit $\sigma \to \infty$ and get zero. In our calculations in the main part of the text we are looking for the square of the scattering matrix integrated over all values of the momentum of the out-propagating particle $\frac{dp'(-)}{2\pi\hbar}|S|^2$. We therefore get for the remaining part of equation (7.34) zero.

In section II we define the uniformly continuous function

$$\varphi_\sigma(p(+)) := \varphi(p(+)) e^{-i(p'(\pm)-p(\pm)-k_3)z_0} \frac{1-e^{i(p'(\pm)-p(\pm)-k_3)\sigma}}{i(p'(\pm)-p(\pm)-k_3)}.$$

Taking the limit $\eta \to \infty$ and using the distributive representation of the delta function given in section 7.3 we get

$$\left(\int \mathcal{P}\delta\right)_{II} = \lim_{\sigma\to\infty} \tfrac{dp(+)}{dp_0} \varphi_\sigma(p(+)(p',k)) \tag{7.35}$$

where $p(+)(p',k) = ((p_0'-k_0-\frac{z0}{2})^2-\mu^2)^{1/2}$. By taking the square of the absolute value we obtain

$$|\left(\int \mathcal{P}\delta\right)|^2 = \lim_{\sigma\to\infty} 2|\tfrac{dp(+)}{dp_0}|^2 \varphi^2(p(+)(p',k)) \tfrac{1-\cos\left((p'(-)-p(-)-k_3)\sigma\right)}{|p'(-)-p(-)-k_3|^2}. \tag{7.36}$$

When integrating over the momentum of the out-propagating particle and transforming the intergration variable from $p'(-)$ to $p(+)(p', k)$ we can take the limit $\sigma \to \infty$ and, for narrow wavepackets, take the integrand, up to the Gaussian function $\varphi(p(+)(p', k))$, out of the integral. The result is

$$\int \frac{dp'(-)}{2\pi\hbar} | \left(\int \mathcal{P}\delta \right) |^2 = 2 | \frac{dp(+)}{dp_0} |^2 \frac{1}{|p'(-) - p(-) - k_3|^2} \frac{p(+)(p',k)}{p'(-)} \frac{\pi'(-)}{\pi(+)(p',k)}. \tag{7.37}$$

Bibliography

[1] J. Jackson, *Classical Electrodynamics, 3 rd ed* (New York, John Wiley & Sons, 1999).

[2] M. O. Scully and M. S. Zubairy, *Quantum Optics* (Cambridge University Press, Cambridge, England, 1997).

[3] R. Schützhold, G. Schaller, and D. Habs, Phys. Rev. Lett. **97**, 121302 (2006).

[4] R. Schützhold, G. Schaller, and D. Habs, Phys. Rev. Lett. **100**, 91301 (2008).

[5] W. G. Unruh, Phys. Rev. D **14**, 870 (1976).

[6] S. Fulling, Phys. Rev. D **7**, 2850 (1973).

[7] S. Hawking, Nature **248**, 30 (1974).

[8] J. Bell and J. Leinaas, Nucl. Phys. B **212** (1983).

[9] V. Ritus and A. Nikishov, Tr. Fiz. Inst. im. PN Lebedeva, Akad. Nauk SSSR **111** (1979).

[10] E. Whittaker and G. Watson, Cambridge Univ. Press , 404 (1952).

[11] R. Brout, R. Parentani, and P. Spindel, Nucl. Phys. B **353**, 209 (1991).

[12] R. Parentani and R. Brout, Nucl. Phys. B **388**, 474 (1992).

[13] R. Brout, S. Massar, R. Parentani, and P. Spindel, Phys. Rep. **260**, 329 (1995).

[14] A. I. Nikishov, Arxiv: hep-th/0111137 (2001).

[15] A. Hansen and F. Ravndal, Physica Scripta **23**, 1036 (1981).

[16] W. Greiner, B. Müller, and J. Rafelski, *Quantum electrodynamics of strong fields: with an introduction into modern relativistic quantum mechanics* (Springer-Verlag, 1985).

[17] M. Berry and K. Mount, Rep. Prog. Phys. **35**, 315 (1972).

[18] J. Schwinger, Phys. Rev. **82**, 664 (1951).

[19] F. Sauter, Z. Phys. A **69**, 742 (1931).

[20] A. I. Nikishov, YAD.FIZ. **67**, 1503 (2004).

[21] N. Tanji, Ann. Phys. (NY) **324**, 1691 (2009).

[22] A. Messiah, *Quantenmechanik Band 2* (Walter de Gruyter, Berlin, 1990).

[23] F. Schwabl, *Quantenmechanik für Fortgeschrittene (QM II)* (Springer, 2005).

[24] H. Dosch and V. Müller, Fortschritte der Physik **23** (1975).

[25] G. Scharf, *Finite quantum electrodynamics* (Springer-Verlag New York, 1989).

[26] P. Blanchard and E. Brüning, *Mathematical methods in physics: distributions, Hilbert space operators, and variational methods* (Birkhauser, 2002).

[27] Mathworld, http://functions.wolfram.com/hypergeometricfunctions/paraboliccylinderd/.

[28] F. Hund, Z. Phys. A **117**, 1 (1941).

[29] R. Parentani and S. Massar, Phys. Rev. D **55**, 3603 (1997).

[30] P. Dirac, *Lectures on quantum mechanics* (Dover, 2001).

[31] C. Cohen-Tannoudji, J. Dupont-Roc, and G. Grynberg, *Photons and atoms* (Wiley New York, 1989).

[32] E. Fradkin, D. Gitman, and S. Shvartsman, *Quantum electrodynamics: with unstable vacuum* (Springer-Verlag, 1991).

[33] C. Itzykson and J. Zuber, *Quantum field theory* (McGraw-Hill, 1980).

[34] B. Delamotte, Am. J. Phys. **72**, 170 (2004).

[35] M. Peskin and D. Schroeder, *An introduction to quantum field theory* (Westview Press, 1995).

[36] M. Duetsch, F. Krahe, and G. Scharf, Nuovo Cimento A **106**, 277 (1993).

[37] A. Higuchi and G. Martin, Foundations of Physics **35**, 1149 (2005).

[38] V. Maslov and M. Fedoriuk, *Semi-classical approximation in quantum mechanics* (Kluwer Academic Publishers, 2002).

[39] S. Rubinow and J. Keller, Phys. Rev. **131**, 2789 (1963).

[40] M. van Exter, A. Aiello, S. Oemrawsingh, G. Nienhuis, and J. Woerdman, Phys. Rev. A **74**, 12309 (2006).

[41] J. Meyer, J. Math. Phys. **11**, 312 (1970).

[42] S. Schnez, E. Loetstedt, U. Jentschura, and C. Keitel, Phys. Rev. A **75** (2007).

[43] A. Belyanin *et al.*, Phys. Rev. A **74**, 023807 (2006).